Fall 2022

Physico-Mechanical Characterization of Prototype Earth Block Material for Constitutive Modeling

Erika Lorena Rengifo-López

PHYSICO-MECHANICAL CHARACTERIZATION OF PROTOTYPE EARTH BLOCK MATERIAL FOR CONSTITUTIVE MODELING

by

Erika Lorena Rengifo-López

Bachelor of Science
Universidad del Valle (Colombia), 2012

Master of Science
Universidad del Valle (Colombia), 2018

Submitted in Partial Fulfillment of the Requirements

For the Degree of Doctor Philosophy in

Civil Engineering

College of Engineering and Computing

University of South Carolina

2022

Accepted by:

Fabio Matta, Major Professor

Michele Barbato, Committee Member

Juan M. Caicedo, Committee Member

Charles E. Pierce, Committee Member

Dr. Tracey L. Weldon, Vice Provost and Interim Dean of the Graduate School

DEDICATION

To my heavenly Father, my beloved mom (mama) Cenoide, my dear dad (papa) Daniel, my sister Daniela, and my little niece Angélica.

ACKNOWLEDGEMENTS

This material is based upon collaborative research supported by the National Science Foundation (NSF) grant 1537776 at University of South Carolina (UofSC), and companion grants 1537078 and 1850777 at Louisiana State University and University of California, Davis, and entitled “Collaborative Research: Engineered Earth Masonry for Affordable Seismic Resistant Low-Rise Buildings”. Any opinions, findings, and conclusions or recommendations expressed herein are those of the authors and do not necessarily reflect the views of the sponsor. Special thanks are extended to Dr. Fabio Matta for his precious and outstanding advisement, and to Dr. Michelle Barbato, Dr. Nitin Kumar, and Dr. Charles Pierce for their significant contributions to this research.

ABSTRACT

The comprehensive understanding and experimental characterization of the overall compressive behavior of earth masonry block materials, such as compressed and stabilized earth blocks (CSEBs), are essential for developing analytical and numerical tools to predict the mechanical response and designing earth masonry structures. Furthermore, advancing the understanding of the extent of the influence of testing parameters on the material's response, such as specimen geometry, is a critical step towards standardization.

CSEBs are produced by compressing a mixture of soil, water, and a stabilizer (e.g., Portland cement). The heterogeneity of the material accrues from the variety of soil particle morphology and potential dry density variations that results from the manufacturing process; both of these factors might affect the homogeneity and directional dependency of the mechanical properties. Yet, there is a lack of conclusive experimental evidence describing these aspects at a scale comparable to that suitable for material characterization, such as in the case of uniaxial compressive strength. On the other hand, the compressive strength and stress-strain response of earth masonry block materials are sensitive to the specimen aspect ratio, cross-sectional shape, and boundary conditions. However, the extent of the effect of these parameters is not fully understood, thus limiting the establishment of a standard test method. Furthermore, the information available on Young’s modulus and Poisson’s ratio is limited and scattered.

This research encompasses three experimental projects and a study on outreach activities for pre-college students. The experimental projects investigated a representative prototype CSEB material. The first project focused on characterizing the material physico-mechanical homogeneity and isotropy based on two criteria: (1) structural and chemical composition of the soil-cement matrix at the micro- and meso-scale, and (2) compressive strength and initial stiffness as a function of the loading direction relative to the compaction pressure and the location within a given block. The second project evaluated the effect of three parameters on the specimen's compressive strength. These parameters included friction at the loading interface and the aspect ratio, and the cross-sectional shape of the specimen. The third project continued the experimental program and data analysis, which included three-dimensional digital image correlation (3D-DIC) deformation measurements to evaluate the specimen geometry effect on the stress-strain response, focusing on the characterization of the constitutive behavior of the material. It was determined that the material investigated can be regarded as homogeneous and isotropic, that the specimen aspect ratio exerts an important influence on the compressive strength whereas the influence of cross-sectional shape is negligible, and that either cylinder or prism specimens with an aspect ratio of 2.0 are suitable to characterize a stress-strain response representative of the material's constitutive behavior.

The study on outreach proposes an adaptable pedagogical framework to provide meaningful structure for on-campus outreach activities for science, technology, engineering, and mathematics (STEM) that emphasize collaborative, hands-on learning experiences for pre-college students. The successful implementation of the framework was demonstrated by designing and assessing a summer workshop on hazard-resistant

earth masonry construction in which 85 high-school students participated over three consecutive years.

TABLE OF CONTENTS

LIST OF TABLES

LIST OF FIGURES

LIST OF SYMBOLS

A	Data group including all specimens.
C	Corner location within a given block.
D	Cylinder specimen diameter.
E	Young's modulus, in MPa.
F	Friction force, in N.
H	Vertically centered distance of the specimen height.
M	Middle third location within a given block.
N	Normal force, in N.
R^2	Coefficient of determination.
SSE	Sum of squared error.
SST	Sum of squared total.
X	Loading direction perpendicular to compaction pressure.
Y	Loading direction perpendicular to compaction pressure.
Z	Loading direction parallel to compaction pressure.
b	Prism specimen minor cross-section dimension.
f_b	Specimen compressive strength, in MPa.
n	Number of data points or number of specimens.
ε_1	Strain on direction 1-1.
ε_2	Strain on direction 2-2.
ε_3	Strain on direction 3-3.

μ_s Static coefficient of friction.

ν Poisson's ratio.

σ_1 Stress on direction 1-1.

σ_2 Stress on direction 2-2.

σ_3 Stress on direction 3-3.

List of Abbreviations

AD	Anderson-Darling test
Al	Aluminum
C	Carbon
Ca	Calcium
CEB	Non-stabilized compressed earth block
CDF	Cumulative distribution function
CL	Lean clay
CoF	Coefficient of friction
CS	Clayey sand
CSEB	Compressed and stabilized earth block
CV	Coefficient of variation
C0.5	Cylinders CSEB specimen with aspect ratio 0.5
C1.0	Cylinders CSEB specimen with aspect ratio 1.0
C2.0	Cylinders CSEB specimen with aspect ratio 2.0
EDS	Energy dispersive spectroscopy
EFFECTs	Environments for fostering effective critical thinking
Fe	Iron
IQR	Interquartile range
K	Potassium
LL	Liquid limit

LSU	Louisiana State University
LVDT	Linear variable displacement transducers
ML	Silt
NBP	Notched box plot
NPS	Net promoter score
NSF	National Science Foundation
O	Oxygen
PBL	Problem based learning
PL	Plastic limit
PMECS	Partners for minorities in engineering & computer science
PTFE	Polytetrafluoroethylene
P0.7	Prism CSEB specimen with aspect ratio 0.7
P1.0	Prism CSEB specimen with aspect ratio 1.0
P1.2	Prism CSEB specimen with aspect ratio 1.2
P1.2S	Prism CSEB specimen with aspect ratio 1.2 with sandpaper insert.
P2.0	Prism CSEB specimen with aspect ratio 2.0
SD	Standard deviation
SEM	Scanning electron microscopy
Si	Silicon
STEM	Technology engineering and mathematics
UCD	University of California Davis
UofSC	University of South Carolina
3D-DIC	Three-dimensional digital image correlation

CHAPTER 1: INTRODUCTION

1.1 BACKGROUND AND LITERATURE REVIEW

Earth masonry made with CSEBs is emerging as a low-cost, environmentally sustainable, and suitable material for building low-rise structures able to resist loads imposed by natural hazards [1]–[3]. Using CSEB materials entails carbon emissions and embodied energy lower than concrete masonry units and fired clay bricks [4]. On the other hand, earth masonry blocks are energy efficient and can passively maintain the indoor humidity within the optimal range for occupant health [5]–[7]. In addition, they suit conventional construction practices, and soils suitable for their production are widely available. Thus, earth masonry using CSEBs offers a feasible and practical response to the demand for affordable, sustainable, and hazard-resilient low-rise buildings. The affordable housing shortage for renter households with extremely low income in the United States is estimated at 7.4 million [8]. Worldwide, it is expected to increase to 440 million by 2025 [9].

1.1.1 CONSTITUTIVE COMPRESSIVE BEHAVIOR OF EARTH BLOCK MATERIALS

CSEBs are produced by compressing a mixture of soil, water, and a stabilizer (e.g., ordinary Portland cement). Research shows that inconsistencies in the dry density of CSEBs may accrue from variations in the pressure distribution during compaction, which depends on the compaction mode (i.e., single-sided or double-sided), amount of pressure applied, and inter-particle and soil mixture-mold friction [10], [11]. On the other hand, because the water content is critical to achieving the maximum dry density [12] of

CSEBs, non-uniform water distribution through the soil-cement mix may lead to density inconsistencies and the non-uniform formation of cement hydrates during curing within a given block. In addition, it has been observed that static compaction produces trajectories of parallel clay particle packets that develop perpendicular to the direction of compaction [13], [14].

To the best of the author's knowledge, only two experimental studies report on CSEB materials' heterogeneity [11] and anisotropy [15]. Yet, when analyzing the strength of earth masonry, the blocks are typically assumed to be homogeneous and isotropic [16], [17]. Similar to CSEB materials, limited literature is available for other earthen materials. For adobe blocks, mainly because of the production process, the distribution of the dry density and compressive strength within a block is typically heterogeneous [18]. For extruded earth bricks, Aubert et al. [19] found that the material is anisotropic with respect to its compressive strength. For the same type of earth brick, Maillard and Aubert [20] determined that the hygrothermal properties in the direction parallel to the clay platelets are different from those in the perpendicular direction to the clay platelets. The anisotropic behavior of extruded earth bricks is attributed to the extrusion process, which facilitates the alignment of clay particles [20]. In contrast, Bui and Morel [21] concluded that rammed earth can be regarded as isotropic in terms of compressive strength and stiffness, provided that the compacted layers adhere sufficiently to one another.

The intrinsic heterogeneity of the CSEB material – linked to dry density variations resulting from the manufacturing process and soil particle morphology –may affect the homogeneity and directional dependency of the mechanical properties.

However, the related evidence available in the literature is limited and based on different material and specimen types, posting difficulties in generalizing conclusions.

Experimental results including compressive strength and stress-strain response are sensitive to a given's specimen aspect ratio (i.e., the ratio between the larger and smaller dimension), cross-sectional shape, and boundary conditions. The aspect ratio effect results from the lateral expansion constraints exerted by the loading plates due to friction at the contact surface and stiffness mismatch between the plates and the specimen [22]. Due to the importance of the uniaxial compression characterization of earth masonry units, the consideration of aspect ratio effects on the compressive behavior becomes significant. However, there is no consensus among the approaches to account for these effects [23]–[25]. For instance, the Spanish standard for compressed earth blocks [23] specifies shape factors to convert the experimental strength of a given block-type specimen to a normalized compressive strength, which corresponds to a block with a height and width of 100 mm; this configuration is similar to the procedure outlined by the European Standards [26] for masonry units. In contrast, the New Zealand standard [24] and Australian handbook [25] specify aspect-ratio correction factors to determine the unconfined compressive strength. It is noted that the factors in [24] and [25] are different from each other; the latter are the same factors specified by the Australian standard for masonry units [27], which were originally proposed based on results from investigations carried out on calcium silicate masonry bricks [28]. These factors are comparable to those determined from experimental results from CSEB specimens [29]. The existing approaches that aim to account for specimen aspect ratio are limited to the experimental

characterization of the compressive strength, and no consideration is given to the stress-strain response.

The literature on the cross-sectional shape effect on the compressive strength of CSEB or similar materials is minimal, and the understanding of the extent of this effect is unclear. Studies on compressive strength behavior and testing methods typically disregard the effect of this parameter. For instance, compression testing methods for CSEBs are assessed in [30] using block and cylinder specimens without considering the cross-sectional shape in interpreting the results, and the testing methods for earth wall materials provided by the Australian earth building handbook [25] and New Zealand standard [24] apply to block type and cylindrical specimens, with no specific provisions per differences in cross-sectional shape. Only one study, reported in [31] on unstabilized compressed earth blocks, presents experimental evidence describing the effect of cross-sectional shape as negligible.

Concerning boundary conditions used to determine the compressive strength of earth masonry materials, different configurations are adopted to provide uniform load distribution and minimize platen lateral restraints. The boundary condition configurations found in the literature provide a combined effect of stiffness mismatch and friction, but there is no reference examining the isolated impact of friction only. Such configurations include sandwiching specimens between plywood sheets [29], [30], [32], [33], combining greased neoprene and Teflon inserts at the loading interface [34], [35] or using bare loading plates [31], [36].

There are limited available investigations aimed at characterizing mechanical parameters that represent the constitutive behavior of earthen materials. These

investigations have focused on compressed earth blocks [34], [37], [38], adobe [18], and rammed earth [39]. Yet, various specimen geometries, measuring methods, and definitions of elastic properties (e.g., Young's modulus) are observed among methodologies from different studies, limiting the interpretation of the results. On the other hand, available experimental results for Poisson's ratio are scattered. For instance, Venkatarama Reddy et al. [40] inform a Poisson's ratio values between 0.19 and 0.24 for earthen mortar and between 0.08 and 0.12 for a CSEB material. For a non-stabilized earth block material, Champiré et al. [38] report results ranging from 0.15 and 0.2, and for rammed earth, Bui et al. [41] found values between 0.22 and 0.40.

The literature review indicates that the extent of the effect of specimen aspect ratio, cross-sectional shape, and boundary conditions on the compressive strength and stress-strain response of earth masonry materials, such as compressed stabilized earth blocks (CSEB), is not fully understood yet. Furthermore, the information available on the overall compressive response (i.e., Young's modulus, Poisson's ratio, and stress-strain relations) of earth masonry blocks is limited.

To address the knowledge gaps described above, the following research questions were formulated: (1) can the mechanical behavior of CSEB material be approximated as homogeneous and isotropic with respect to uniaxial compressive strength, which is a key mechanical property for the structural analysis and design of earth masonry? (2) What specimen configuration should one use to characterize strength and stress-strain response that are suitable to define constitutive models for CSEB materials? Addressing these research questions is essential to develop analytical and numerical tools for the analysis, design, and computational simulation of earth masonry structures. In addition, related

contributions to the state of the art are necessary steps towards the standardization of the mechanical characterization of earth block materials.

1.1.2 K-12 Outreach programs for STEM

The STEM workforce in the United States is essential for improving the quality of life, sustaining economic growth, and maintaining global competitiveness [42]. Demand for STEM workers continues to rise as more occupations require their expertise [43]. Meeting this demand requires a sustained and multifaceted effort to inform and motivate pre-college students to pursue STEM in higher education. Most K-12 outreach programs become important recruitment tools for increasing enrollment and broadening representation in STEM majors at colleges and universities [44]–[46]. Furthermore, the broader impacts of outreach on changing negative perceptions of engineers and scientists [47] and improving scientific literacy [48] are significant. However, one of the challenges with K-12 outreach is the lack of knowledge about how to construct and deliver an experience that maximizes potential impact.

EFFECTs are problem-based learning (PBL) modules that feature active learning and collaborative learning. Modules constructed within this framework have proven successful across a range of instructional environments, including undergraduate engineering courses in a conventional classroom setting [49], [50], laboratory courses [51], [50], and high school science classes [52]. While civil engineering has been the focus for most modules, EFFECTs have been structured around other STEM content such as solar power [53] and software engineering [54]. Such broad application of this PBL framework in formal STEM instruction suggests it can be adapted for informal learning environments, including outreach programs.

1.2 OBJECTIVES

The scope of this dissertation entails two research projects. The first one refers to the experimental characterization of the compressive constitutive behavior of a representative prototype earth block material. The second one refers to the integrated outreach component conceived as part of the broader impacts for the research project that supported this dissertation through the NSF grant 1537776 at UofSC, and companion grants 1537078 and 1850777 at Louisiana State University (LSU) and University of California, Davis (UCD), and entitled "Collaborative Research: Engineered Earth Masonry for Affordable Seismic Resistant Low-Rise Buildings"[55]–[57]. The specific objectives are as follows.

1. To experimentally characterize the physico-mechanical homogeneity and isotropy of a prototype CSEB material based on structural and chemical composition, and to statistically analyze compressive strength and initial stiffness data.

2. To experimentally assess the effect of specimen aspect ratio, cross-sectional shape, and friction at the loading interface on the resulting compressive strength of specimens made of the prototype material.

3. To determine a suitable configuration to characterize both the uniaxial compressive strength and stress-strain response of the prototype CSEB material, and to demonstrate the definition of the critical parameters for constitutive modeling.

4. To propose, demonstrate, and assess an adaptable pedagogical framework to provide meaningful structure for on-campus STEM outreach activities for pre-college students through a workshop on hazard-resistant earth masonry construction.

1.3 METHODOLOGY

This section summarizes the methodology followed in conducting the three articulated experimental projects and the study on STEM outreach activities. Further details are described in the Methodology section of each chapter.

The experimental component investigated a CSEB material prototyped at the UofSC by Cuéllar-Azcárate [58]. The material's physico-mechanical homogeneity and isotropy were assessed based on two criteria: (1) structural and chemical composition of the soil-cement matrix and (2) compressive strength and initial stiffness as a function of the loading direction relative to the compaction pressure and the location within a given block. First, scanning electron microscopy (SEM) and energy dispersive spectroscopy (EDS) were used to visually examine the structural composition and characterize the chemical composition of the material. Then, uniaxial compression tests were carried out on cube specimens to collect strength and stiffness data, differentiated by the cube's sourced location within a given block and the compressive load direction. Finally, statistical analysis was conducted to quantify the significance of the statistical differences between the mean values and variances of the collected data, pertaining to different location and loading direction groups for homogeneity and isotropy assessment, respectively.

Following the homogeneity and isotropy characterization, the assessment of the extent of friction, cross-sectional shape, and aspect ratio effects on the compressive strength was conducted. To that end, the coefficient of friction (CoF) between different inserts and the CSEB surface was characterized to estimate the friction levels at the specimen-loading platen interface and select two inserts with statistically significant

different CoFs. Next, prism and cylinder specimens having different aspect ratios and friction inserts were tested in uniaxial compression to collect strength data. The specimen manufacturing process was considered in the interpretation of the results to facilitate the discussion based on the observed effects of the parameter in consideration.

After assessing the effects on strength of the specimen geometry and friction at the loading interface, the research continued to identify a suitable configuration for stress-strain response measurement and complete the constitutive behavior characterization. The compressive stress-strain response of cylinder and prism specimens was determined based on pointwise and 3D-DIC deformation measurements. The 3D-DIC-based strain maps were analyzed to gain a comprehensive insight into the effects of the specimen geometry and platen lateral restraints on the full-field strain distribution and to quantitatively identify a suitable specimen height portion to retrieve data that potentially represent the uniaxial behavior of the material.

The methodology of the pedagogical framework for on-campus STEM outreach activities consists of five steps that emphasize collaborative, hands-on learning experiences for pre-college students. The core component of the methodology is establishing a situated learning environment in which activities develop around tangible applications and allocate within meaningful contexts. The proposed framework was demonstrated by designing a hazard-resistant earth masonry construction workshop. The workshop was delivered to underrepresented gifted K-12 students within a summer camp program for STEM disciplines throughout three consecutive years. The results of the analysis of student feedback, collected throughout a post-workshop survey, were used to measure the successful implementation of the framework.

1.4 RESEARCH NOVELTY AND SIGNIFICANCE

This research offers the following novel contributions:

1. Physico-mechanical characterization of a prototype earth block material as homogeneous and isotropic at a scale comparable to which one can use in laboratory settings for material characterization. This contribution is critical for defining constitutive models of the material and defining testing methods. The loading direction relative to the compaction direction is not a critical component of the testing methodology.

2. Identification of appropriate probability distributions for the compressive strength and initial tangent stiffness of a representative earth block material. The normal distribution is recommended as the most suitable distribution for applications focused on the body of the distribution (e.g., probabilistic response, stochastic dynamics) whereas the truncated normal distribution is recommended for use in applications focused on the distribution tails (e.g., structural reliability).

3. Identification of a specimen configuration suitable for characterization of strength and constitutive behavior of earth block materials. Using prisms and cylinders with an aspect ratio of 2.0 allows for deformation measurements within a specimen height portion where the restraining effects of the loading platens are sufficiently minimized.

4. Practical recommendations concerning critical components to define a methodology for experimental characterization of earth block materials. Considerations are offered for specimen manufacturing, deformation measurement instrumentation (pointwise contact and 3D-DIC full-field measurement methods), and data interpretation. This contribution is a relevant step towards standardization.

5. Extensive and rigorously collected database describing the stress-strain response and elastic properties (i.e., Young's modulus and Poisson's ratio) of the material and their variability. This contribution constitutes a robust and reliable input to define the constitutive models for the numerical modeling of earth block masonry structures.

6. Adaptable pedagogical framework to provide meaningful structure for on-campus STEM outreach activities that emphasize collaborative, hands-on learning experiences for pre-college students.

1.5 OUTLINE OF DISSERTATION

In Chapter 2, the physico-mechanical homogeneity and isotropy of a representative prototype earth block material are characterized based on microanalysis of the physical and chemical composition and statistical analysis of compressive strength and initial stiffness data. Chapter 3 presents the results of an experimental investigation on the compressive strength of the same material studied in Chapter 2, focusing on the effect of friction at the loading interface and specimen geometry. Chapter 4 expands the experimental program and data analysis to evaluate the specimen geometry effect on the stress-strain response, focusing on the characterization of the constitutive behavior of the material. In Chapter 5, an adaptable pedagogical framework is proposed to provide meaningful structure for on-campus STEM outreach activities that emphasize collaborative, hands-on learning experiences for pre-college students. The successful implementation of the framework was demonstrated through the design and evaluation of a workshop on hazard-resistant earth masonry construction. Chapter 6 presents a summary of the key conclusions and recommendations drawn from the research presented in Chapter 2 through Chapter 5.

1.6 REFERENCES

[1] P. J. Yttrup, “Strength of earth walls subjected to lateral wind load forces,” in *In Proc., 1st National local government engineering conference*, Adelaine, Australia, 1981, pp. 181–185.

[2] H. W. Morris, R. Walker, and T. Drupsteen, “Modern and historic earth buildings: Observations of the 4th September 2010 Darfield earthquake,” presented at the Ninth Pacific Conference on Earthquake Engineering Building an Earthquake-Resilient Society, Auckland, New Zealand, Apr. 2011. Accessed: Mar. 28, 2017. [Online]. Available: http://nzsee.org.nz/db/2011/133.pdf

[3] F. Matta, M. C. Cuéllar-Azcárate, and E. Garbin, “Earthen masonry dwelling structures for extreme wind loads,” *Eng. Struct.*, vol. 83, pp. 163–175, Jan. 2015, doi: 10.1016/j.engstruct.2014.10.043.

[4] F. P. Torgal and S. Jalali, “Construction and Demolition (C&D) Wastes,” in *Eco-efficient Construction and Building Materials*, F. Pacheco Torgal and S. Jalali, Eds. London: Springer, 2011, pp. 51–73. doi: 10.1007/978-0-85729-892-8_4.

[5] T. Morton, *Earth masonry design and construction guidelines*. Bracknell: IHS BRE Press, 2008.

[6] F. Pacheco-Torgal and S. Jalali, “Earth construction: Lessons from the past for future eco-efficient construction,” *Constr. Build. Mater.*, vol. 29, pp. 512–519, Apr. 2012, doi: 10.1016/j.conbuildmat.2011.10.054.

[7] D. Allinson and M. Hall, “Humidity buffering using stabilised rammed earth materials,” 2012.

[8] NLIHC, “The GAP: A shortage of affordable homes,” National Low Income Housing Coalition, Washington, DC, Mar. 2017.

[9] J. R. Woetzel, S. Ram, J. Mischke, N. Garemo, and S. Sankhe, “A blueprint for addressing the global affordable housing challenge,” McKinsey Global Institute, Executive summary, 2014. [Online]. Available: www.mckinsey.com/mgi

[10] D. E. M. Gooding, “Quasi-static compression forming of stabilised soil-cement building blocks,” *Dev. Technol. Unit Work. Pap.*, no. 40, 1993.

[11] D. E. M. Gooding, “Improved processes for the production of soil-cement building blocks,” Doctoral dissertation, University of Warwick, Coventry, UK, 1994.

[12] M. Olivier and A. Mesbah, “Le matériau terre: Essai de compactage statique pour la fabrication de briques de terre compressées [The earth as a material: use of the proctor static test to optimize the making of compacted earth bricks],” *Bull Liaison Lab Ponts Chaussées*, vol. 146, pp. 37–43, 1986.

[13] R. L. Sloane, T. R. Kell, and Foundation and Materials Branch, U.S. Army Corpe Engineers, Southwest Division, Dallas, Texas, "The fabric of mechanically compacted kaolin," in *In Proc., 14th National Conference on Clays and Clay Minerals*, Berkeley, California, Jan. 1966, pp. 289–296. doi: 10.1016/B978-0-08-011908-3.50027-X.

[14] O. M. de Oliveira, "Estudo sobre a resistência ao cisalhamento de um solo residual compactado não saturado," Doctoral dissertation, Universidade de São Paulo, São Paulo, 2004. doi: 10.11606/T.3.2004.tde-08032005-160218.

[15] J. R. González-López, C. A. Juárez-Alvarado, B. Ayub-Francis, and J. M. Mendoza-Rangel, "Compaction effect on the compressive strength and durability of stabilized earth blocks," *Constr. Build. Mater.*, vol. 163, pp. 179–188, Feb. 2018, doi: 10.1016/j.conbuildmat.2017.12.074.

[16] L. Miccoli, A. Garofano, P. Fontana, and U. Müller, "Experimental testing and finite element modelling of earth block masonry," *Eng. Struct.*, vol. 104, pp. 80–94, Dec. 2015, doi: 10.1016/j.engstruct.2015.09.020.

[17] Q.-B. Bui, J.-C. Morel, S. Hans, and N. Meunier, "Compression behavior of non-industrial materials in civil engineering by three scale experiments: the case of rammed earth," *Mater. Struct.*, vol. 42, no. 8, pp. 1101–1116, Oct. 2009, doi: 10.1617/s11527-008-9446-y.

[18] C. H. Kouakou and J. C. Morel, "Strength and elasto-plastic properties of non-industrial building materials manufactured with clay as a natural binder," *Appl. Clay Sci.*, vol. 44, no. 1–2, pp. 27–34, Apr. 2009, doi: 10.1016/j.clay.2008.12.019.

[19] J. E. Aubert, P. Maillard, J. C. Morel, and M. Al Rafii, "Towards a simple compressive strength test for earth bricks?," *Mater. Struct.*, vol. 49, no. 5, pp. 1641–1654, 2016, doi: 10.1617/s11527-015-0601-y.

[20] P. Maillard and J. E. Aubert, "Effects of the anisotropy of extruded earth bricks on their hygrothermal properties," *Constr. Build. Mater.*, vol. 63, pp. 56–61, Jul. 2014, doi: 10.1016/j.conbuildmat.2014.04.001.

[21] Q.-B. Bui and J.-C. Morel, "Assessing the anisotropy of rammed earth," *Constr. Build. Mater.*, vol. 23, no. 9, pp. 3005–3011, Sep. 2009, doi: 10.1016/j.conbuildmat.2009.04.011.

[22] P. Domone, "Strength and failure of concrete," *Constr. Mater.*, pp. 155–168, 1994.

[23] AEN/CTN 41, *UNE 41410: Bloques de tierra comprimida para muros y tabiques. Definiciones, especificaciones y métodos de ensayo [Compressed earth blocks for walls and partitions. Definitions, specifications and test methods]*, AENOR. Madrid: AENOR, 2008.

[24] NZS, *NZS 4298: Materials and construction for earth buildings*. Wellington, N.Z.: Standards New Zealand, 2020.

[25] P. Walker and Standards Australia, *The Australian earth building handbook*. Australia: Standards Australia International, 2002.

[26] CEN/TC 125, *EN 772-1:2011+A1:2015: Methods of test for masonry units–Part 1: Determination of compressive strength*. Brussels: European Committee for Standardization, 2015.

[27] Standards Australia, *AS/NZS 4456: Masonry units, segmental pavers and flags - Methods of test*. Sydney, 2003.

[28] A. W. Page and R. Marshall, "The influence of brick and brickwork prism aspect ratio on the evaluation of compressive strength," in *Proc., 7th International Brick Masonry Conference*, Melbourne, Australia, 1985, vol. 1, pp. 653–664.

[29] K. A. Heathcote and E. Jankulovski, "Aspect ratio correction factors for soilcrete blocks," *Trans. Inst. Eng. Aust. Civ. Eng.*, vol. 34, no. 4, pp. 309–312, 1992.

[30] P. Walker, "Strength and durability testing of earth blocks," in *Proceedings of the 6th international seminar on Structural Masonry for developing countries*, 2000, pp. 110–118.

[31] G. Lan, Y. Wang, and S. Chao, "Influences of specimen geometry and loading rate on compressive strength of unstabilized compacted earth block," *Adv. Mater. Sci. Eng.*, pp. 1–10, Jul. 2018, doi: 10.1155/2018/5034256.

[32] P. Walker, "Characteristics of pressed earth blocks in compression," in *Proceedings of the 11th international brick/block masonry conference, Shanghai, China*, Shanghai, China, 1997, pp. 14–16.

[33] P. J. Walker, "Strength, Durability and Shrinkage Characteristics of Cement Stabilised Soil Blocks," *Cem. Concr. Compos.*, vol. 17, no. 4, pp. 301–310, Jan. 1995, doi: 10.1016/0958-9465(95)00019-9.

[34] A. Hakimi, O. Fassi-Fehri, H. Bouabid, S. C. D'ouazzane, and M. E. Kortbi, "Comportement mécanique non linéaire du bloc de terre comprimée par couplage élasticité endommagement [Non-linear behaviourof the compressed earthen block by elasticity-damage coupling]," *Mater. Struct.*, vol. 32, no. 7, pp. 539–545, Aug. 1999, doi: 10.1007/BF02481639.

[35] D. Ciancio and J. Gibbings, "Experimental investigation on the compressive strength of cored and molded cement-stabilized rammed earth samples," *Constr. Build. Mater.*, vol. 28, no. 1, pp. 294–304, Mar. 2012, doi: 10.1016/j.conbuildmat.2011.08.070.

[36] K. Heathcote, “Compressive strength of cement stabilized pressed earth blocks,” *Build. Res. Inf.*, vol. 19, no. 2, pp. 101–105, Mar. 1991, doi: 10.1080/09613219108727106.

[37] G. Ruiz, X. Zhang, W. F. Edris, I. Cañas, and L. Garijo, “A comprehensive study of mechanical properties of compressed earth blocks,” *Constr. Build. Mater.*, vol. 176, pp. 566–572, Jul. 2018, doi: 10.1016/j.conbuildmat.2018.05.077.

[38] F. Champiré, A. Fabbri, J.-C. Morel, H. Wong, and F. McGregor, “Impact of relative humidity on the mechanical behavior of compacted earth as a building material,” *Constr. Build. Mater.*, vol. 110, pp. 70–78, May 2016, doi: 10.1016/j.conbuildmat.2016.01.027.

[39] P. Chauhan, A. El Hajjar, N. Prime, and O. Plé, “Unsaturated behavior of rammed earth: Experimentation towards numerical modelling,” *Constr. Build. Mater.*, vol. 227, p. 116646, Dec. 2019, doi: 10.1016/j.conbuildmat.2019.08.027.

[40] B. V. Venkatarama Reddy, R. Lal, and K. S. Nanjunda Rao, “Enhancing bond strength and characteristics of soil-cement block masonry,” *J. Mater. Civ. Eng.*, vol. 19, no. 2, pp. 164–172, Feb. 2007, doi: 10.1061/(ASCE)0899-1561(2007)19:2(164).

[41] Q.-B. Bui, S. Hans, J.-C. Morel, and A.-P. Do, “First exploratory study on dynamic characteristics of rammed earth buildings,” *Eng. Struct.*, vol. 33, no. 12, pp. 3690–3695, Dec. 2011, doi: 10.1016/j.engstruct.2011.08.004.

[42] National Science Board, “The STEM labor force of today: scientists, engineers, and skilled technical workers,” National Science Foundation, Alexandria, VA, Special reports NSB 2021-2, 2021. Accessed: Mar. 10, 2022. [Online]. Available: https://ncses.nsf.gov/pubs/nsb20212

[43] Bureau of Labor Statistics, “Special tabulations of 2019–29,” 2020.

[44] R. Hammack, T. Ivey, J. Utley, and K. High, “Effect of an engineering camp on students’ perceptions of engineering and technology,” *J. Pre-Coll. Eng. Educ. Res. J-PEER*, vol. 5, no. 2, Nov. 2015, doi: 10.7771/2157-9288.1102.

[45] X. Kong, K. P. Dabney, and R. H. Tai, “The association between science summer camps and career interest in science and engineering,” *Int. J. Sci. Educ. Part B*, vol. 4, no. 1, pp. 54–65, Jan. 2014, doi: 10.1080/21548455.2012.760856.

[46] J. Vennix, P. den Brok, and R. Taconis, “Do outreach activities in secondary STEM education motivate students and improve their attitudes towards STEM?,” *Int. J. Sci. Educ.*, vol. 40, no. 11, pp. 1263–1283, Jul. 2018, doi: 10.1080/09500693.2018.1473659.

[47] M. F. Bugallo and A. M. Kelly, “Engineering outreach: yesterday, today, and tomorrow [SP education],” *IEEE Signal Process. Mag.*, vol. 34, no. 3, pp. 69–100, May 2017, doi: 10.1109/MSP.2017.2673018.

[48] A. T. Jeffers, A. G. Safferman, and S. I. Safferman, “Understanding K–12 engineering outreach programs,” *J. Prof. Issues Eng. Educ. Pract.*, vol. 130, no. 2, pp. 95–108, Apr. 2004, doi: 10.1061/(ASCE)1052-3928(2004)130:2(95).

[49] C. E. Pierce, J. M. Caicedo, J. R. Flora, N. D. Berge, R. Madarshahian, and B. Timmerman, “Integrating professional and technical engineering skills with the EFFECTs pedagogical framework,” *Int. J. Eng. Educ.*, vol. 30, no. 6, pp. 1579–1589, 2014.

[50] C. E. Pierce, S. L. Gassman, and J. T. Huffman, “Environments for fostering effective critical thinking in geotechnical engineering education (Geo-EFFECTs),” *Eur. J. Eng. Educ.*, vol. 38, no. 3, pp. 281–299, Jun. 2013, doi: 10.1080/03043797.2013.800021.

[51] R. D. Starcher and C. E. Pierce, “Problem-based learning with EFFECTs: part II–ground improvement module for lab courses,” presented at the International Conference on Geo-Engineering Education, ISSMGE, Belo Horizonte, Brazil, 2016.

[52] N. Berge, D. D. Thompson, C. Ingram, and C. Pierce, “Engineering design and EFFECTs,” *Sci. Scope*, vol. 38, no. 3, pp. 16–27, Nov. 2014.

[53] I. W. Wait, “Solar power system design to promote critical thinking in freshman engineering students,” in *Proc. 2012 ASEE Annual Conference & Exposition*, 2012, pp. 25–1167.

[54] C. E. Pierce *et al.*, “Infusing STEM courses with problem-based learning about transportation disruptive technologies,” presented at the ASEE Annual Conference & Exposition, 2019.

[55] “NSF Award Search: Award # 1537776 - Collaborative Research: Engineered Earth Masonry for Affordable Seismic Resistant Low-Rise Buildings.” https://nsf.gov/awardsearch/showAward?AWD_ID=1537776 (accessed Apr. 03, 2022).

[56] “NSF Award Search: Award # 1537078 - Collaborative Research: Engineered Earth Masonry for Affordable Seismic Resistant Low-Rise Buildings.” https://nsf.gov/awardsearch/showAward?AWD_ID=1537078 (accessed Apr. 03, 2022).

[57] “NSF Award Search: Award # 1850777 - Collaborative Research: Engineered Earth Masonry for Affordable Seismic Resistant Low-Rise Buildings.” https://www.nsf.gov/awardsearch/showAward?AWD_ID=1850777 (accessed Apr. 03, 2022).

[58] M. C. Cuéllar-Azcárate, “Engineered earthen masonry structures for extreme wind loads,” Doctoral dissertation, University of South Carolina, Columbia, 2016. Accessed: Mar. 28, 2017. [Online]. Available: http://scholarcommons.sc.edu/etd/3396/?utm_source=scholarcommons.sc.edu%2Fetd%2F3396&utm_medium=PDF&utm_campaign=PDFCoverPages.

CHAPTER 2: PHYSICO-MECHANICAL CHARACTERIZATION OF HOMOGENEITY AND ISOTROPY OF PROTOTYPE EARTH BLOCK MATERIAL[1]

[1] Erika L. Rengifo-López., Nitin Kumar, Fabio Matta, and Michele Barbato. To be submitted to *ASCE Journal of Materials in Civil Engineering*.

ABSTRACT. Compressed and stabilized earth blocks (CSEBs) are typically manufactured through one-side compaction. The resulting soil matrix-cement hydrate microstructure is inhomogeneous, posing the question of whether CSEB materials can be considered homogeneous and isotropic. As earth masonry is emerging as an affordable and sustainable material for high-quality and hazard-resistant houses, addressing this question becomes relevant to define constitutive models for analysis and design, and interpret material test data for quality assurance/control.

This paper reports the results of an extensive experimental program and data analysis aimed to study the homogeneity and directional dependence of the compressive strength and initial stiffness of CSEBs manufactured with one-sided hydraulic compaction. Based on microanalysis methods, qualitative and quantitative data were collected to describe the soil-cement composition and distribution of stabilization at the micro- and meso-scale. Furthermore, 84 cube specimens were tested under uniaxial compression by applying the load either parallel or perpendicular to the compaction direction used for manufacturing, to characterize strength and stiffness. Statistical analyses were enlisted to characterize the statistical significance of the difference between mean values of the mechanical properties for different specimen groups based on loading direction and location in the source CSEBs. It was concluded that the representative CSEB material can be regarded as homogeneous and isotropic.

2.1 INTRODUCTION

CSEB is a low-cost, environmentally sustainable and suitable material for building low-rise structures able to resist loads imposed by natural-hazards [1]–[3]. Since CSEB suits conventional practices of production and construction, it becomes a feasible

and appealing alternative to alleviate the affordable housing shortage. For renter households with extremely low income in the United States of America, the affordable housing shortage is estimated in 7.4 million [4], and worldwide, it is expected to increase in 440 million by 2025 [5]. CSEBs are produced by compressing the mixture of soil, water, and a stabilizer, which is commonly a chemical binder. The combined action of compression and chemical reaction of the stabilizer results in a density increment and provides a water-resistant strengthening mechanism, which enhances the dimensional stability, reduces permeability and increases the bearing capacity [6].

The intrinsic heterogeneity of the CSEB material – linked to dry density variations resulting from the manufacturing process and soil particle morphology –may affect the homogeneity and directional dependency of the mechanical properties. The variety of sizes and shapes of the soil particles constitute a plausible source of inherent heterogeneity. Concerning the compaction process, variables such as pressure distribution, water content, and potential particle alignment may be identified as possible sources of heterogeneity and or isotropy. Research shows that inconsistencies in the dry density of CSEBs may accrue from variations in the pressure distribution during compaction, which depends on the compaction mode (i.e., single-sided or double-sided), amount of pressure applied, and inter-particle and soil mixture-mold friction [6], [7]. Gooding [6] measured the pressure transmitted to the mold walls through the compacting soil and identified that the values on the mold's bottom are higher than on the mold's sides in a single-sided compaction process; thus, the nearest material to the compacting piston results denser. Furthermore, Gooding's results showed that friction between soil particles and friction between soil mixture and mold surfaces affect the applied pressure's

effectiveness in the block compaction. The pressure reduction observed in the compacting piston is attributed to internal shear due to friction. Water content is critical to achieving the maximum dry density of CSEBs [8]. Consequently, any extent of nonuniform water distribution through the soil-cement mix may lead to density inconsistencies and the non-uniform formation of cement hydrates products during the curing process within a given block. Finally, it has been observed that static compaction produces trajectories of parallel clay particle packets that appear to orient perpendicular to the direction of compaction direction [9], [10]. Since the soil used to produce CSEBs typically has a clay content that ranges between 5 and 40 % [11], it is plausible that clay particle alignment resulting from the compaction process might constitute a source of anisotropy. However, the available evidence on homogeneity and isotropy of the mechanical properties of earth block materials is limited and based on different material and specimen types, posting difficulties in generalizing conclusions. Therefore, the following question regarding the constitutive laws of the material arises: can the mechanical behavior of CSEB material be approximated as homogeneous and isotropic for structural analysis and design of earth masonry structures?

The development of numerical tools for the structural analysis and design is fundamental to extendedly understand the response of any material under different configurations and loading conditions. When analyzing the strength of earth masonry, the blocks are typically assumed as homogeneous and isotropic. Miccoli et al. [12] propose a macro-model, for earth block masonry, based on isotropic plasticity and a micro-model whose blocks are defined as homogeneous and isotropic elements. Bui et al. [13] propose an experimental approach to determine equivalent mechanical properties of rammed earth

elements based on test results of CSEB that are assumed as homogeneous and isotropic to apply homogenization procedures.

To the best of the author's knowledge, only two experimental studies report on CSEB materials' heterogeneity [7] and anisotropy [14]. However, the methodologies and results of these studies do not seem to support their conclusions fully. Gooding [7] finds statistically significant differences between the compression strength of samples cut from different locations of CSEBs and concludes that regions closest to the mold walls result in increased strength; however, Gooding's sample size limits the robustness of the experimental evidence to draw reliable conclusions regarding the homogeneity of the material. Another study concludes that the compressive strength of CSEB material is anisotropic based on results from compression tests carried out on specimen configurations in which geometry effects are not reasonably isolated [14].

Like for the CSEB material, limited literature is available for other earthen materials. For adobe block, mainly because of the production process, the distribution of the dry density and compressive strength within a block is typically heterogeneous [15]. Whereas for extruded earth bricks, Aubert et al. [16] conclude that the material is anisotropic regarding its compressive strength. The authors compare the compressive strength drawn from cubic samples that were tested along different directions. For the same type of earth brick, Maillard and Aubert [17] determine that the hygrothermal properties in the direction parallel to the clay platelets are different from those in the perpendicular direction to the clay platelets. The anisotropic behavior of extruded earth bricks is attributed to the extrusion process, which potentiates the alignment of clay particles [17]. In contrast, Bui and Morel [18] conclude that rammed earth can be

regarded as isotropic in terms of compressive strength and stiffness provided that the compacted layers adhere sufficiently to one another.

This paper reports the results of an extensive experimental program and data analysis aimed to study the homogeneity and directional dependence of the compressive strength and initial stiffness of CSEBs manufactured with one-sided hydraulic compaction. The initial section of the paper describes the materials and methods used in two experimental sub-programs carried out in a representative CSEB material. In the first sub-program, the structural and chemical composition of the soil-cement matrix were characterized using microanalysis techniques. In the second sub-program, cube specimens were tested under uniaxial compression by applying the load parallel to one of the three perpendicular directions and identifying the specimen's location regarding the sourced block. The following section presents and discusses the experimental results of the microanalysis and compression tests. Microanalysis results included micrographs of the soil-cement matrix, calcium mapping, and identification of main chemical elements at different magnifications. Compression test results consisted of load-displacement curves and data of compressive strength and initial stiffness. The closing section presents a statistical analysis conducted to identify the effects of cube location and loading direction on the mechanical properties of CSEBs. To that end, the compressive strength and stiffness data's dispersion and statistical differences of their mean values and variance were analyzed. Furthermore, the appropriateness of the sample size and the statistical distribution of the data were assessed.

2.2 SIGNIFICANCE

Identifying whether CSEB material can be approximated as homogeneous or not, as well as understanding the directional dependence of its mechanical properties (i.e., isotropic or anisotropic behavior) is significant for analytical modeling purposes and interpretation of compression tests results. The results of this investigation provide experimental evidence for selecting suitable constitutive models to be used in the development of analysis and design tools. Furthermore, the extensive database of load-displacement response depicts the characteristics and variability of the material, which becomes meaningful for modeling purposes. On the other hand, compressive strength is typically related to other mechanical properties, and it is used as an indicator of quality control. Therefore, determining if the compressive strength depends on the direction is relevant in uniaxial compression test procedures, in which typically the load is applied parallel to the direction of the manufacturing compression [19]–[23].

2.3 EXPERIMENTAL PROGRAM

2.3.1 MATERIALS

The CSEB prototype used in this study was previously developed and characterized by Cuellar-Azcarate [24]**.** The blocks were manufactured with local soil sourced from Lexington (SC). Following crushing and sieving through a standard mesh No. 8, the soil was classified as either a lean clay (CL), silt (ML) or clayey sand (CS) per ASTM D2487 [25]. Figure 2.1 shows representative particle size distribution curves, determined per ASTM D422 [26], corresponding to three different batches collected at the same location. Atterberg limits and optimum moisture content were characterized per ASTM D4318 [27] and ASTM D698 [28], respectively. The salient soil properties,

summarized in Table 2.1, fall within the ranges recommended for selecting soils for earth construction [11], [29].

The prototyped block was manufactured using a commercial hydraulic press (model EPH-2008, Fernco Metal Products, Capitan, NM), which can apply a one-sided compaction pressure of 10 MPa to form units with nominal dimensions of 178 × 254 × 89 mm^3. The soil was stabilized by adding 6% of Type I ordinary Portland cement by weight proportion. The mean compressive strength, determined by testing half-block specimens, and its specific weight after a 28-day curing were 5.64±1.85 MPa and 1640±96 kg/m^3 respectively.

2.3.2 MICROANALYSIS

Scanning electron microscopy (SEM) was enlisted to visually examine the structural composition of the CSEB soil-cement matrix at the microscale (i.e., where particles smaller than 1 μm are identified) and mesoscale (i.e., where particles between 1 μm - 1 mm are identified). Furthermore, in combination with SEM, energy dispersive spectroscopy (EDS) analysis was used to characterize the chemical composition of the CSEB material. The secondary electron detector of the system (model VEGA3, TESCAN) was used for SEM and EDS microanalysis on plate-type samples, with an approximate surface of 10-mm^2, that were cut from the prototype CSEB. The samples were mounted on aluminum stubs using sticky carbon tabs and then coated twice using a gold target (Desk II Sputter Coater, Denton Vacuum). Each sample's surface was analyzed throughout at least four different areas, as illustrated in Figure 2.2. The analysis process yielded 120 micrographs (magnification ranging from 50X to 25,000X) and 42 EDS analyses. Table 2.2 summarizes the breakdown of the test matrix.

2.3.3 MECHANICAL TESTING

2.3.3.1 TEST MATRIX

Uniaxial compression load tests were carried out on 76-mm cube specimens (denoted as P1.0 in Chapter 3) saw-cut from CSEBs and stored under laboratory conditions. The purpose was to investigate the extent to which the inherent physical heterogeneity of the CSEB material affects the variability of compressive strength and stiffness as a function of location within a given block and compressive load direction (vis-à-vis the compaction pressure direction). To that end, the effect of two variables was examined independently, as illustrated in Figure 2.3. The first variable was the cube's sourced location within a given block, identified as either corner (*C*) or middle third (*M*). The second variable was the compressive load direction. Each specimen was tested by applying the load either parallel (i.e., along *Z*) or perpendicular (i.e., along *X* or *Y*) to the direction of the compaction pressure used to manufacture the sourced CSEB. The results were interpreted as a function of the location to assess the material homogeneity and the load direction to evaluate the material directional dependence.

From each sourced CSEB, two specimens were tested per loading direction (i.e., *X*, *Y*, and *Z*). Moreover, the specimen location (*C* or *M*) was considered when assigning the loading direction to guarantee the random combination of both variables. Table 2.3 summarizes the final test matrix.

2.3.3.2 TEST SETUP AND PROCEDURE

Figure 2.4 illustrates the test setup. The cubic specimens were loaded continuously in uniaxial compression up to failure using a servo-controlled hydraulic test frame of 245-kN capacity at a displacement control rate of 0.03 mm/sec (395 με/sec). The

load and displacement data were monitored using a 45-kN external load cell and the integrated displacement transducer of the test frame, respectively. Additionally, four linear displacement transducers were rigidly attached to the steel loading plates to measure vertical deformations along the perpendicular axes of the specimen. Polytetrafluoroethylene (PTFE) sheets, 0.4 mm thick, were placed between the specimens and the loading plates to minimize the effects of restraint due to friction.

2.4 Results and discussion

This session presents the experimental results of the microanalysis and compression tests. First, the structure and physical composition of the soil-cement matrix are described based on micrographs, calcium mapping, and identification of main chemical elements at different magnifications resulting from SEM and EDS microanalysis. Then, the failure mode and load-displacement response are described, followed by the discussion of compressive strength and initial stiffness results as a function of cube location and load direction. It is noted that compressive strength and stiffness data were available for 84 and 83 samples, respectively.

2.4.1 Microanalysis

Representative SEM micrographs of the structure of the CSEB soil-cement matrix at different magnifications are shown in Figure 2.5. Figure 2.5(a-b) shows a representative micrograph of the structure of the CSEB visualized at a mesoscale, in which grain-like particles (0.2 mm- to 1 mm-size) are confined by a compacted matrix of finest particles. In the micrograph shown in Figure 2.5(c) the morphology of a grain-like particle is observed in detail, as well as the discontinuities between the interface of the grain surface and the surrounding compacted finest particles. The typical porosity of the

finest soil matrix portion is illustrated by the micrograph shown in Figure 2.5(d). Across the different magnifications shown herein, it is noted that the pores are 10 μm or less in diameter and are relatively good distributed through the CSEB soil-cement matrix. A visualization of the microscale structure of the CSEB soil-cement matrix is shown in Figure 2.5(e-f), in which the characteristic flaky shape of clay particles in a variety of sizes and alignments is observed. The SEM micrographs depict how a relatively low porosity resulting from the compaction and stabilization process contributes to mitigating the heterogeneity linked to the morphology of the soil particles.

Figure 2.6 shows Calcium (Ca) mapping at different magnifications for a given sample in which a relatively uniform distribution of cement hydrates byproducts can be observed through the matrix. It is noted that the presence of Ca in the soil-cement matrix is exclusive of the formation of cement hydrates due to the stabilization [24].

The chemical composition of the CSEB soil-cement matrix was characterized by SEM and EDS analysis. A standardless quantitative analysis was used, in which the salient EDS spectra of the CSEB samples are correlated with default data, available in the analysis system, corresponding to all the chemical elements [30]. Figure 2.7 plots the weight concentration of the chemical elements identified in three different samples at different magnifications. In is noted that the results shown in Figure 2.7(a) correspond to the field of view of the micrographs shown in Figure 2.6. Major components were identified as oxygen (O), aluminum (Al), and silicon (Si), which are the main peaks of the characteristic ED spectra of the clay mineral kaolinite. Potassium (K), carbon (C), iron (Fe) and calcium (Ca) are identified in less concentration but consistently through the sample.

The microanalysis results indicated that the CSEB material has a consistent chemical composition through the matrix, and the Ca mapping provided visual evidence of the relatively uniform distribution of cement hydrates due to the stabilization.

2.4.2 Failure mode and axial load-displacement response

The cracking pattern observed in cube specimens is illustrated in Figure 2.8. The formation of cracks on the specimen's lateral sides and approximately parallel to the direction of the compression load, as shown in Figure 2.8 (a-b), indicates minimization of the effects of lateral restraining forces (i.e., by using PTFE sheets). All cubes were split into slabs towards the side surfaces Figure 2.8 (c-d) and developed a double pyramid shape towards the core Figure 2.8(e-f), indicating a triaxial stress state.

The axial load-displacement response of the CSEBs cube specimens under compression loading was observed as comparable to the non-linear stress-strain behavior described by Domone [31] for concrete. Figure 2.9 and Figure 2.10 present the load-displacement curves from all specimens differentiating them by cube location and load direction, respectively. All specimens showed linearity up to approximately 50% of the peak load.

2.4.3 Compressive strength

Table 2.4 summarizes the resulting mean and coefficient of variation (CV) of compressive strength (f_b) obtained from 84 cube specimens. The results are grouped by sourced block (e.g., B01, B02), load direction (*X*, *Y*, *Z*), and cube's location within the sourced block (*C*, *M*). The CV observed among specimens sourced from the same block ranged between 8.88 -21.23%. The mean f_b of specimens tested parallel to the compaction direction (*Z*) was approximately 90% of the mean values drawn from those

tested along the perpendicular directions (*X* and *Y*) to the manufacturing compaction. These results indicate that the higher f_b is not necessarily achieved in the direction parallel to the direction of single-sided compaction, as suggested by Gooding [6]. When the results are compared based on location, it is observed that cubes sourced from the middle third reached a higher mean f_b than the value of those sourced from the corners (approximately by 6%). The fact that corner sourced specimens yielded a lower mean f_b than the middle-third sourced ones could be associated with the non-uniform distribution of compaction within the block because of the friction between soil particles and walls of the mold [6], [32].

2.4.4 Initial tangent stiffness

Table 2.5 summarizes the results of the initial tangent stiffness, calculated as the slope of the linear response of the axial load-displacement curve, which was defined up to 50% of the maximum load. The data are presented in the same fashion as the results of f_b. For one of the specimens, no displacement data were recorded; therefore, the stiffness results were drawn from 83 cubes. The axial deformation, corresponding to the maximum load, ranged between 1.51-3.03 mm. The CV observed among cubes sourced from the same block ranged between 10.13% -22.65%. Similar to results for f_b, the mean stiffness of specimens tested parallel to the compaction direction (*Z*) was lower than the mean values drawn from those tested along the perpendicular directions (*X* and *Y*) to the manufacturing compaction. In fact, the mean stiffness of cubes tested along the *Z* direction was 84% and 91% of the mean of specimens tested along the *X* and *Y* direction, respectively. Likewise, the mean stiffness of samples sourced from the middle exceeded the corresponding values of those from the corners by approximately 4%.

The difference between mean values of f_b and initial tangent stiffness obtained along *X*, *Y* and *Z* may suggest that there is a directional dependence regarding the mechanical properties of CSEB material. Similarly, the differences between the mean results drawn from middle and corner specimens may indicate that the heterogeneity of CSEB material affects the uniformity of its mechanical properties. The significance of the differences among mean values is statistically analyzed in the following section.

2.5 Statistical analysis

The effects of location and loading direction on the mechanical properties of CSEBs were studied through statistical analysis. First, the dispersion of the experimental data was analyzed graphically by using Notched Box Plots (NBPs). Next, analysis of variance (ANOVA) and Levine's test were employed to investigate the statistical differences between the mean values and variances of f_b and initial tangent stiffness for data groups characterized by different locations and loading directions. Then, confidence intervals of the mean and standard deviation estimators were calculated and used to determine the appropriateness of the experimental sample sizes. Finally, a goodness-of-fit test was performed to identify appropriate statistical distributions for the obtained experimental data.

2.5.1 Visualization of data dispersion using Notched Box Plots

The experimental data of f_b and initial tangent stiffness are presented using NBPs, as shown in Figure 2.11 NBPs represent a convenient tool to graphically describe the statistical variability of data batches. In an NBP, the central mark represents the median; the lower and upper hinges of the box enclose the interquartile range (IQR), i.e., identify the 25^{th} and 75^{th} percentiles, respectively, of the data group. The notches indicate the 95%

confidence intervals of the median values, which can be used as rough indicators of statistical differences between medians of different data sets [33]. Extreme values are linked to the hinges through dashed lines, called whiskers, and the difference between these extreme values is referred to as range. The spacing between the different parts of the box (i.e., the median, upper hinges, lower hinges, and extreme values) signifies the degree of dispersion and skewness of data in the group [33].

For the statistical analysis, the data is classified into six different groups, following the experimental test matrix described in Table 2.3**.** Group "*A*" entails data from all specimens, groups "*C*" and "*M*" comprise data of cubes sourced from the corner and middle location respectively (location groups) and, groups "*X*", "*Y*", and "*Z*" contain the data according to the loading direction (loading direction groups).

Figure 2.11(a) plots the NBPs for f_b data. The range of the six different groups varies between 3.60 - 4.20 MPa, and their IQR varies between 1.23 - 1.96 MPa. Moreover, the CV of the different groups varies between 26.11% - 32.83%, which shows that the compressive strength groups exhibit a significant variability. It is observed that the data is roughly symmetrically distributed about the medians for all groups, except for group *Z*. The location groups' notches overlap, thus indicating that the differences between the medians of groups *C* and *M* are not statistically different. However, the notches of groups *Z* and *Y* do not overlap, hence signifying that the difference between the f_b medians of these two groups is statistically significant.

Figure 2.11(b) presents the NBPs for the initial tangent stiffness of the six batches of experimental data. The range and IQR of initial tangent stiffness groups vary between 15.8 - 17.4 kN/mm and 6.1 - 9.8 kN/mm, respectively. The CV of the different groups

varies betwwen 33.75% - 38.56%, which shows that the initial tangent stiffness groups also exhibit a significant variability. Similar to the compressive strength results, the initial tangent stiffness data for all groups are symmetrically distributed about their median. The data do not indicate statistically significant differences between the different groups since their confidence intervals overlap.

2.5.2 Comparison of means through ANOVA

One-way ANOVA was employed to identify statistical differences among sample means of different groups by comparing the sample variation among different groups with the sample variation within each group [34]. The statistical test used in this study is based on three assumptions: (1) independence of observations, (2) normal distribution of residuals, and (3) homogeneity of data variances [34], [35]. The first assumption is satisfied in the present study because the specimens from any given same block were randomly selected and assigned to the different experimental conditions (i.e., location and direction samples). In addition, although each cube is representative of a single loading direction and location, the effect of each variable was analyzed independently. The discussion of the second and third assumptions is presented in the following sections of this paper. It is noted here that the results from the ANOVA are only weakly sensitive to departures from normality [35], [36]; however, the effects of violating the variance homogeneity assumption can significant when groups sizes are not equal [35], as for the case of the location groups considered here (i.e., groups *M* and *C* with 28 and 56 specimens, respectively).

Table 2.6 provides the *p*-values corresponding to the ANOVA of both compressive strength and initial stiffness data for all groups, which exceed the critical

value of 0.05 in all cases. Thus, neither mean compressive strength nor mean initial tangent stiffness differ among the groups at a 5% of significance level. This result suggests that all groups have the same mean values for both compressive strength and initial tangent stiffness.

2.5.3 Comparison of variances through Levene's test

The Levene's test was employed in this study to investigate variance homogeneity among different data groups because of its simplicity and its insensitivity to the violation of the normality assumption [37], [38]. The variance homogeneity assumption is satisfied when the error variance across all predicted values of a dependent variable is constant [34]. In this case, the Levene's test was used to verify if the population's variances for the different groups have statistically significant differences at a significance level equal to 0.05.

Table 2.7 lists the results of the variance homogeneity test performed for the compression strength and initial tangent stiffness data among the different groups of analysis, according to the cube location within the block (*C* and *M*) and the loading direction (*X*, *Y*, and *Z*). All *p*-values obtained for both compressive strength and initial tangent stiffness are greater than 0.05, which indicates that the differences among groups' variances are not statistically significant. Therefore, the results of the Levene's test indicate that the assumption of variance homogeneity for the ANOVA is satisfied and that all groups have the same variance values for both compressive strength and initial tangent stiffness.

The combined results of ANOVA and Levine's test suggest that all data groups belong to the same population and that a single probability distribution can be used to

describe the variability of all results. Therefore, it is concluded that the compression strength and initial tangent stiffness are homogeneous and isotropic properties for earth blocks fabricated with the technique used in this paper.

2.5.4 Assessment of the suitability of sample sizes through confidence intervals of mean and standard deviation estimators

The appropriateness of the sample sizes used in this research to estimate the mean and standard deviations of the different groups was investigated through the use of confidence intervals and the coefficient of variation (CV) of the mean and standard deviation estimators. These confidence intervals provide a graphical representation of the estimated range of variation for each of the unknown population parameters (i.e., mean and standard deviation). In particular, the 95% confidence intervals used hereinafter indicate the range within which each parameter estimator is expected to be found 95% of the times that the same experiment is repeated [39], [40].

In the present study, confidence intervals and standard errors of means and standard deviation were calculated according to the approximate equations given in Harding et al. [39]. These equations are valid for sample sizes larger than or equal to 10 for the mean and 20 for the standard deviation. All sample groups considered in this research satisfy the above conditions and contain at least 28 samples. The confidence intervals for the estimators of the mean and standard deviation estimators of the compressive strength and initial tangent stiffness are shown in Figure 2.12. The CVs of the mean and standard deviation estimators of the compressive strength and initial tangent stiffness are given in Table 2.8 and Table 2.9.

The 95% confidence intervals of the means and standard deviation estimators for the different location (*C* and *M*) and loading direction (*X*, *Y*, and *Z*) groups overlap each other, which indicates that the differences among the different estimators are not statistically significant for both compression strength and initial tangent stiffness. The CVs of the mean estimator for different sample groups assume values between 3.2-6.2%, whereas the CVs of the standard deviation estimator of different sample groups assume values between 7.7%-13.7%, which is considerably high. Customarily, a CV ≤ 14% is considered acceptable for the estimation of a statistical parameter, e.g., see the recommendations given on sample sizes for concrete compressive strength given in FEMA 356 (ASCE 2000 sec. 6.3.2.4.1). Thus, the mean and standard deviation estimates obtained in this research are sufficiently accurate for all data groups.

2.5.5 Suitable statistical distribution of the experimental data

A goodness-of-fit technique was used to identify appropriate probability distributions for the compressive strength and initial tangent stiffness for the earth blocks tested in this research [42], [43]. The probability distribution of earth block's mechanical parameters is important information needed for applications such as structural reliability, probabilistic structural response, structural dynamics, uncertainty quantification, risk management, and probabilistic life-cycle cost analysis.

The Anderson-Darling (AD) test for continuous distributions with unknown parameters, in which both location (mean) and scale (variance) are estimated from the samples, was used in the present study [44], [45]. The probability distributions considered in the test are normal, lognormal, and truncated normal (with a lower truncation for values lower than zero). The AD test was selected because it is one of the

most powerful statistical tools for detecting departures from normality [46], [47] and gives more weight to the distribution tails than other equivalent tests, e.g. the Kolmogorov–Smirnov test [46].

The AD test was performed on data group *A* (i.e., on all 84 specimens), because the results of ANOVA and Levene's test indicated that the earth block material is homogeneous and isotropic for both compression strength and initial tangent stiffness. A significance level equal to 0.05 was chosen to determine if a given distribution is acceptable. The maximum difference between the empirical cumulative distribution function (CDF) and the proposed analytical CDF was compared with the critical value corresponding to the desired significance level [45]. The corresponding *p*-values were calculated for each distribution type and both compression strength and initial tangent stiffness [47]. The calculated *p*-values are reported in Table 2.10. It is observed that the *p*-values for the lognormal distribution of both compressive strength and initial tangent stiffness are less than the selected 5% significance level. Thus, the lognormal distribution can be rejected at a 5% significance level. For normal and truncated-normal distributions, the calculated *p*-values are greater than 0.05 for both compressive strength and initial tangent stiffness data. Thus, both distributions can be accepted to represent the experimental data. The two distribution have very similar *p*-values, are practically equivalent for practical purposes, and can be both to describe the variability of compressive strength and initial tangent stiffness for earth block materials fabricated using a one-sided compaction technique.

It is noted that the *p*-values for the normal distribution are slightly higher than those of the truncated normal distribution. In addition, a greater mathematical complexity

is associated with the use of a truncated normal distribution when compared with that of a normal distribution. However, the truncated normal distribution has the theoretical advantage of excluding physically unrealizable negative values for the mechanical properties considered in this study. Based on the previous consideration, the normal distribution is recommended as the most suitable distribution for applications focused on the body of the distribution (e.g., probabilistic response, stochastic dynamics), whereas the truncated normal distribution is recommended for use in applications focused on the distribution tails (e.g., structural reliability).

2.6 Conclusions

The homogeneity and directional dependence of the mechanical properties of CSEB manufactured with one-sided compaction were investigated through uniaxial compression tests and the statistical analysis of the collected experimental data. Based on the results, the following conclusions are drawn:

1. The difference between mean values of compressive strength and initial tangent stiffness obtained along *X*, *Y* and *Z* may indicate that there is directional dependence regarding the mechanical properties of CSEB material. Similarly, the differences between the mean results drawn from middle or corner specimens may indicate that the heterogeneity of CSEB material affects the uniform distribution of its mechanical properties.

2. The combined results of ANOVA and Levine's test suggest that all data groups belong to the same population and that a single probability distribution can be used to describe the variability of all results. Therefore, it is concluded that the compression

strength and initial tangent stiffness are homogeneous and isotropic properties for earth blocks fabricated with the technique used in this paper.

3. For practical purposes, the inherent heterogeneity of the soil used for manufacturing CSEBs, the variability of its properties (e.g., particle size distribution, plastic limits) and the factors associated with the block manufacturing process (e.g., internal friction, particle alignment), do not significantly affect the uniform distribution of the mechanical properties within a given block.

4. The coefficients of variation of the mean estimator and standard deviation estimator suit the acceptance criterion commonly used for statistical parameters. Therefore, the resulting coefficients of variation indicate that the sample sizes used in this investigation are suitable for obtaining an accurate mean and standard deviation estimates of the mechanical properties assessed.

5. A normal distribution is recommended for applications focused on the body of the distribution (e.g., probabilistic response, stochastic dynamics), whereas the truncated normal distribution is recommended for use in applications focused on the distribution tails (e.g., structural reliability).

2.7 REFERENCES

[1] P. J. Yttrup, “Strength of earth walls subjected to lateral wind load forces,” in *In Proc., 1st National local government engineering conference,* Adelaine, Australia, 1981, pp. 181–185.

[2] H. W. Morris, R. Walker, and T. Drupsteen, “Modern and historic earth buildings: Observations of the 4th September 2010 Darfield earthquake,” presented at the Ninth Pacific Conference on Earthquake Engineering Building an Earthquake-Resilient Society, Auckland, New Zealand, Apr. 2011. Accessed: Mar. 28, 2017. [Online]. Available: http://nzsee.org.nz/db/2011/133.pdf

[3] F. Matta, M. C. Cuéllar-Azcárate, and E. Garbin, “Earthen masonry dwelling structures for extreme wind loads,” *Eng. Struct.*, vol. 83, pp. 163–175, Jan. 2015, doi: 10.1016/j.engstruct.2014.10.043.

[4] NLIHC, “The GAP: A shortage of affordable homes,” National Low Income Housing Coalition, Washington, DC, Mar. 2017.

[5] J. R. Woetzel, S. Ram, J. Mischke, N. Garemo, and S. Sankhe, “A blueprint for addressing the global affordable housing challenge,” McKinsey Global Institute, Executive summary, 2014. [Online]. Available: www.mckinsey.com/mgi

[6] D. E. M. Gooding, “Quasi-static compression forming of stabilised soil-cement building blocks,” *Dev. Technol. Unit Work. Pap.*, no. 40, 1993.

[7] D. E. M. Gooding, “Improved processes for the production of soil-cement building blocks,” Doctoral dissertation, University of Warwick, Coventry, UK, 1994.

[8] M. Olivier and A. Mesbah, “Le matériau terre: Essai de compactage statique pour la fabrication de briques de terre compressées [The earth as a material: use of the proctor static test to optimize the making of compacted earth bricks],” *Bull Liaison Lab Ponts Chaussées,* vol. 146, pp. 37–43, 1986.

[9] R. L. Sloane, T. R. Kell, and Foundation and Materials Branch, U.S. Army Corpe Engineers, Southwest Division, Dallas, Texas, “The fabric of mechanically compacted kaolin,” in *In Proc., 14th National Conference on Clays and Clay Minerals,* Berkeley, California, Jan. 1966, pp. 289–296. doi: 10.1016/B978-0-08-011908-3.50027-X.

[10] O. M. de Oliveira, “Estudo sobre a resistência ao cisalhamento de um solo residual compactado não saturado,” Doctoral dissertation, Universidade de São Paulo, São Paulo, 2004. doi: 10.11606/T.3.2004.tde-08032005-160218.

[11] M. C. Jiménez Delgado and I. C. Guerrero, “The selection of soils for unstabilised earth building: A normative review,” *Constr. Build. Mater.*, vol. 21, no. 2, pp. 237–251, Feb. 2007, doi: 10.1016/j.conbuildmat.2005.08.006.

[12] L. Miccoli, A. Garofano, P. Fontana, and U. Müller, “Experimental testing and finite element modelling of earth block masonry,” *Eng. Struct.*, vol. 104, pp. 80–94, Dec. 2015, doi: 10.1016/j.engstruct.2015.09.020.

[13] Q.-B. Bui, J.-C. Morel, S. Hans, and N. Meunier, “Compression behavior of non-industrial materials in civil engineering by three scale experiments: the case of rammed earth,” *Mater. Struct.*, vol. 42, no. 8, pp. 1101–1116, Oct. 2009, doi: 10.1617/s11527-008-9446-y.

[14] J. R. González-López, C. A. Juárez-Alvarado, B. Ayub-Francis, and J. M. Mendoza-Rangel, “Compaction effect on the compressive strength and durability of stabilized earth blocks,” *Constr. Build. Mater.*, vol. 163, pp. 179–188, Feb. 2018, doi: 10.1016/j.conbuildmat.2017.12.074.

[15] C. H. Kouakou and J. C. Morel, “Strength and elasto-plastic properties of non-industrial building materials manufactured with clay as a natural binder,” *Appl. Clay Sci.*, vol. 44, no. 1–2, pp. 27–34, Apr. 2009, doi: 10.1016/j.clay.2008.12.019.

[16] J. E. Aubert, P. Maillard, J. C. Morel, and M. Al Rafii, “Towards a simple compressive strength test for earth bricks?,” *Mater. Struct.*, vol. 49, no. 5, pp. 1641–1654, 2016, doi: 10.1617/s11527-015-0601-y.

[17] P. Maillard and J. E. Aubert, “Effects of the anisotropy of extruded earth bricks on their hygrothermal properties,” *Constr. Build. Mater.*, vol. 63, pp. 56–61, Jul. 2014, doi: 10.1016/j.conbuildmat.2014.04.001.

[18] Q.-B. Bui and J.-C. Morel, “Assessing the anisotropy of rammed earth,” *Constr. Build. Mater.*, vol. 23, no. 9, pp. 3005–3011, Sep. 2009, doi: 10.1016/j.conbuildmat.2009.04.011.

[19] P. Walker and T. Stace, “Properties of some cement stabilised compressed earth blocks and mortars,” *Mater. Struct.*, vol. 30, no. 9, pp. 545–551, 1997.

[20] P. J. Walker, “Strength and erosion characteristics of earth blocks and earth block masonry,” *J. Mater. Civ. Eng.*, vol. 16, no. 5, pp. 497–506, Oct. 2004, doi: 10.1061/(ASCE)0899-1561(2004)16:5(497).

[21] B. V. Venkatarama Reddy, S. M. Rao, and M. K. Arum Kumar, “Characteristics of stabilized mud blocks using ash-modified soils.,” *Indian Concr. J.*, vol. 77, no. 2, pp. 903–911, 2003.

[22] Q. Piattoni, E. Quagliarini, and S. Lenci, “Experimental analysis and modelling of the mechanical behaviour of earthen bricks,” *Constr. Build. Mater.*, vol. 25, no. 4, pp. 2067–2075, Apr. 2011, doi: 10.1016/j.conbuildmat.2010.11.039.

[23] A. S. Muntohar, “Engineering characteristics of the compressed-stabilized earth brick,” *Constr. Build. Mater.*, vol. 25, no. 11, pp. 4215–4220, Nov. 2011, doi: 10.1016/j.conbuildmat.2011.04.061.

[24] M. C. Cuéllar-Azcárate, “Engineered earthen masonry structures for extreme wind loads,” Doctoral dissertation, University of South Carolina, Columbia, 2016. Accessed: Mar. 28, 2017. [Online]. Available: http://scholarcommons.sc.edu/etd/3396/?utm_source=scholarcommons.sc.edu%2Fetd%2F3396&utm_medium=PDF&utm_campaign=PDFCoverPages

[25] ASTM, *Standard practice for classification of soils for engineering purposes (Unified Soil Classification System)*. West Conshohocken, PA: ASTM, 2011.

[26] ASTM, *Standard test method for particle-size analysis of soils*. West Conshohocken, PA: ASTM, 2007.

[27] ASTM, *Standard test methods for liquid limit, plastic limit, and plasticity index of soils*. West Conshohocken, PA: ASTM, 2010.

[28] ASTM, *Standard test methods for laboratory compaction characteristics of soil using standard effort (12 400 ft-lbf/ft3 (600 kN-m/m3))*. West Conshohocken, PA: ASTM, 2007.

[29] T. Morton, *Earth masonry design and construction guidelines*. Bracknell: IHS BRE Press, 2008.

[30] D. E. Newbury and N. W. M. Ritchie, "Is Scanning Electron Microscopy/Energy Dispersive X-ray Spectrometry (SEM/EDS) Quantitative?," *Scanning*, vol. 35, no. 3, pp. 141–168, May 2013, doi: 10.1002/sca.21041.

[31] P. Domone, "Strength and failure of concrete," *Constr. Mater.*, pp. 155–168, 1994.

[32] H. Houben, V. Rigassi, and P. Garnier, *Compressed earth blocks: production equipment*, 2nd ed. Brussels: CDI and CRATerre-EAG, 1996. [Online]. Available: https://books.google.com/books?id=g1ogAAAACAAJ

[33] R. McGill, J. W. Tukey, and W. A. Larsen, "Variations of box plots," *Am. Stat.*, vol. 32, no. 1, pp. 12–16, 1978.

[34] A. Rutherford, *ANOVA and ANCOVA: a GLM approach*, 2nd ed. Hoboken, NJ: Wiley, 2011. Accessed: Apr. 28, 2017. [Online]. Available: http://library.sc.edu/catalog/off campus.html?url=http://site.ebrary.com/lib/usca/Doc?id=10595380

[35] L. M. Lix, J. C. Keselman, and H. J. Keselman, "Consequences of assumption violations revisited: a quantitative review of alternatives to the one-way analysis of variance F test," *Rev. Educ. Res.*, vol. 66, no. 4, pp. 579–619, Diciembre 1996, doi: 10.3102/00346543066004579.

[36] G. V. Glass, P. D. Peckham, and J. R. Sanders, "Consequences of failure to meet assumptions underlying the fixed effects analyses of variance and covariance," *Rev. Educ. Res.*, vol. 42, no. 3, pp. 237–288, Sep. 1972, doi: 10.3102/00346543042003237.

[37] G. V. Glass, "Testing homogeneity of variances," *Am. Educ. Res. J.*, vol. 3, no. 3, pp. 187–190, 1966.

[38] H. Levene, "Robust tests for equality of variances," in *Contributions to Probability and Statistics: essays in honor of Harold Hotelling*, vol. 1, Stanford, CA: Stanford University Press, 1960, pp. 278–292.

[39] B. Harding, C. Tremblay, and D. Cousineau, "Standard errors: A review and evaluation of standard error estimators using Monte Carlo simulations," *Quant. Methods Psychol.*, vol. 10, no. 2, pp. 107–123, 2014.

[40] D. L. Streiner, “Maintaining standards: differences between the standard deviation and standard error, and when to use each,” *Can. J. Psychiatry*, vol. 41, no. 8, pp. 498–502, 1996.

[41] ASCE, *Prestandard and commentary for the seismic rehabilitation of buildings*, vol. 1. Washington, DC: ASCE, 2000.

[42] J. D. Gibbons and S. Chakraborti, *Nonparametric statistical inference*, 6th ed. Boca Raton, FL: CRC press, 2020.

[43] D. C. Montgomery, G. C. Runger, and N. F. Hubele, *Engineering statistics*. John Wiley & Sons, 2009.

[44] R. B. D’Agostino and M. A. Stephens, *Goodness-of-fit-techniques*, vol. 68. Boca Raton, FL: CRC Press, 1986.

[45] D. Kececioglu, *Reliability & life testing handbook*, vol. 2. Lancaster, PA: DEStech Publications, Inc, 2002.

[46] M. A. Stephens, “EDF Statistics for goodness of fit and some comparisons,” *J. Am. Stat. Assoc.*, vol. 69, no. 347, pp. 730–737, 1974, doi: 10.2307/2286009.

[47] M. A. Stephens, “Tests based on EDF statistics,” in *Goodness-of-Fit Techniques*, Boca Raton, FL: CRC Press, 1986, pp. 97–193.

2.8 TABLES

Table 2.1 Soil properties

Sand content, passing No.4 sieve and retained on No. 200 sieve	21-59%
Silt content, particle size 0.074 to 0.005 mm	11-46%
Clay content, particle size smaller than 0.005 mm	22-63%
Liquid limit	37-46%
Plastic limit	14-29%
Plasticity index	10-23%
Optimum moisture content	12-18%

Table 2.2 Microanalysis test matrix

Sample	Output data	
	SEM	EDS
1	47	27
2	58	Not available
3	2	1
4	13	7
Total	120	35

Table 2.3 Text matrix

Specimen location in source CSEB		Corner (*C*)	Middle third (*M*)	Total
Load direction	*X*	18	10	28
	Y	18	10	28
	Z	20	8	28
Total		56	28	

Table 2.4 Compressive strength (f_b) results [MPa]

Block	*X*		*Y*		*Z*		Mean	% COV
	C	*M*	*C*	*M*	*C*	*M*		
B01	4.48	4.14	4.07	5.08	3.91 3.66		4.22	11.81
B02	4.79 4.62		4.39	4.51	5.49	4.38	4.70	8.88
B03	3.31	3.28	3.03	3.63	2.69 3.66		3.27	11.32
B04	4.12	4.65	3.86 3.70		3.75	3.49	3.93	10.46
B05	2.92	2.73	3.03	2.63	2.24 2.83		2.73	10.11
B06	2.41	2.38	2.30	2.15	1.89 1.87		2.17	11.07
B07	1.29	2.11	1.48 1.74		1.41	1.80	1.64	18.49
B08	2.26 3.08		3.20	3.51	2.81	2.93	2.96	14.26
B09	4.31 4.00		3.37	3.34	2.85	3.79	3.61	14.63
B10	3.26	4.73	4.38	4.31	3.51 3.86		4.01	14.02
B11	2.38 2.44		2.49	2.66	2.50	1.93	2.40	10.31
B12	4.61	4.35	4.36 4.25		2.64	5.42	4.27	21.23
B13	4.92	3.50	4.03	3.98	2.53 4.47		3.91	21.14
B14	4.74	4.04	3.62 4.34		2.57	3.63	3.83	19.57

	X	*Y*	*Z*	*C*	*M*	*All*
Mean	3.57	3.48	3.16	3.33	3.54	3.40
% CV	28.84	26.11	32.83	30.17	27.74	29.30

Table 2.5 Initial tangent stiffness results [kN/mm]

Block	*X*		*Y*		*Z*		Mean	% COV
	C	*M*	*C*	*M*	*C*	*M*		
B01	15.64	19.25	22.71	22.14	15.12 16.77		18.61	17.67
B02	21.87 18.42		15.01	19.62	15.97	19.98	18.48	13.99
B03	10.59	N.A.	10.90	12.85	8.04 9.55		10.38	17.09
B04	14.99	14.34	12.27 12.51		11.62	12.45	13.03	10.13
B05	9.55	8.46	9.81	8.43	10.57 7.76		9.10	11.54
B06	9.46	7.06	7.88	7.98	6.69 5.83		7.48	16.73
B07	6.57	6.79	5.61 5.46		6.17	5.34	5.99	10.14
B08	6.07 10.22		10.05	12.01	7.91	8.61	9.14	22.65
B09	18.03 16.14		13.81	13.45	13.05	17.55	15.34	14.27
B10	15.15	19.01	15.40	14.19	14.78 15.98		15.75	10.82
B11	10.45 11.93		11.86	9.83	8.72	7.71	10.08	16.75
B12	21.70	16.15	17.80 17.98		10.76	21.13	17.59	22.50
B13	21.28	15.70	15.87	14.56	12.35 20.80		16.76	21.18
B14	22.50	21.05	16.73 18.53		16.22	12.46	17.92	20.17

	X	*Y*	*Z*	*C*	*M*	*All*
Mean	14.38	13.40	12.14	13.13	13.63	13.30
% CV	36.84	33.75	38.56	36.53	37.32	36.62

Table 2.6 ANOVA results

	Source	sum of squares	d.o.f.	mean squared error	*F*-statistic	*p*-value
Compressive strength	By location					
	Groups	0.52	1	0.52	0.48	0.49
	Error	88.33	82	1.08		
	Total	88.85	83			
	By direction					
	Columns	2.54	2	1.27	1.29	0.28
	Error	79.93	81	0.99		
	Total	82.47	83			
Initial stiffness	By location					
	Groups	0.34	1	0.34	0.01	0.91
	Error	2086.6	81	25.76		
	Total	2086.9	82			
	By direction					
	Groups	69.81	2	34.9	1.49	0.23
	Error	1873.9	80	23.42		
	Total	1943.7	82			

Table 2.7 Levene's test results for variance homogeneity

Compressive strength, f_b				Initial stiffness			
Source	d.o.f.	Levene's statistic	*p*-value	Source	d.o.f.	Levene's statistic	*p*-value
By location							
Groups	1	0.017	0.896	Groups	1	0.003	0.956
Total	82			Total	81		
By direction							
Groups	2	0.386	0.681	Groups	2	0.758	0.472
Total	81			Total	80		

Table 2.8 CV of mean and SD of different data groups for f_b

Data group	No. of data	Mean [MPa]	SD [MPa]	Standard error [MPa]		CV	
				Mean	SD	Mean	SD
A	84	3.40	1.00	0.109	0.077	3.2%	7.7%
C	56	3.33	0.97	0.129	0.092	3.9%	9.5%
M	28	3.54	1.05	0.199	0.144	5.6%	13.7%
X	28	3.57	1.03	0.194	0.140	5.5%	13.6%
Y	28	3.48	0.91	0.172	0.124	4.9%	13.6%
Z	28	3.16	1.04	0.196	0.141	6.2%	13.6%

Table 2.9 CV of mean and SD of different data groups for initial tangent stiffness

Data group	No. of data	Mean [kN/mm]	SD [kN/mm]	Standard error [kN/mm]		CV	
				Mean	SD	Mean	SD
All	84	13.30	4.87	0.531	0.378	4.0%	7.8%
C	56	13.13	4.80	0.641	0.457	4.9%	9.5%
M	28	13.63	5.09	0.962	0.692	7.1%	13.6%
X	28	14.38	5.30	1.001	0.721	7.0%	13.6%
Y	28	13.40	4.52	0.855	0.615	6.4%	13.6%
Z	28	12.14	4.68	0.884	0.637	7.3%	13.6%

Table 2.10 *p*-values from AD test for different statistical distributions

No. of data	Normal	Truncated normal	Log Normal
Compressive strength			
84	0.155	0.154	0.002
Initial stiffness			
83	0.072	0.065	0.020

2.9 FIGURES

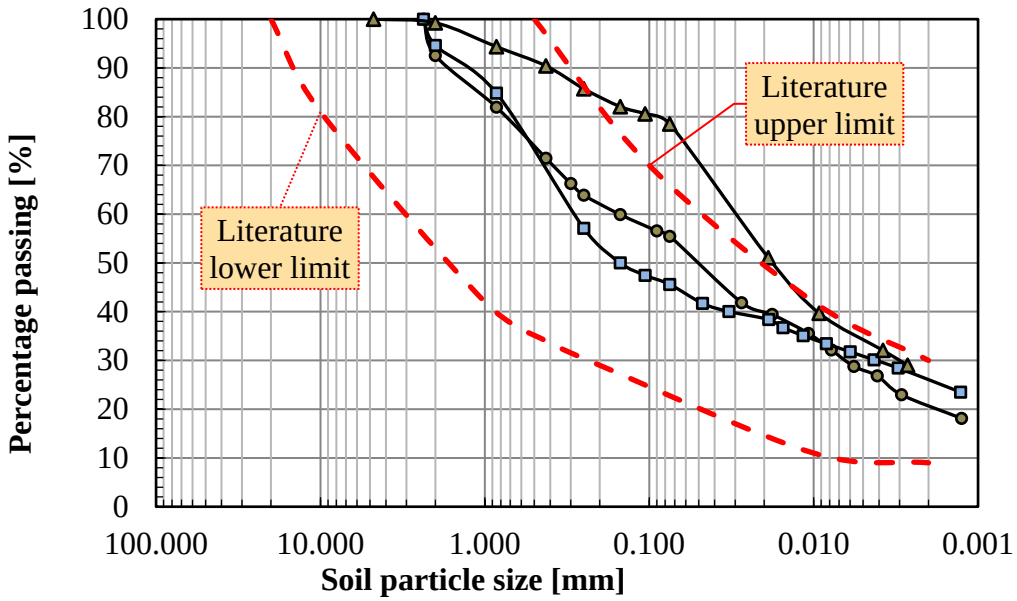

Figure 2.1 Representative particle size distributions curves of soil used to manufacture CSEBs

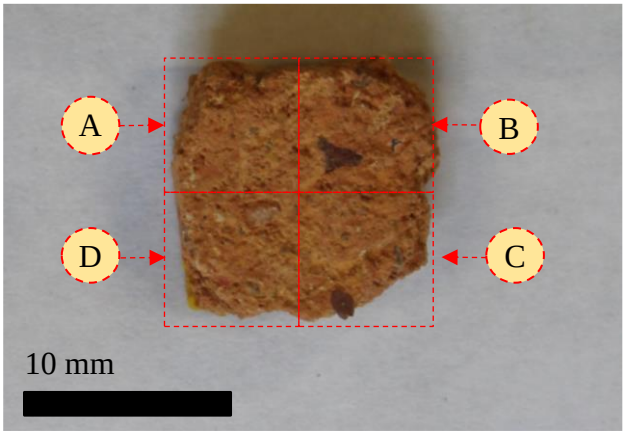

Figure 2.2 Representative CSEB plate-type sample with annotations indicating areas, A, B, C and D, in which SEM and EDS analysis were performed

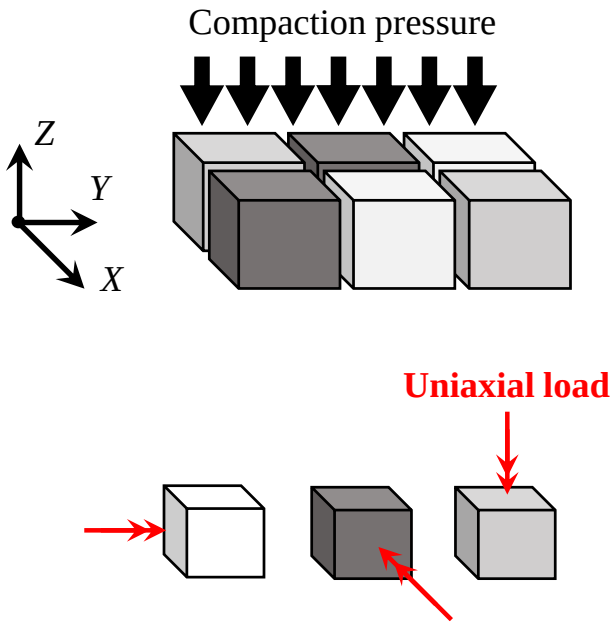

Figure 2.3 Sketch indicating cube's location and loading direction regarding compaction pressure for a given CSEB

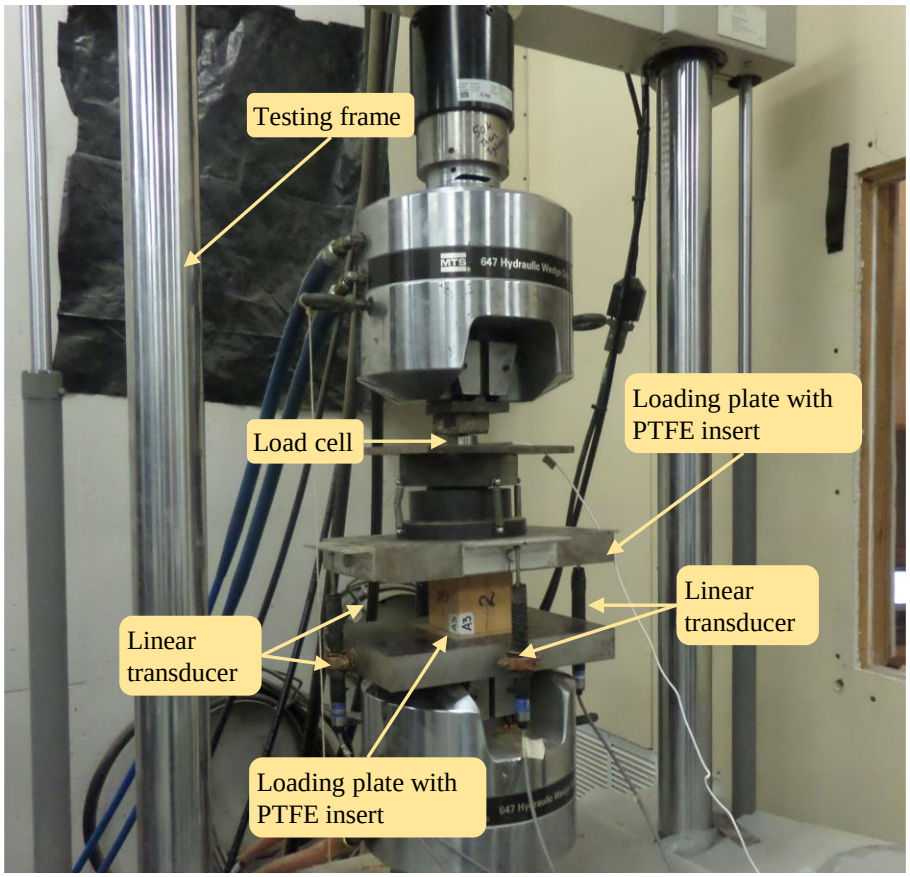

Figure 2.4 Uniaxial compression test setup

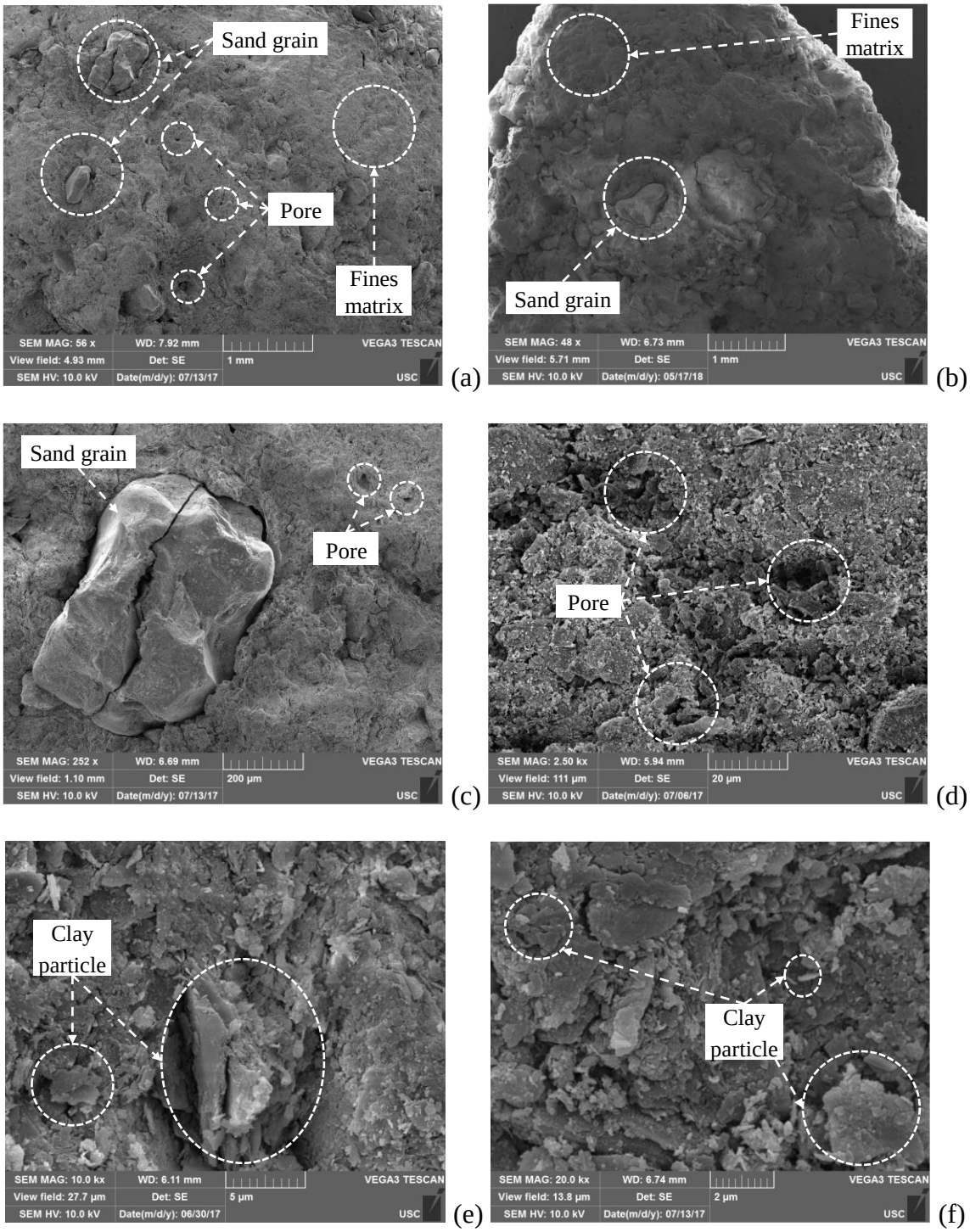

Figure 2.5 SEM images of CSEB soil-cement matrix: (a-b) different sizes and shapes of sand grains and (c) discontinuities between sand grains and clumps of finest particles observed at a mesoscale; (d) detail of pore size and pore distribution among finest particles; (e-f) different sizes and alignments of flaky shape clay particles identified at a microscale

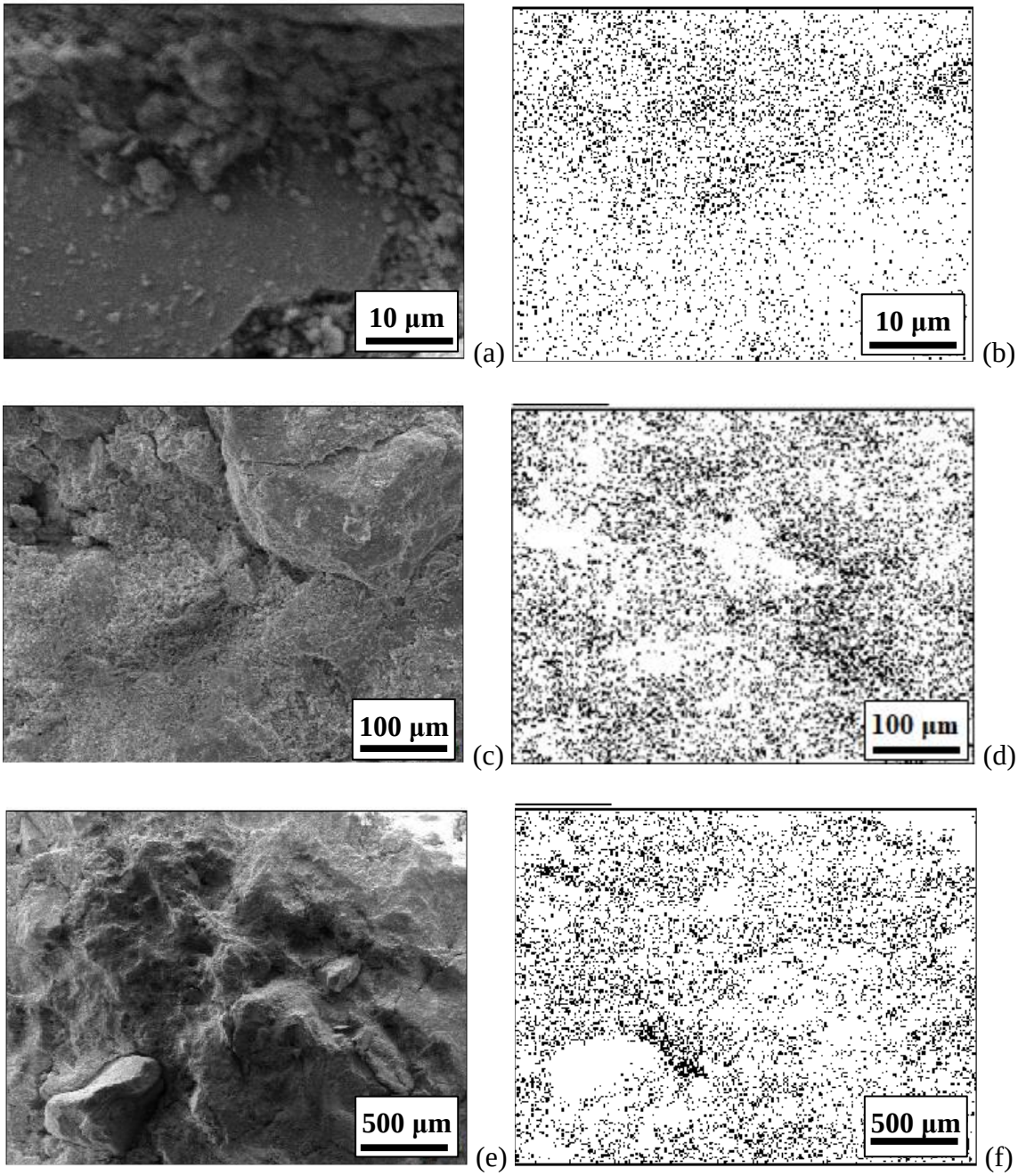

Figure 2.6 Calcium mapping of CSEB soil-cement matrix identified in sample 4 at magnification (a-b) 5000X, (c-d) 500X, and (e-f) 100X

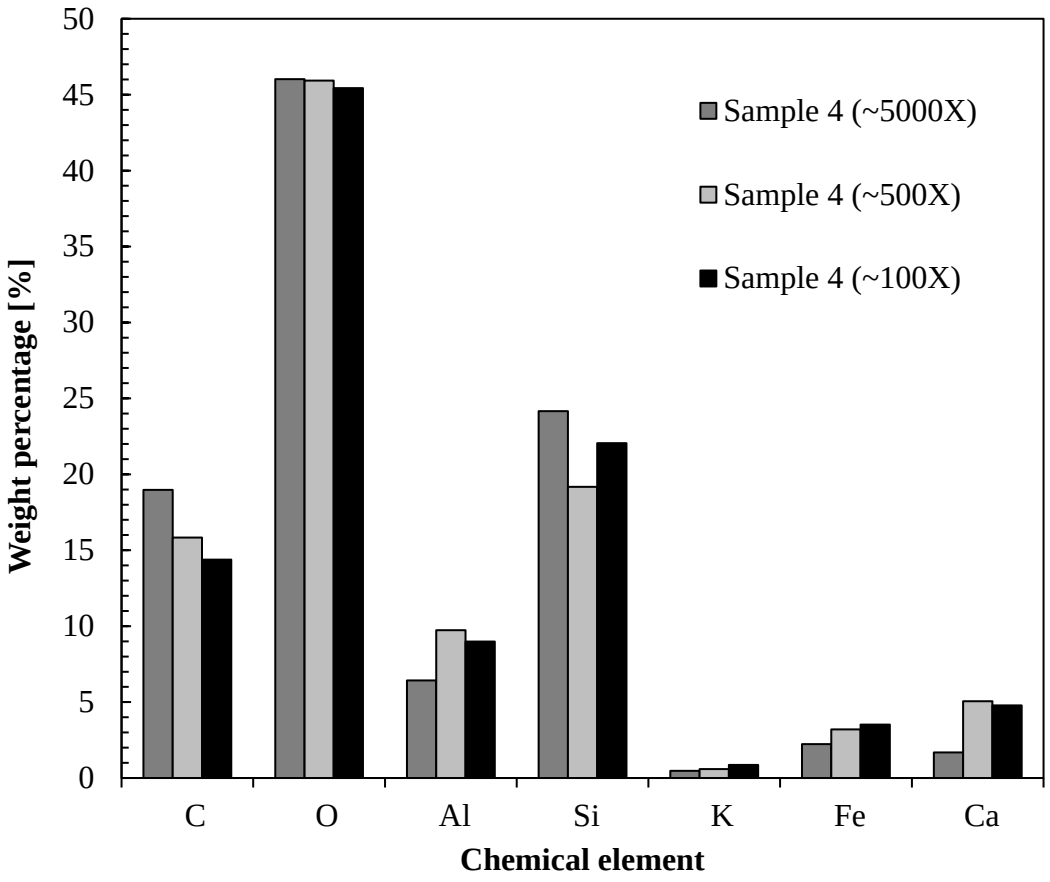

Figure 2.7 Histogram of weight percentage concentration of chemical elements identified with EDS analysis at different magnifications in sample 4

(a) (b) (c) (d) (e) (f)

Figure 2.8 Failure mode: (a-b)) vertical cracks development indicating friction minimization achieved by PTFE inserts; (c-d) sample split into slabs towards side surfaces and (e-f) double pyramid shape failure towards the core

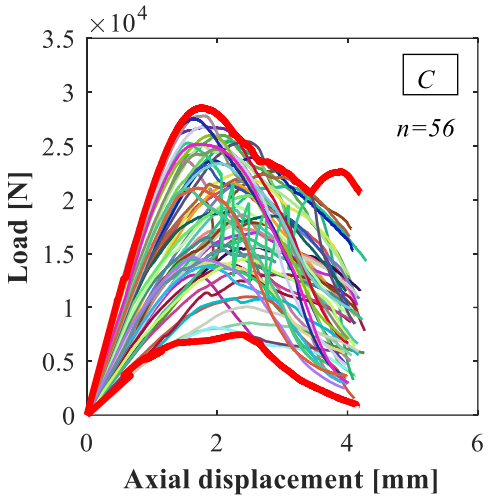

(a)

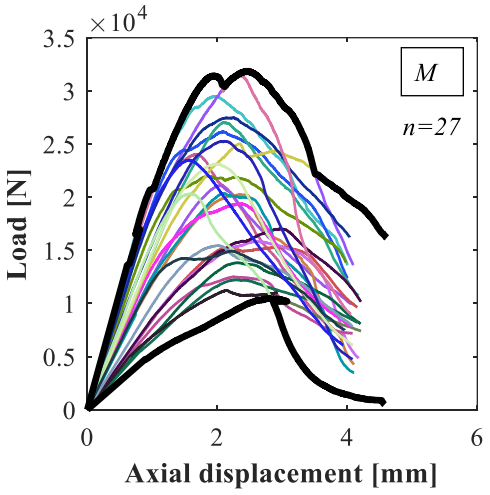

(b)

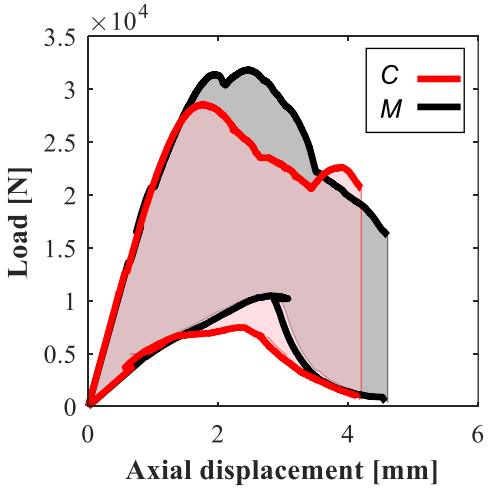

(c)

Figure 2.9 Compressive load-displacement curves from all specimens grouped by load location: (a) corner location, (b) middle location, (c) envelopes

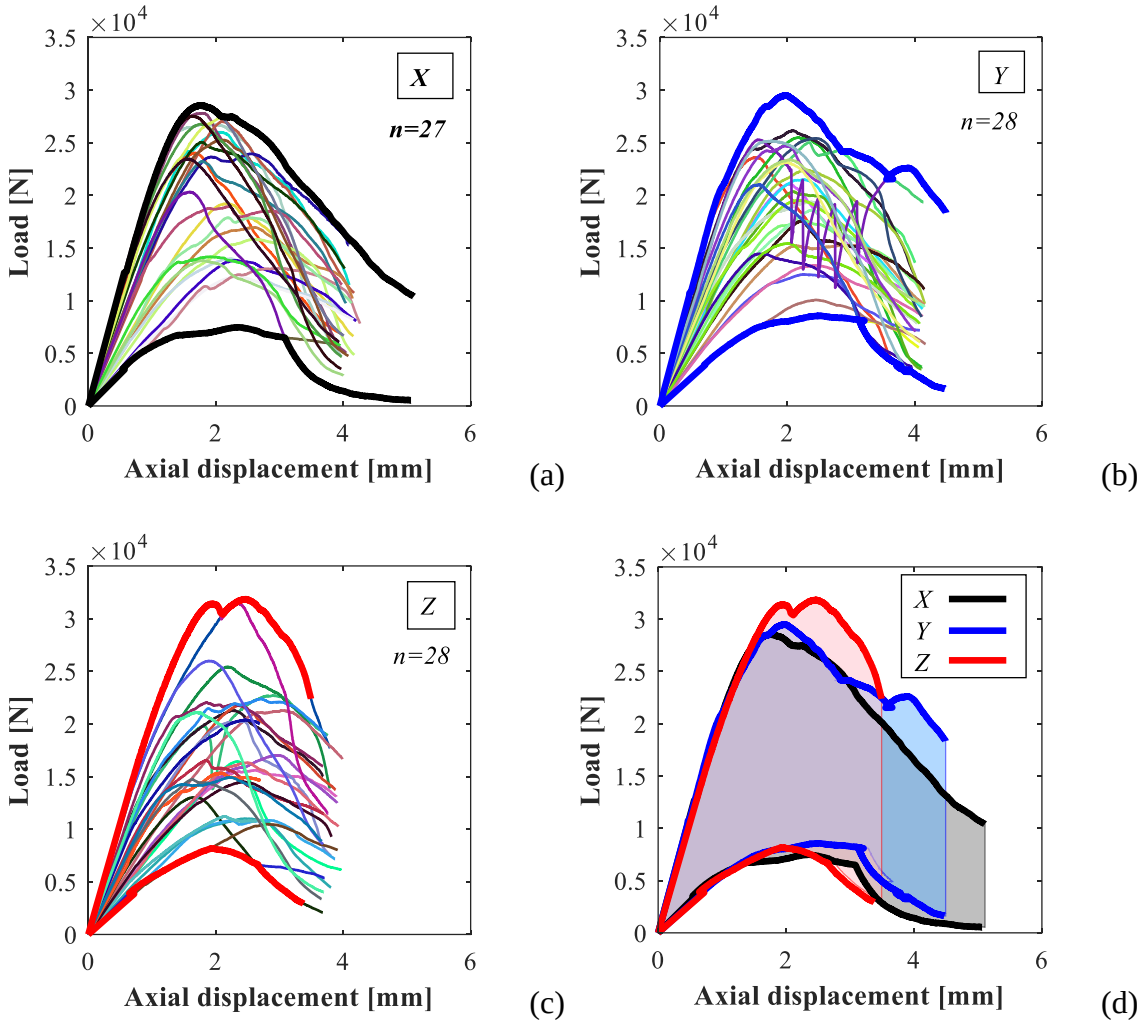

Figure 2.10 Compressive load-displacement curves from all specimens grouped by load direction: (a) *X* direction, (b) *Y* direction, (c) *Z* direction and (d) envelopes

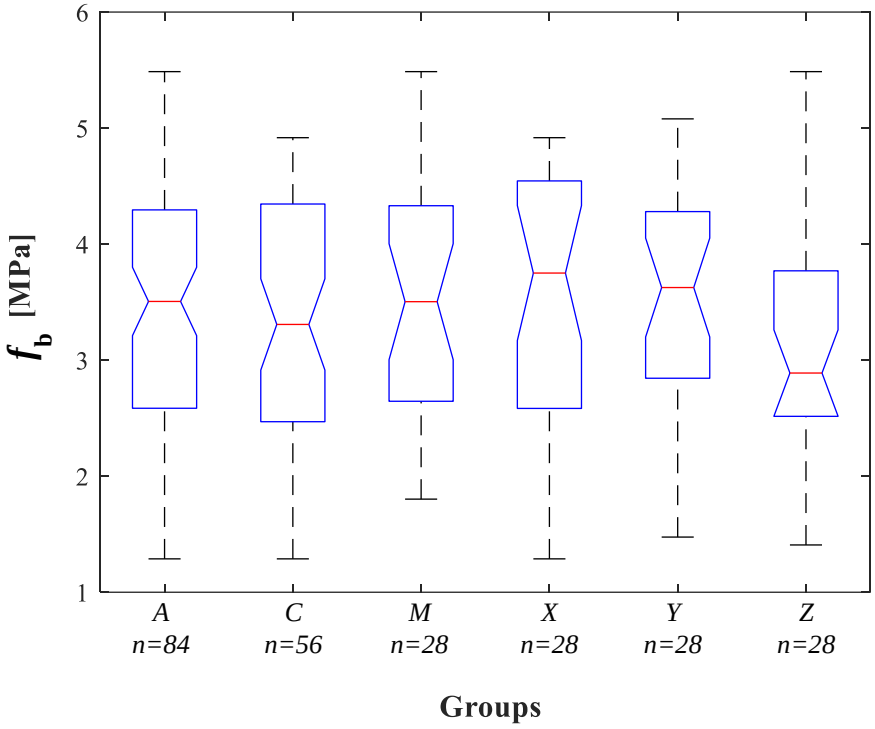

(a)

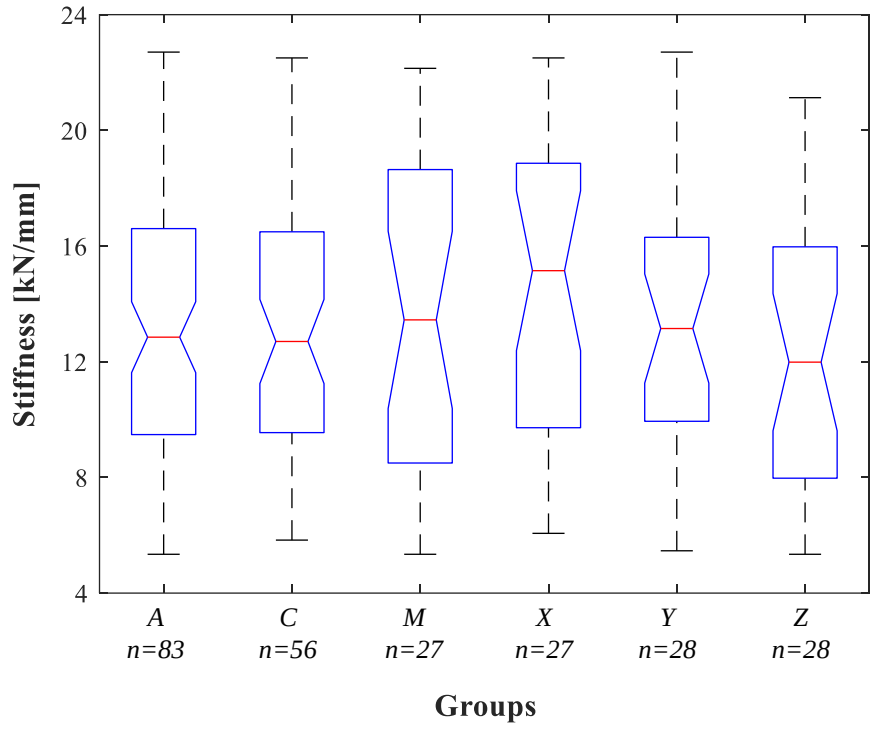

(b)

Figure 2.11 NBPs of results by data groups: (a) compressive strength; (b) stiffness

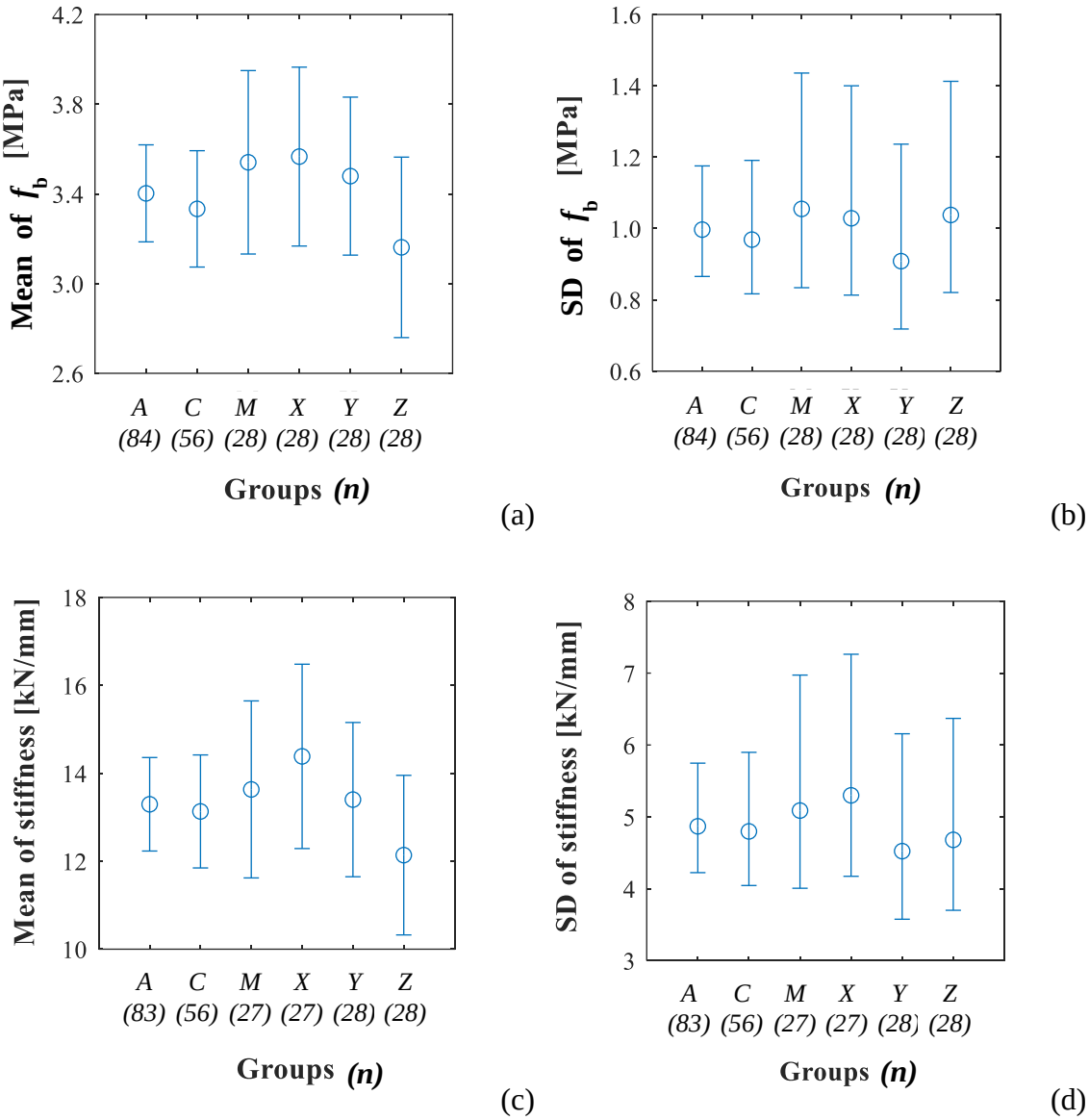

Figure 2.12 95% confidence intervals of different data groups for (a) mean of compressive strength; (b) standard deviation of compressive strength; (c) mean of stiffness; (d) standard deviation of stiffness

CHAPTER 3: COMPRESSIVE STRENGTH OF COMPRESSED EARTH BLOCK MATERIAL SPECIMENS: ASPECT RATIO, CROSS-SECTIONAL SHAPE AND FRICTION EFFECTS[2]

[2] Erika L. Rengifo-López., Nitin Kumar, Fabio Matta, and Michele Barbato. To be submitted to *ASCE Journal of Materials in Civil Engineering*.

ABSTRACT. The compressive strength of earth masonry materials, such as compressed stabilized earth blocks (CSEB), is sensitive to the specimen's aspect ratio, cross-sectional shape, and boundary conditions. However, the extent of the effect of these parameters on the compressive strength of earth masonry specimens is not fully understood yet, which restricts the definition of a well-established test method. In fact, a lack of consensus on the specimen geometry and boundary conditions is evident among testing methods specified by different earth construction standards. This aspect becomes more significant as the sustainability advantages of earth masonry prompt its use in structural applications in developed countries worldwide.

This paper reports on an experimental investigation on the compressive strength of a representative CSEB material, focusing on the effect of friction at the loading interface and specimen geometry (i.e., cross-sectional shape and aspect ratio). The prototype CSEB was manufactured with on-side hydraulic compaction using a mixture of local South Carolina soil, water, and 6% (by weight) of Type I ordinary Portland cement. Uniaxial compression tests were conducted on cylinder and prism specimens with different aspect ratios and varying friction inserts at the specimen-loading plate interface. The results were interpreted to describe the effects of the parameters in consideration on CSEB specimens' compressive strength. Furthermore, the specimen manufacturing process was included in the discussion to facilitate the interpretation of the results.

3.1 INTRODUCTION

The compressive strength of a masonry specimen is sensitive to its aspect ratio (i.e., the ratio between the larger and smaller dimension), cross-sectional shape, and boundary conditions. However, the extent of the effect of these parameters on the

compressive strength of earth masonry materials, such as CSEB, is not fully understood yet. This knowledge gap is a limitation for defining a testing methodology.

The aspect ratio effect accrues from the lateral expansion constraints produced by friction at the specimen-loading plate interface and the difference in stiffness between the loading plates and the specimen [1], as Figure 3.1 illustrates. As a result of the lateral expansion constraints, the compressive strength increases as the aspect ratio decreases. For CSEB materials, two studies examine this aspect and report experimental evidence suggesting that the strength increment becomes significant for specimens with aspect ratios lower than three [2], [3]. However, each study recommends different strength correction factors per specimen aspect ratio. The factors proposed by Heathcote and Jankulovski [2] resulted from strength data regression analysis of a CSEB material made with hydraulic compaction, 8% cement by weight proportion, and 1900 kg/m^{3}dry density. In this investigation, CSEBs with nominal dimensions of 103 × 186 × 60 mm^3 were cut to generate block-type specimens with aspect ratios ranging from 0.27 to 6.21, then oven-dried and tested in compression. On the other hand, Walker [3] concludes that correction factors derived from investigations on calcium silicate masonry bricks [4] seem appropriate to account for the aspect ratio effect observed in CSEB specimens. This investigation refers to two CSEB materials formed with a manual press and nominal dimensions of 295 × 140 × 120 mm^3, for which either pressed or cut specimens were generated for dry and saturated conditions testing. Pressed specimens were made of cement-stabilized (5% by weight) plastic soil with a cross-section of 140 × 70 mm^2 and aspect ratio ranging from 0.33 to 1.61 by inserting dividers in the mold. Cut specimens

had a cross-section of 40 × 20 mm^2 and aspect ratios ranging from 0.62 to 5.35 and were extracted from CSEBs made of cement-stabilized (10% by weight) non-plastic soil.

The literature on the cross-sectional shape effect on the compressive strength of CSEB or similar materials is minimal, and the understanding of the extent of this effect is unclear. Studies on compressive strength behavior and testing methods typically disregard the effect of this parameter. For instance, compression testing methods for CSEBs are assessed in [5] using block and cylinder specimens without considering the cross-sectional shape in interpreting the results. In this case, a blended soil, stabilized with 5% cement by weight proportion, was used. Block specimens were made using a manual press, having different dimensions with aspect ratios ranging from 0.32 to 0.88. Cylinder specimens had nominal dimensions of 101 × 117 mm^2 (height × diameter) and were formed by following the Proctor test compaction method. On the other hand, the testing methods for earth wall materials provided by the Australian earth building handbook [6] and New Zealand standard [7] apply to block type and cylindrical specimens, with no specific provisions per differences in cross-sectional shape. Only one study, reported in [8] on unstabilized compressed earth blocks, presents experimental evidence describing the effect of cross-sectional shape as negligible. This description agrees with the behavior exhibited by concrete specimens [9]. Lan et al. [8] compare compressive strength data from pressed specimens corresponding to 100-mm cubes and 100-mm diameter × 100-mm height cylinders. The average strength of specimens with circular cross-sections exceeded the corresponding value of those with a square shape by 2% to 8%. These differences are ascribed to the distribution of stresses through the cross-section. With a cylindrical specimen, the case of uniform confining stress (i.e., $\sigma_2 = \sigma_3$)

can be approximated. In contrast, the unrestrained corners of prisms result in non-uniform stress distribution [9], [10], [1].

Concerning boundary conditions used to determine the compressive strength of earth masonry materials, different configurations are adopted to provide uniform load distribution and minimize platen lateral restraints. The boundary condition configurations found in the literature provide a combined effect of stiffness mismatch and friction, but there is no reference examining the isolated impact of friction only. Such configurations include sandwiching specimens between plywood sheets [2], [3], [5], [11], combining greased neoprene and Teflon inserts at the loading interface [12], [13] or using bare loading plates [8], [14]. Particularly for CSEBs, Ruiz et al. [15] observed that the lateral restraint effects exerted by inserts of plywood and bare plates are comparable to each other and both higher than the effect exerted by rubber inserts. The related material was made with 6% cement by weight proportion, nominal dimensions of 290 × 140 × 70 mm^3, and 2,055 kg/m^3 dry density. The mean compressive strength of specimens tested with either 3-mm plywood or bare plates was approximately 80% higher than the value corresponding to 3-mm rubber inserts tests. The authors attribute these results to the rubber's effectiveness in reducing friction at the loading interface; however, it is reasonable to consider the effect of stiffness mismatch at the loading interface as a more plausible explanation.

This paper presents the results of an experimental investigation on the compressive strength of a representative CSEB material, focusing on the effect of friction at the loading interface and specimen geometry. The first section describes the experimental plan to collect compressive strength data. The plan entails (1) experimental

characterization of coefficients of friction (CoF) to select inserts representative of low- and high-friction conditions, and (2) uniaxial compression tests on cylinder and prism specimens with different aspects ratios and friction inserts. The second section presents the results, followed by a discussion on the observed effects of the parameters under consideration.

3.2 SIGNIFICANCE

The lack of a well-established specimen geometry and testing method to characterize the compressive strength of earth masonry units reflects the limited understanding of the influence of specimen geometry and boundary conditions. This research contributes to filling the gap concerning the effect of friction and specimen aspect ratio and cross-sectional shape on the compressive strength of a representative CSEB material.

The uniaxial compression test where the load is applied parallel to the compaction direction is the procedure adopted by earthen construction manuals and standards [6], [16]–[19]. However, as shown in Table 3.1, the corresponding testing methods present significant differences concerning specimen geometry, boundary condition, and strength definition. Testing earth masonry units following this configuration generally results in aspect ratios lower than 0.8 due to their manufactured dimensions. However, only the New Zealand standard [7], Australian handbook [6], and Spanish standard [16] specify correction factors to account for the aspect ratio effect; still, there is no consensus among them. For instance, for a specimen with an aspect ratio of 1.0, the correction factor specified in [7] is 0.88, whereas it is 0.70 in [6]. On the other hand, the method outlined in [16] refers to the European standard for masonry unis [20], which for the case of

aspect ratio 1.0, provides factors ranging from 0.85 to 1.15, depending on the size of the specimen. It is noted that the factors in [6] are identical to those specified by the Australian standard for masonry units [21], whose provisions rely on correlations derived from investigations conducted on calcium silicate masonry bricks [4]. Interestingly, none of the standards consider the effect of the cross-sectional shape despite the lack of evidence describing its extent.

The lack of consensus in testing methodologies is also observed among investigations on the relationship of the compressive strength of CSEB with soil properties (i.e., gradation, clay type, plasticity), cement content, density, water content, and compaction method. For instance, Olivier and Mesbah [22] used pressed cylinders sandwiched between greased neoprene and Teflon inserts, while Walker [11], [3] tested block-type specimens in saturated and dry conditions between plywood sheets. In other cases, cubes [23] or whole blocks, lengthwise loaded, [14] have been tested between bare loading plates without any capping.

Given the missing evidence to understand the effects of specimen geometry on the compressive strength of earth masonry materials, existing standards refer to methods specified for materials from which a comparable mechanical response is expected, such as concrete and clay masonry. Furthermore, related provisions are scattered concerning potentially important parameters, thus imposing limitations to interpret and compare results among methods.

3.3 METHODOLOGY

3.3.1 MATERIALS

3.3.1.1 SOIL

The CSEB material used in this investigation was manufactured with 13 batches of soil collected from a construction lot located in Lexington (SC). Each soil batch was classified in conformance with ASTM D2487 [24] as either a lean clay (CL), clayey sand (CS), or silt (ML). Figure 3.2 presents representative results from the particle size distribution, Atterberg limits and optimum moisture content determined per ASTM D6913 [25] and D7928 [26], ASTM D4318 [27] and ASTM D698 [28], respectively. The soil sand content varied from 14% to 59%, and fines content ranged between 41% and 86%. Furthermore, the liquid limit (LL) and plastic limit (PL) ranges were 30%-49% and 10%-23%, respectively. The results served to verify that the soil properties were in good agreement with gradation (e.g., 20%-70% fines) and plasticity ranges (e.g., 16%-28% LL) that have been identified to be suitable for earth construction materials [29], [30].

3.3.1.2 CESB MATERIAL

The nominal dimensions of the CSEB material were 254 × 178 × 89 mm^3, and the average dry density, estimated from 16 randomly selected blocks, was 1640±96 kg/m^3. The manufacturing process, illustrated in Figure 3.3, started by crushing the raw soil using a rotating concrete mixer containing 12 steel spheres (48-mm diameter), followed by sieving through a standard mesh No. 8. Once prepared, the soil was mixed manually with 6% (by weight) Type I ordinary Portland cement and water until attaining a uniform consistency. The optimal moisture content of each soil batch, ranging between 12% to 22%, and determined per ASTM D698 [31], was used as a benchmark to proportion the

water for wet mixing. the final moisture content of the soil-cement mix was adjusted based on the drop test results [6] performed per production batch as mixing. The CSEBs were formed using a commercial hydraulic press (model EPH-2008, Fernco Metal Products, Capitan, NM), applying one-sided compaction pressure of 10 MPa. Finally, the curing was completed indoors and away from sun exposure for a total of 28 days, from which the first 14 days the CSEBs were wrapped in plastic.

3.3.2 FRICTION CHARACTERIZATION

The CoF between the CSEB surface and different inserts representing low- and high- friction conditions was experimentally characterized. The purpose was to estimate the friction levels at the specimen-loading platen interface and select two inserts with statistically significant different CoF. The procedures outlined by ASTM G115 [32] and ASTM D1894 [33] were followed to design the experimental setup shown in *Figure 3.4*.

The CoF was defined as the static friction coefficient (μ_s), determined by (1), where F is the friction force (pulling force), and N is the force normal to the surface of interest. This definition corresponds to Coulomb friction which states that the ratio of the friction force to the normal force is constant and independent of the area in contact [34].

$$\mu_s = \frac{F}{N} \tag{1}$$

The test setup included 0.4-mm thick polytetrafluoroethylene (PTFE) sheets and sandpaper (60- and 220-grit) sheets as representative low- and high-friction inserts, respectively. Additionally, bare steel plates, both polished and non-polished, were considered. The specimens were cut from whole CSEBs into nominal dimensions of 76 × 76 × 89 mm^3 and had an average weight of 9 N. The procedure to determine each CoF consisted of three trials with different normal forces, N. The first trial was performed by

considering the specimen's self-weight only and the second and third ones by superimposing a standard slotted weight of 4.5 N and 8.9 N, respectively. This procedure was repeated twice using two different faces of the same specimen. Since there were three specimens per interface, the procedure yielded 18 replicates per CoF, thus exceeding the minimum of 10 recommended in [32].

3.3.3 Mechanical testing

3.3.3.1 Test matrix

The test matrix, listed in Table 3.2, was designed to investigate the effect of friction at the loading interface, aspect ratio, and cross-sectional shape on the compressive strength of CSEB specimens. The CSEB's nominal dimensions limited the diameter of the cylinders and minor dimensions of the prisms. Furthermore, the specimens intended to assess the effect of friction (i.e., P1.2 and P1.2S) were selected having an aspect ratio of 1.2 to trigger the confinement exerted by the two inserts.

3.3.3.2 Specimen manufacturing

Figure 3.5 illustrates the process followed in manufacturing the different CSEB specimens. A brick diamond saw was used to cut whole CSEBs into prism specimens by applying one to five cutting planes and generating the desired aspect ratios. Cylinder specimens came from cores extracted continuously along the width, length, or height of CSEBs using the same drill. Then, one to two cutting planes were made perpendicular to the longitudinal axis of each core to generate different aspect ratios. The potential abrasion extent introduced to the specimens due to the drilling and cutting involved in their manufacturing is illustrated in Figure 3.6. For cylinder specimens, the drilling causes abrasion of the perimeter, and the cutting, used to generate different aspect ratios,

introduces abrasion to the surface at the cylinder bases. In the case of prism specimens, the extent of surface abrasion is limited to the number of cut surfaces.

3.3.3.3 SETUP AND PROTOCOL

Quasi-static uniaxial compression tests were carried out on the CSEB specimens listed in Table 3.2. All specimens were tested up to failure using a servo-hydraulic frame (model 810, MTS Systems Corporation, Eden Prairie, MN). For specimens C0.5, C1.0, C2.0, P1., P1.2, and P2.0, the force was measured using a 98-kN load cell. For specimens P0.7, the load cell capacity was 445 kN. The loading rate is indicated in Table 3.2 for each specimen.

3.4 RESULTS AND DISCUSSION

3.4.1 FRICTION CHARACTERIZATION

Table 3.3 summarizes the CoF's mean, standard deviation (SD), and coefficient of variation (CV) for the five interfaces in consideration. The results indicate that the level of friction at the interfaces CSEB-PTFE, CSEB-polished steel, and CSEB-not polished steel are comparable between each other. For repeatability reasons, the PTFE insert was selected to represent a low-friction condition, with an associated mean CoF of 0.49±0.12. On the other hand, the sandpaper grit-60 insert, with a mean CoF of 0.85±0.06, was selected to represent a high-friction condition.

One-way ANOVA was conducted to quantify the statistical significance of the difference between the mean CoF values of the selected inserts. Table 3.4 summarizes the related results. The *p*-value is far below the cutoff value of 0.05, indicating that the mean CoF associated with the PTFE and sandpaper grit-60 inserts differ from each other at a 5% of significance level.

The outcomes of the friction characterization show that the selected inserts for compression testing can reasonably simulate two substantially different friction conditions at the specimen-loading platen interface, as initially intended.

3.4.2 FRICTION EFFECT ON COMPRESSIVE STRENGTH

Figure 3.7 presents the compressive strength (f_b) results as a function of the CoF at the specimen-loading platen interface, where the square marks indicate the mean, and the error bars indicate the standard deviation. The mean f_b from specimens tested with the high-friction insert (i.e., P1.2S) exceeded the value from those tested with the low-friction insert (i.e., P1.2), as expected due to the lateral restraints associated with each friction level. The results show that an increment of 68% in the mean CoF at the specimen-loading platen interface increases by 13% the mean f_b of CSEB prisms with an aspect ratio of 1.2. The statistical significance of such difference was identified by conducting a One-way ANOVA. Table 3.5 summarizes the outcome, where it is observed that the *p*-value exceeded the 0.05 threshold, indicating that the mean f_b of specimens tested with high- and low-friction do not differ from each other at a 5% of significance level.

The results indicate that the CoFs associated with low- and high- friction inserts representative of those that one could use in a laboratory setting (e.g., higher than 0.37) exert a negligible change in the f_b of CSEB specimens. Similar behavior to the one inferred before is observed in results from numerical simulations of compression tests in 150-mm concrete cubes reported in [35]. In this investigation, Indelicato and Paggi [35] find that the compressive strength-friction relation is nearly linear up to a CoF of 0.2.

Beyond that point, the strength decays at a higher rate and then approximates an asymptote, exhibiting negligible changes in the compressive strength.

On the other hand, from a practical standpoint, the results describe the limitation of using only low-friction inserts (e.g., PTFE sheets) to generate a sufficiently low friction level at the contact surface with the CSEB, such that the lateral restraint effect on the compressive strength can be minimized. This observation agrees with compressive strength results from an extruded earth material reported in [36], where cube specimens tested between 2-mm PTFE sheets and between bare plates yielded comparable mean values, highlighting the negligible effect of the low-friction inserts. It is noted that combining low-friction inserts with lubricants or using highly deformable insert materials, such as rubber, are configurations effective in reducing lateral restraining effects on CSEB specimens or similar earthen material [13], [15].

3.4.3 Geometry effects on compressive strength

Figure 3.8 summarizes the f_b results of cylinder and prism specimens with different aspect ratios tested with PTFE inserts. In Figure 3.8, the markers (square and circle) indicate the mean, and the error bars indicate the standard deviation. The data labels note the specimen identification with the associated mean value and the number of data points, *n*, indicated within parentheses.

3.4.3.1 Cross-sectional shape

The effect of the cross-sectional shape is assessed by comparing P2.0 and C2.0 data sets. These specimen types are selected for having comparable sizes and aspect ratios; thus, it is assumed that the influence of such parameters is reasonably isolated and that the results primarily describe the cross-sectional shape effect.

The mean f_b of specimens with a rectangular cross-section (i.e., P2.0) was 3.32±0.67, and the value of those with a circular cross-section (i.e., C2.0) was 3.09±0.79. This result might appear counterintuitive to the expected behavior based on the distribution of stresses through a circular and rectangular cross-section. A cylinder should attain a higher strength than a prism because the confining stresses (i.e., $\sigma_2 = \sigma_3$) can be approximated as uniform across its circular cross-section [10], [1]. In contrast, a non-uniform stress distribution results from the unrestraint corners of a square or rectangular cross-section [9]. This behavior is observed in experimental evidence reported for molded specimens made of stabilized rammed earth [13] and an unstabilized earth block material [8]. Ciancio and Gibbings [13] refer to compression test results from 100-mm diameter cylinder specimens and 100-mm base prism specimens with aspect ratios ranging from 0.7 to 2.0. Unconfined compressive strength data were measured by testing the specimens between 4.5-mm thick PTFE sheets with a layer of grease. The results indicate that the mean strength from cylinders was 16% higher than the strength from prisms. Similarly, [8] informs compressive strength data showing that the mean value determined with 100-mm diameter × 100-mm height cylinders exceed the value measured with 100-mm cubes by 2% to 8%. A possible explanation for the resulting higher mean strength from specimens P2.0 is the potential strength impairment caused by drilling or cutting, which may have counteracted the cross-sectional shape effect if any. This aspect is discussed in detail after discussing the results in terms of aspect ratio.

The results showed that the difference between the average f_b of CSEB prisms and cylinders with comparable size, aspect ratio, and tested between PTFE inserts does not exceed 9%. From the comparison of strength ranges estimated from specimens C2.0 and

P2.0, it is inferred that both specimens yield comparable results; thus, the cross-sectional shape effect on the compressive strength can be regarded as negligible.

3.4.3.2 ASPECT RATIO

The trend observed within the data of P0.7, P1.2, and P2.0 corresponds to the expected aspect ratio effect, exhibiting a progressive and consistent strength decay as the aspect ratio increases. The mean f_b of P0.7 and P1.2 exceeded P2.0 by 70% and 30%, respectively. Instead, the mean f_b of P1.0 specimens dropped with respect to the trend of the data set, with a mean value lower than P1.2 and comparable to P2.0 (i.e., P1.0-to-P2.0 ratio of 1.03). Similar to prisms, within the cylinders data set, the f_b decay is evident for C2.0 compared to C0.5, but such an effect is unclear compared to C1.0. The mean f_b of C0.5 was 50% higher than the mean value corresponding to C2.0, whereas C1.0 was 3% lower than C2.0.

The results indicate that the aspect ratio of CSEB specimens significantly affects the compressive strength. The compressive strength decreases as the aspect ratio increases due to the minimization of platen restraining effects, and this effect becomes clear for aspect ratios higher than one. Furthermore, the unclear aspect ratio effect observed in specimens C1.0 and P1.0 poses a question regarding the potential of manufacturing processes for influencing the strength of CSEB specimens. Hence, the specimen manufacturing process is discussed in detail in the following section to facilitate a completion of interpretation of the results and draw conclusions.

3.4.4 SPECIMEN MANUFACTURING PROCESS

The specimen manufacturing process, described in the methodology section and illustrated in Figure 3.5 and Figure 3.6, constitutes a plausible explanation for the

inconsistency observed in the results from P1.0 and C1.0. As the affected surface depth could be assumed as constant, the extent of any associated strength impairment would be inversely proportional to the length of the dimension perpendicular to the cut surface. Thus, the strength results from specimens with the highest number of cut surfaces and the lowest aspect ratios are more likely to be significantly affected. This inference can be justified by examining the correlation between the results' dispersion with the cutting extent associated with each specimen.

Table 3.6 relates the compressive strength coefficient of variation (CV) with the number of saw-cut surfaces of each specimen type. It is identified that the data sets associated to the least number of saw-cut surfaces exhibited the lowest variability. For instance, prisms for which three or fewer surfaces were saw-cut (i.e., P2.0, P1.2, and P0.7) had a CV ranging from 15% to 18%, whereas P1.0, for which more than three surfaces were saw-cut, resulted in a 29% CV. Likewise, the drilling and cutting used for cylinder specimens appear to connect with the relatively high dispersion observed in their data sets, ranging from 25% to 34% CV. This observation agrees with dispersion data reported in investigations conducted with comparable earthen materials for which cut specimens resulted in a higher CV and lower strength than molded counterparts [37], [38], [36], [15], [13].

The description of the procedure followed to manufacture the CSEB specimens included in the test matrix (Table 3.2) provides an insight into its effect on the compressive strength. From the results it is inferred that the surface abrasion, produced by cutting and or drilling, may introduce micro-cracks in the specimen. Such micro-cracking affects the consistency of the specimen strength, resulting in increased

variability and possibly strength impairment. This effect is reduced as the specimen aspect ratio increases and cutting involved in the specimen preparation is minimized. Furthermore, the cross-sectional shape assessment results can be further explained by the influence of the manufacturing process on strength. It is reasonable to assume that specimens P2.0 resulted in higher compressive strength than C2.0 due to the smaller extent of cutting involved in its manufacturing. Therefore, the related strength impairment might have counteracted the cross-sectional shape effect, if any.

3.5 CONCLUSIONS

Based on the results obtained for the representative CSEB material investigated, the following conclusions are drawn:

1. There is a negligible difference between the effect of using either low- or high-friction inserts at the loading interface, in a uniaxial compression test, on the compressive strength of CSEB specimens. The experimental results indicate that the order of magnitude of the CoF developed between the CSEB material surface and inserts of either PTFE or sandpaper (i.e., CoF higher than 0.37) pertains to a range in which the relation between friction and compressive strength approaches an asymptote.

2. The use of low friction inserts only, such as PTFE sheets, has limited effectiveness in reducing friction at the loading interface of CSEB specimens in a compression test. The friction characterization results describe the practical limitation imposed by the CSEB material texture to attain a relatively low friction coefficient when in contact with a smooth surface. For that purpose, the interface preparation should include additional steps (e.g., plaster caping, lubrication or highly deformable materials).

3. The cross-sectional shape has a negligible effect on the compressive strength of CSEB specimens. CSEB prisms and cylinders with comparable size and aspect ratio yield comparable compressive strength results.

4. In uniaxial compression tests, the CSEB specimens' aspect ratio (i.e., minor dimension-to-height ratio) has a significant effect on the resulting compressive strength. The compressive strength decreases as the aspect ratio increases due to the minimization of platen restraining effects, and such effect becomes clear for aspect ratios higher than one.

5. The extent of cutting to manufacture CSEB laboratory specimens affects uniaxial compression tests results. The surface abrasion, caused by cutting and or drilling used to manufacture prism and cylinder specimens, increases the test results' variability and impair, to some extent, the specimen's strength. This effect is mitigated as the specimen aspect ratio increases and cutting involved in its manufacturing is minimized.

6. Prisms and cylinders with an aspect ratio of 2.0 are suitable configurations to characterize the compressive strength of CSEB materials. Using specimens with an aspect ratio of 2.0 provides minimization of platen restraining and manufacturing effects on the compressive strength. In contrast, for cut CSEB specimens with an aspect ratio equal to or lower than 1.0, the interplay between the extent of strength increments due to platen restraining effect and the extent of strength impairment due to manufacturing effect is unclear.

7. When using CSEB specimens extracted from whole blocks to characterize the compressive strength of the material, it is recommended to opt for prisms with an aspect ratio of 2.0 and minimize the number of cut surfaces to manufacture the specimens.

When practical constraints oblige extracting drilled cores (e.g., in existing structures), it is recommended to use specimens with an aspect ratio near two.

3.6 REFERENCES

[1] P. Domone, "Strength and failure of concrete," *Constr. Mater.*, pp. 155–168, 1994.

[2] K. A. Heathcote and E. Jankulovski, "Aspect ratio correction factors for soilcrete blocks," *Trans. Inst. Eng. Aust. Civ. Eng.*, vol. 34, no. 4, pp. 309–312, 1992.

[3] P. Walker, "Characteristics of pressed earth blocks in compression," in *Proceedings of the 11th international brick/block masonry conference, Shanghai, China*, Shanghai, China, 1997, pp. 14–16.

[4] A. W. Page and R. Marshall, "The influence of brick and brickwork prism aspect ratio on the evaluation of compressive strength," in *Proc., 7th International Brick Masonry Conference*, Melbourne, Australia, 1985, vol. 1, pp. 653–664.

[5] P. Walker, "Strength and durability testing of earth blocks," in *Proceedings of the 6th international seminar on Structural Masonry for developing countries*, 2000, pp. 110–118.

[6] P. Walker and Standards Australia, *The Australian earth building handbook*. Australia: Standards Australia International, 2002.

[7] NZS, *NZS 4298: Materials and construction for earth buildings*. Wellington, N.Z.: Standards New Zealand, 2020.

[8] G. Lan, Y. Wang, and S. Chao, "Influences of specimen geometry and loading rate on compressive strength of unstabilized compacted earth block," *Adv. Mater. Sci. Eng.*, pp. 1–10, Jul. 2018, doi: 10.1155/2018/5034256.

[9] H. F. Gonnerman, "Effect of size and shape of test specimen on compressive strength of concrete," in *Procedings of ASTM*, 1925, vol. 25, pp. 237–250.

[10] A. M. Neville, *Properties of concrete*. New York, Wiley, 1963. [Online]. Available: http://hdl.handle.net/2027/mdp.39015036310863

[11] P. J. Walker, "Strength, Durability and Shrinkage Characteristics of Cement Stabilised Soil Blocks," *Cem. Concr. Compos.*, vol. 17, no. 4, pp. 301–310, Jan. 1995, doi: 10.1016/0958-9465(95)00019-9.

[12] A. Hakimi, O. Fassi-Fehri, H. Bouabid, S. C. D'ouazzane, and M. E. Kortbi, "Comportement mécanique non linéaire du bloc de terre comprimée par couplage élasticité endommagement [Non-linear behaviourof the compressed earthen block by elasticity-damage coupling]," *Mater. Struct.*, vol. 32, no. 7, pp. 539–545, Aug. 1999, doi: 10.1007/BF02481639.

[13] D. Ciancio and J. Gibbings, “Experimental investigation on the compressive strength of cored and molded cement-stabilized rammed earth samples,” *Constr. Build. Mater.*, vol. 28, no. 1, pp. 294–304, Mar. 2012, doi: 10.1016/j.conbuildmat.2011.08.070.

[14] K. Heathcote, “Compressive strength of cement stabilized pressed earth blocks,” *Build. Res. Inf.*, vol. 19, no. 2, pp. 101–105, Mar. 1991, doi: 10.1080/09613219108727106.

[15] G. Ruiz, X. Zhang, W. F. Edris, I. Cañas, and L. Garijo, “A comprehensive study of mechanical properties of compressed earth blocks,” *Constr. Build. Mater.*, vol. 176, pp. 566–572, Jul. 2018, doi: 10.1016/j.conbuildmat.2018.05.077.

[16] AEN/CTN 41, *UNE 41410: Bloques de tierra comprimida para muros y tabiques. Definiciones, especificaciones y métodos de ensayo [Compressed earth blocks for walls and partitions. Definitions, specifications and test methods]*, AENOR. Madrid: AENOR, 2008.

[17] Indian Standards, “IS 1725: Stabilized soil blocks used in general building construction. Specification.” Bureau of indian standard, 2013.

[18] International Code Council, *International building code*. Falls Church, Va: International Code Council, 2021.

[19] NMAC, “2015 New Mexico Earthen Building Materials Code,” in *New Mexico Administrative Code*, 2015, p. Title 14, Chapter 7, Part 4, 31 p.

[20] CEN/TC 125, *EN 772-1:2011+A1:2015: Methods of test for masonry units–Part 1: Determination of compressive strength*. Brussels: European Committee for Standardization, 2015.

[21] Standards Australia, *AS/NZS 4456: Masonry units, segmental pavers and flags - Methods of test*. Sydney, 2003.

[22] M. Olivier and A. Mesbah, “Le matériau terre: Essai de compactage statique pour la fabrication de briques de terre compressées [The earth as a material: use of the proctor static test to optimize the making of compacted earth bricks],” *Bull Liaison Lab Ponts Chaussées*, vol. 146, pp. 37–43, 1986.

[23] B. V. Venkatarama Reddy and K. S. Jagadish, “Influence of soil composition on the strength and durability of soil-cement blocks,” *Indian Concr. J.*, vol. 69, pp. 517–526, 1995.

[24] ASTM, *Standard practice for classification of soils for engineering purposes (Unified Soil Classification System)*. West Conshohocken, PA: ASTM, 2011.

[25] ASTM, *Standard test method for particle-size distribution (gradation) of soils using sieve analysis*. West Conshohocken, PA: ASTM, 2017.

[26] ASTM, *Standard test method for particle-size distribution (gradation) of fine-grained soil using the sedimentation (hydrometer) analysis*. West Conshohocken, PA: ASTM, 2017.

[27] ASTM, *Standard test methods for liquid limit, plastic limit, and plasticity index of soils*. West Conshohocken, PA: ASTM, 2017.

[28] ASTM, *Standard test methods for laboratory compaction characteristics of soil using standard effort (12 400 ft-lbf/ft3 (600 kN-m/m3))*. West Conshohocken, PA: ASTM, 2012.

[29] M. C. Jiménez Delgado and I. C. Guerrero, "The selection of soils for unstabilized earth building: A normative review," *Constr. Build. Mater.*, vol. 21, no. 2, pp. 237–251, Feb. 2007, doi: 10.1016/j.conbuildmat.2005.08.006.

[30] T. Morton, *Earth masonry design and construction guidelines*. Bracknell: IHS BRE Press, 2008.

[31] ASTM, *Standard test methods for laboratory compaction characteristics of soil using standard effort (12 400 ft-lbf/ft3 (600 kN-m/m3))*. West Conshohocken, PA: ASTM, 2007.

[32] ASTM, *Standard Guide for Measuring and Reporting Friction Coefficients*. West Conshohocken, PA, 2013.

[33] ASTM, *Standard Test Method for Static and Kinetic Coefficients of Friction of Plastic Film and Sheeting*. West Conshohocken, PA, 2014.

[34] M. Escudier and T. Atkins, "coefficient of friction," in *A Dictionary of Mechanical Engineering*, Oxford University Press, 2019. Accessed: Feb. 18, 2021. [Online]. Available: https://www.oxfordreference.com/view/10.1093/acref/9780198832102.001.0001/acref-9780198832102-e-937

[35] F. Indelicato and M. Paggi, "Specimen shape and the problem of contact in the assessment of concrete compressive strength," *Mater. Struct.*, vol. 41, no. 2, p. 431, Mar. 2008, doi: 10.1617/s11527-007-9256-7.

[36] J. E. Aubert, P. Maillard, J. C. Morel, and M. Al Rafii, "Towards a simple compressive strength test for earth bricks?," *Mater. Struct.*, vol. 49, no. 5, pp. 1641–1654, 2016, doi: 10.1617/s11527-015-0601-y.

[37] P. J. Walker, "Strength and erosion characteristics of earth blocks and earth block masonry," *J. Mater. Civ. Eng.*, vol. 16, no. 5, pp. 497–506, Oct. 2004, doi: 10.1061/(ASCE)0899-1561(2004)16:5(497).

[38] D. Silveira, H. Varum, and A. Costa, “Influence of the testing procedures in the mechanical characterization of adobe bricks,” *Constr. Build. Mater.*, vol. 40, pp. 719–728, Mar. 2013, doi: 10.1016/j.conbuildmat.2012.11.058.

[39] Bureau of Indian Standards, *IS 1725: Stabilized soil block used in general building construction - specification*. New Delhi: Bureau of Indian Standards, 2013.

[40] ASTM, *Standard test methods for sampling and testing brick and structural clay tie*. West Conshohocken, PA: ASTM, 2021.

[41] Bureau of Indian Standards, “Part I: Determination of compressive strength,” in *IS 3495-1: Methods of test of burnt clay building bricks*, New Delhi: Bureau of Indian Standards, 1992.

[42] Bureau of Indian Standards, “IS 5454: Methods for sampling of clay building bricks,” in *IS 5454-1978: Methods of test of burnt clay building bricks*, New Delhi: Bureau of Indian Standards, 1978.

3.7 TABLES

Table 3.1 Comparison of compression test methods for earth masonry materials

	Australia [6], [21]	**New Zealand** [7]	**USA – NM** [19]	**USA – IBC** [18]	**India** [39]	**Spain** [16]
Block specimen	Whole or cut part-units	1.0 ≤ aspect ratio ≤ 2.0	Length ≥ 2 Width	½ - ¼ brick. Cross-sectional area ≥ 90.3 cm^2	Whole	
Moisture condition	Any	Air dry	Saturated	Oven-dry	Saturated	Air dry
Capping[1]	Plywood	Not specified		Gypsum with oil coating or sulfur-filler	Plywood	Not specified
Loading ratio	1 - 5 mm/min or 9 - 42 MPa/min	Not specified	3.4 MPa/min	Any up to 1/2 max. load, then increases such that max. is attained in between 1 and 2 minutes	14 MPa/min	Any up to 1/2 max. load, then increases such that max. is attained in not less than 1 minute
Orientation	Not specified	Horizontal[2]				
Correction factor	Per aspect ratio	Per aspect ratio	Not specified			Per size and aspect ratio
Strength definition	Unconfined[3]		Apparent[4]			Normalized [5]
Min. samples	Five					Six
Strength performance	1.0 MPa (saturated) 2.0 MPa (dry) Characteristic	Individual results ≥1.4 MPa	Individual results > 2.0 MPa	Average ≥ 2.0 MPa Individual results ≥ 1.72 MPa	Average ≥ 3.5 MPa	1.3 MPa ≤ Characteristic ≤ 5 MPa
Additional remarks	Apply to earth wall materials cylinder and block specimens		Specification for CSEB	Specification for adobe. Test method refers to [40] for brick and structural clay tie	Test method refers to [41] and [42] for burnt clay brick	Test method refers to [20] for masonry units

[1] Generally, standards recommend using mortar or plaster filling when voids, recessions, lack of flatness, or parallel faces need to be corrected.
[2]Horizontal orientation refers to laying the block on a face parallel to the compression plane, formed perpendicular to the compression ram during manufacturing.
[3]Obtained by applying an aspect ratio correction factor to measured values.
[4]Obtained without minimizing nor correcting the strength gain due to lateral platen restraints.
[5]Equivalent to a 100 mm height and 100 mm width block.

Table 3.2 Mechanical testing matrix

ID	Aspect ratio	Loading interface insert[1]	Nominal dimensions [mm]			Number of specimens	Loading rate	
			Diameter or base	Length	Height		mm/ sec	με/ sec
Cylinders								
C0.5	0.5	PTFE	64	—	32	23	0.01	313
C1.0	1.0	PTFE	64	—	64	21	0.01	156
C2.0	2.0	PTFE	64	—	127	28	0.01	79
Prisms								
P0.7	0.7	PTFE	127	178	90	12	0.03	333
P1.0	1.0	PTFE	76	76	76	84	0.03	395
P1.2	1.2	PTFE	76	76	89	8	0.03	337
P1.2S	1.2	Sandpaper	76	76	89	9	0.03	337
P2.0	2.0	PTFE	84	89	178	10	0.01	79
[1]0.4-mm thick PTFE sheets and sandpaper grit-60.								

Table 3.3 CoF characterization results

Interface	Mean	SD	CV
CSEB-PTFE	0.49	0.12	24%
CSEB-sandpaper 220	0.77	0.11	15%
CSEB-sandpaper 60-grit	0.82	0.06	7%
CSEB-polished steel	0.36	0.06	17%
CSEB-not polished steel	0.49	0.17	35%

Table 3.4 One-way ANOVA results for CoF

Source of variation	SS	DF	MS	*F*-statistic	*p*-value
Among groups	1.00	1	1.00	119	1.20e-12
Within groups	0.29	34	0.01		
Total	1.29	35			
SS: Sum of squares; DF: Degrees of freedom; MS: Mean square error					

Table 3.5 One-way ANOVA results for friction effect on compressive strength

Source of variation	SS	DF	MS	*F*-statistic	*p*-value
Among groups	1.29	1	1.29	3.4	0.085
Within groups	5.70	15	0.38		
Total	6.99	16			
SS: Sum of squares; DF: Degrees of freedom; MS: Mean square error					

Table 3.6 Relation between strength dispersion and sampling saw-cutting extent

Specimen	CV	Number of saw-cut surfaces
C2.0	25%	1-2[1]
C1.0	24%	1-2[1]
C0.5	34%	1-2[1]
P2.0	18%	1-2
P1.2	15%	2-3
P1.0	29%	3-5
P0.7	16%	1
[1]Drilling added to saw-cutting perpendicular to longitudinal axis		

3.8 FIGURES

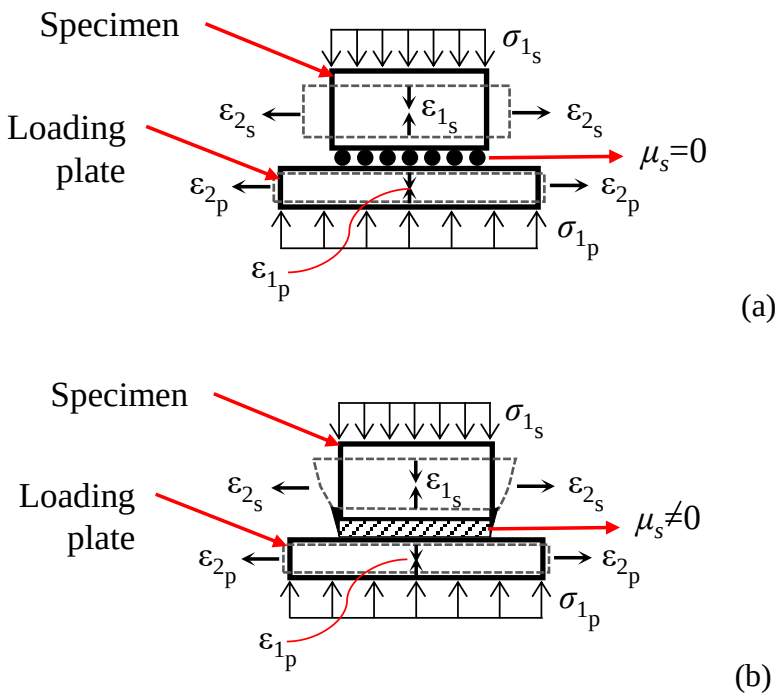

Figure 3.1 Platen lateral restraint mechanism schematic: (a) zero friction case at the specimen-loading plate interface, (b) non-zero friction case at the specimen-loading plate interface

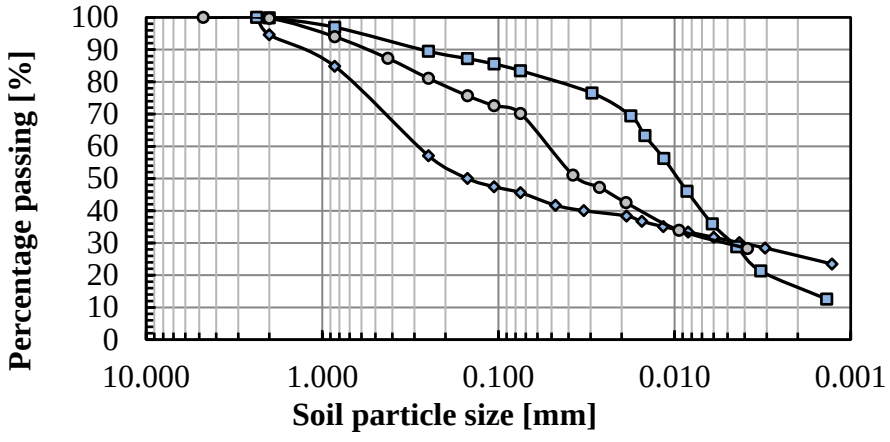

(a)

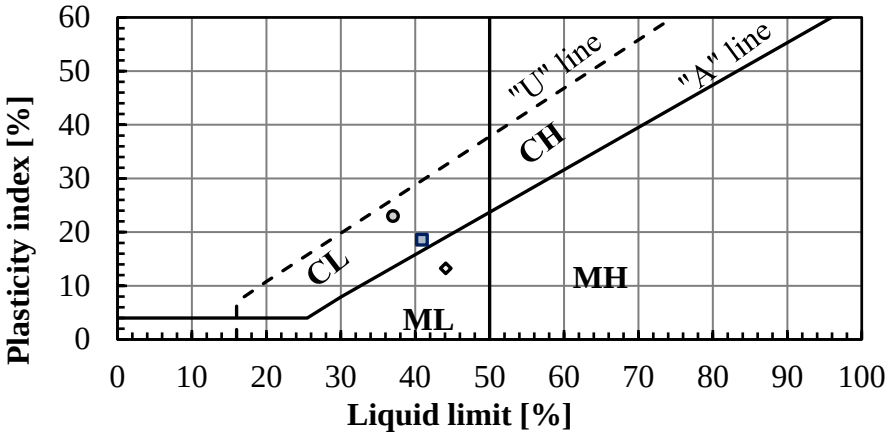

(b)

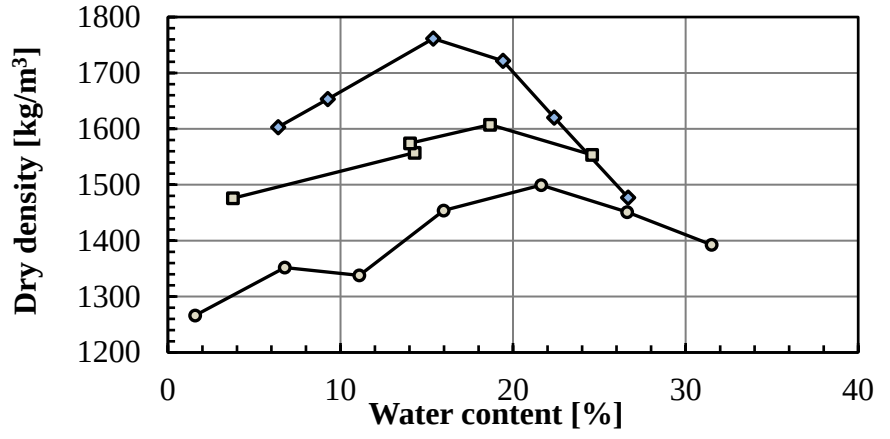

(c)

Figure 3.2 Representative soil characterization results: (a) particle-size distribution curves, (b) plasticity chart, (c) compaction curves


(a)

(b)

(c)

(d)

Figure 3.3 CSEB manufacturing process: (a) soil collection from construction pit in Lexington, SC, (b) crushing and sieving, (c) manual mixing and compaction, and (d) curing

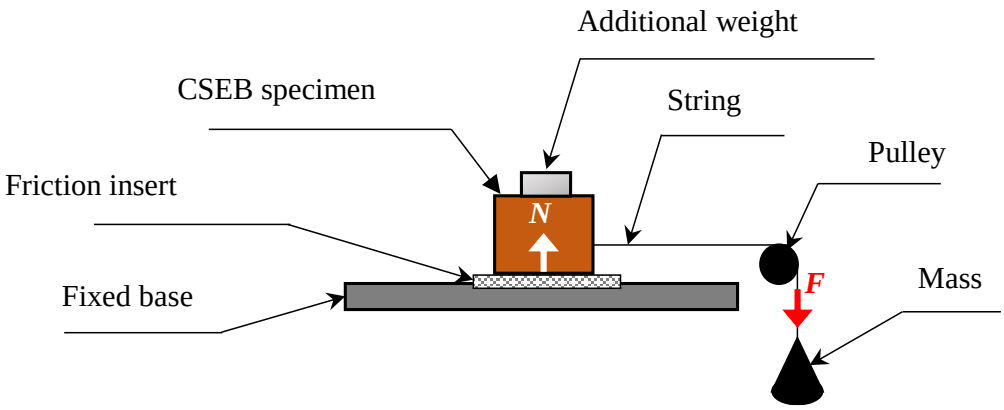

(a)

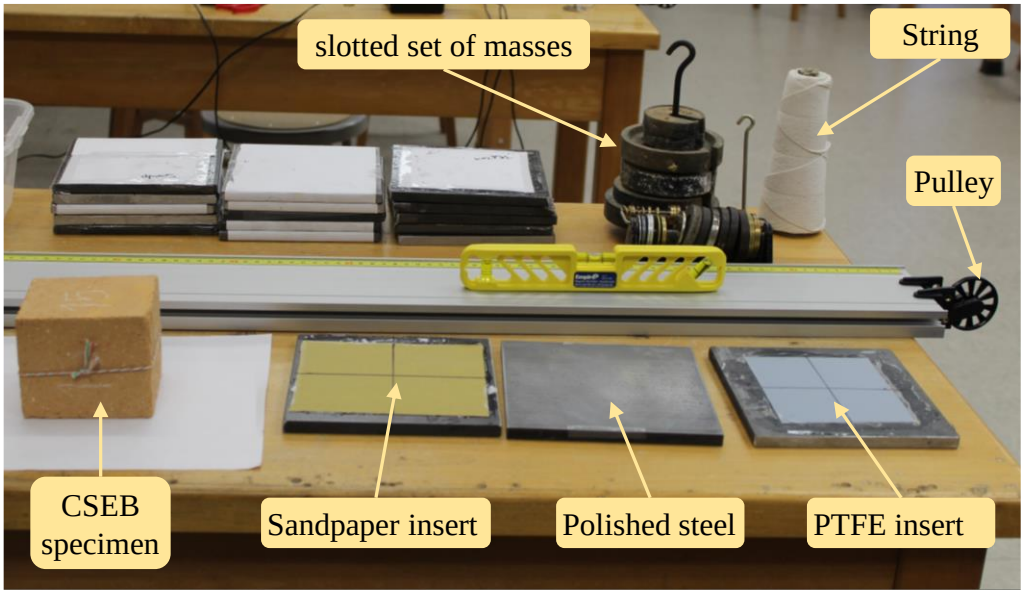

(c)

Figure 3.4 CoF characterization setup: (a) test schematic; (b) actual picture setting including friction inserts, slotted set of masses, low-friction pulley, string, and level platform


(a)

(b)

(c)

(d)
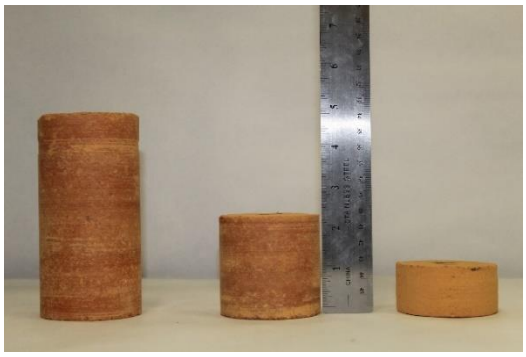
(e)

(f)

Figure 3.5 CSEB specimens manufacturing: (a) width-wise, (b) length-wise, and (c) height-wise drilled cores, (d) saw-cutting to generate desired aspect ratios, (e) C0.5, C1.0, C2.0 and (f) P2.0 specimens

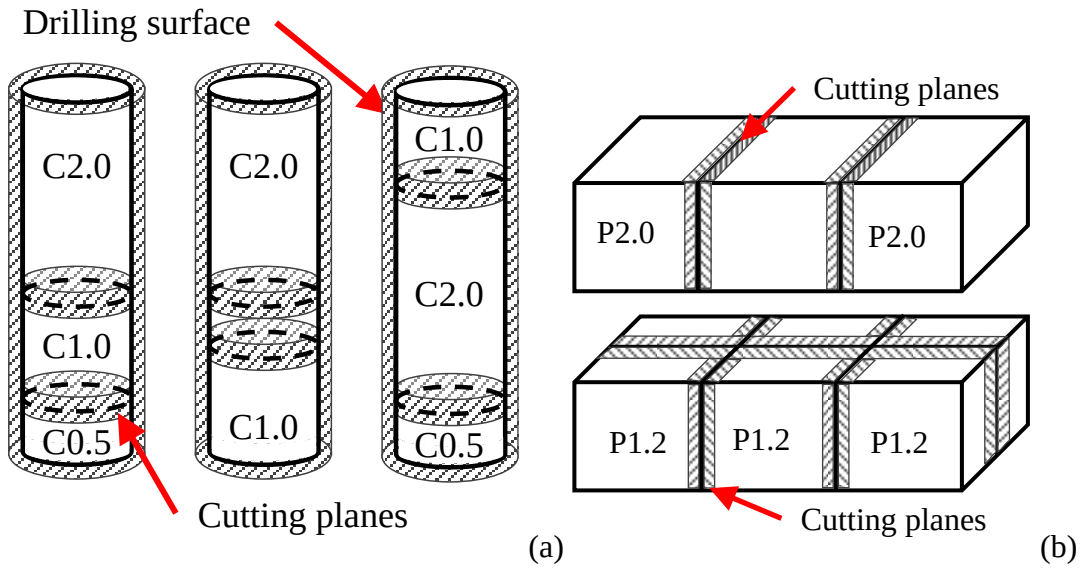

Figure 3.6 Cutting and drilling schematics to manufacture (a) cylinder and (b) prism specimens

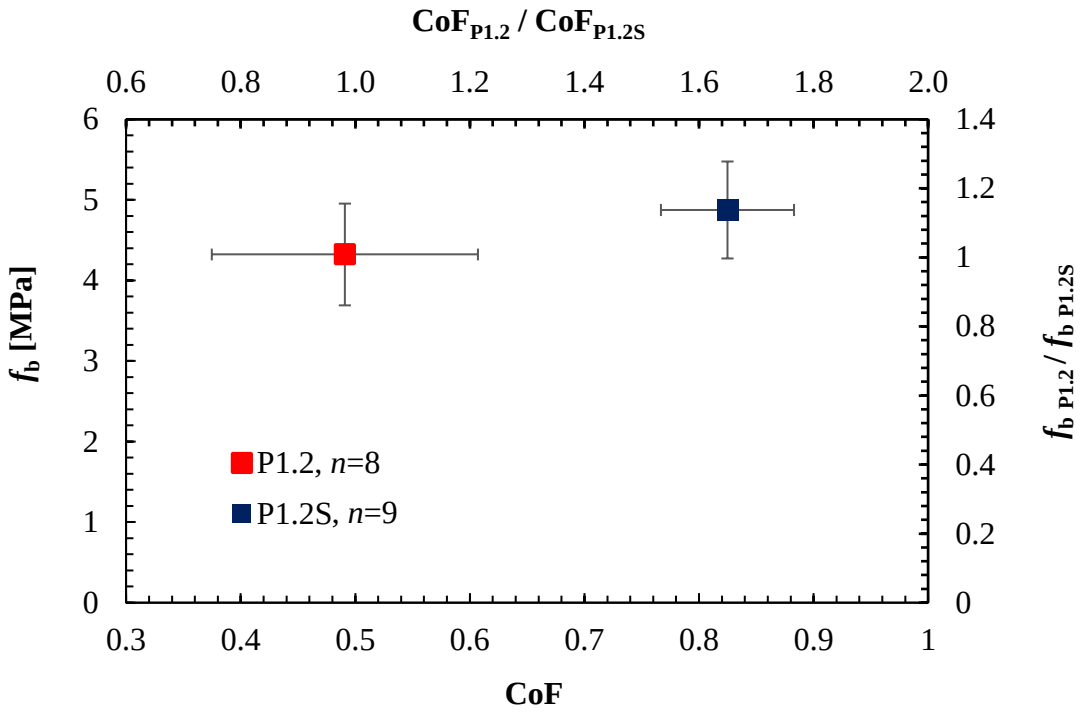

Figure 3.7 f_b of CSEB specimens as a function of friction

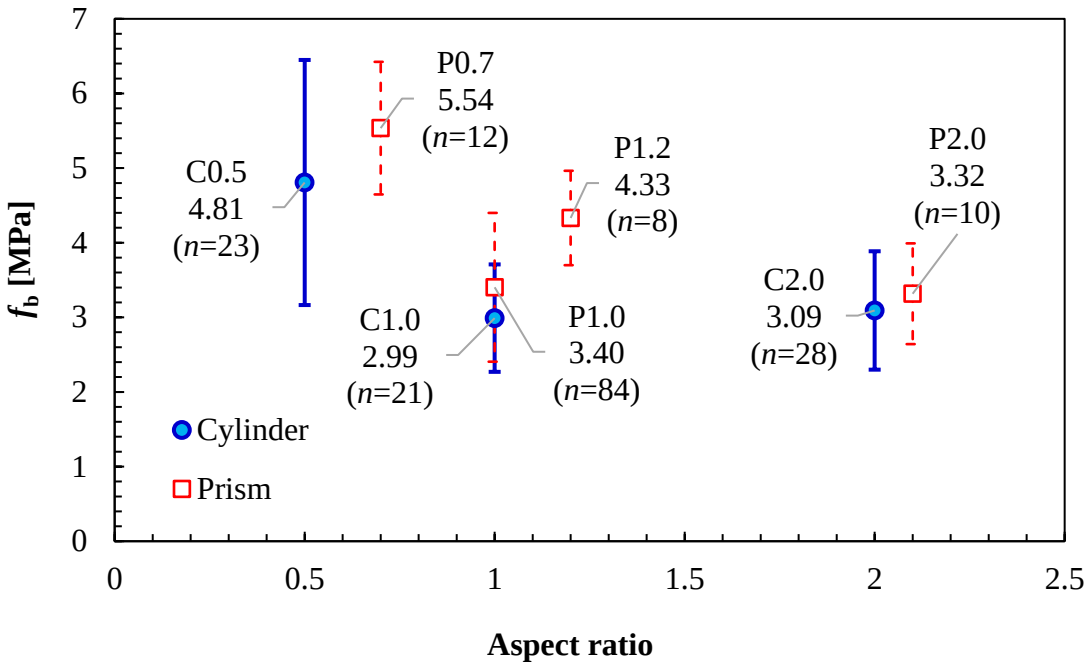

Figure 3.8 f_b of CSEBs cylinder and prism specimens with different aspect ratios

CHAPTER 4: EXPERIMENTAL CHARACTERIZATION OF CONSTITUTIVE COMPRESSIVE STRESS-STRAIN BEHAVIOR OF PROTOTYPE EARTH BLOCK MATERIAL [3]

[3]Erika L. Rengifo-López., Nitin Kumar, Fabio Matta, and Michele Barbato. To be submitted to *Materials and Structures*.

ABSTRACT. Typically, the compressive response of compressed and stabilized earth block (CSEB) materials is characterized by performing uniaxial compression tests on blocks or block portions. However, the effects of specimen geometry and shape on the stress-strain response are not well understood. This paper reports on an experimental investigation of the compressive behavior of a representative CSEB material, focusing on the characterization of the uniaxial stress-strain response. Cylinder and prism specimens, having different aspect ratios, were tested in uniaxial compression to collect stress-strain data. Three-dimensional digital image correlation (3D-DIC) was enlisted to measure full-field deformations and better understand the platen lateral restraining effect on the axial strain distribution throughout the specimen height.

The analysis of the results indicated that specimens with an aspect ratio of 2.0 (either cylinder or prism) are a suitable configuration to characterize a stress-strain response representative of the material's constitutive behavior. To this end, the region where strains are measured should be way from the loading plates by at least a distance equal to one-fourth of the height. The findings of this investigation make a relevant contribution towards the standardization of the experimental characterization of the overall compressive response of earth block materials, which is critical for the design and analysis of earth masonry structures.

4.1 INTRODUCTION

The information available on the overall compressive response (i.e., Young's modulus, Poisson's ratio, and stress-strain relations) of earth masonry blocks is limited. Furthermore, the extent of specimen geometry effect on the compressive behavior is not fully understood. This knowledge gap becomes relevant as the experimental

characterization of the compressive stress-strain response, which is representative of uniaxial behavior, is essential to define constitutive models and develop numerical tools for the effective design and simulation of the mechanical behavior of earth masonry systems.

Experimental results, including compressive strength and stress-strain response, are sensitive to a given specimen's size, cross-sectional shape, and aspect ratio (i.e., the ratio between the larger and smaller dimension). In Chapter 3, it was concluded that for a representative prototype CSEB material, the specimen cross-sectional shape has a negligible effect on the compressive strength. In contrast, the specimen aspect ratio effect on the resulting compressive strength was significant. The aspect ratio effect results from the lateral expansion constraints exerted by the loading plates due to friction at the contact surface and stiffness mismatch between the plates and the specimen [1]. Due to the importance of the uniaxial compression characterization of earth masonry units, the consideration of aspect ratio effects on the compressive behavior becomes significant. However, there is no consensus on how to account for these effects [2]–[4]. For instance, the Spanish standard for compressed earth blocks [2] specifies shape factors to convert the experimental strength of a given block-type specimen to a normalized compressive strength, which corresponds to a block with a height and width of 100 mm; this configuration is similar to the procedure outlined by the European Standards [5] for masonry units. In contrast, the New Zealand standard [3] and Australian handbook [4] provide aspect-ratio correction factors to determine the unconfined compressive strength. It is noted that the factors in [3] and [4] are different from each other, and the latter ones are identical to those specified in the Australian standard for masonry units [6], which

were originally proposed based on results from investigations carried out on calcium silicate masonry bricks [7]. These factors are comparable to those determined from experimental results from CSEB specimens [8]. The existing approaches that aim to account for specimen aspect ratio are limited to the experimental characterization of the compressive strength, and no consideration is given to the stress-strain response. In fact, to the best of the authors' knowledge, there is no available investigation focused on the specimen's geometry effect on the stress-strain response of earth masonry block materials. Therefore, a question arises regarding how to consider aspect ratio effects to characterize a stress-strain response that is representative of the constitutive behavior of earth masonry blocks.

This paper presents the results of a rigorous experimental investigation aimed to characterize the constitutive compressive stress-strain response of a representative CSEB material. The first section describes the methodology followed to collect compressive stress-strain data from cylinder and prism specimens having different aspect ratios. The experimental plan entails 3D-DIC deformation measurements and pointwise deformation measurements. The second section presents the results and discussion of the aspect ratio effects observed on the strain distribution through full-field (3D-DIC) strain maps. To this end, strain non-uniformities were quantified over the height of specimens with an aspect ratio of 2.0 to identify a region in which strain disturbances due to lateral platen restraints were reasonably minimized. The stress-strain data from specimens with aspect ratio 2.0 were analyzed to identify elastic parameters, which are critical to define the constitutive elastic properties of the material.

4.2 SIGNIFICANCE

The experimental characterization of the constitutive behavior of earthen materials is critical to develop numerical models to predict the mechanical response of associated structural systems. However, there are limited available investigations aimed at characterizing mechanical parameters that represent the constitutive behavior of earthen materials. These investigations have focused on compressed earth blocks [9]–[11], adobe [12], and rammed earth [13]. Yet, various specimen geometry, measuring methods, and definitions of elastic properties (e.g., Young's modulus) are observed among methodologies from different studies, limiting the interpretation of the results. To illustrate this point, Table 4.1 summarizes the modulus of elasticity values and descriptions of related methods reported in the literature.

On the other hand, available experimental results for Poisson's ratio are scattered. For instance, Venkatarama Reddy et al. [14] reports Poisson's ratio values between 0.19 and 0.24 for earthen mortar and between 0.08 and 0.12 for a CSEB material. For a non-stabilized compressed earth block (CEB) material, Champiré et al. [11] report results ranging from 0.15 and 0.2, and for rammed earth, Bui et al. [15] found values between 0.22 and 0.40 for different water contents. These ranges are plotted in Figure 4.1, in which characteristic values of lightweight concrete [16] and cementitious materials [17], [18] are included for further reference.

The literature review showed that the information available is insufficient to define constitutive models needed for the numerical modeling of CSEB structures. This investigation contributes to the comprehensive understanding of the material's compressive behavior and effects of the specimen geometry and boundary conditions on

the stress-strain response. Furthermore, the resulting data collection constitutes a robust source to define, calibrate and validate numerical models of earth block materials.

4.3 METHODOLOGY

4.3.1 MATERIALS

4.3.1.1 SOIL

The soil used to produce the prototype CSEB material, sourced from a construction lot in Lexington (SC), was collected in 13 batches. Each batch was characterized through standard tests [19]–[22] and classified as either a lean clay (CL), clayey sand (CS), or silt (ML) per ASTM D2487 [23]. Table 4. summarizes the characterized soil properties ranges, and Figure 4. shows representative particle size distribution curves. These results are comparable to ranges of gradation (e.g., 20%-70% fines) and plasticity (e.g., 16%-28% LL) that have been identified to be suitable for earth construction materials [24], [25]**.**

4.3.1.2 CSEB MATERIAL

The prototype CSEB investigated herein was produced by compacting a mix of soil, Type I ordinary Portal cement (6% by weight proportion), and water into a mold with nominal dimensions of 254 × 178 × 89 mm^3. To that end, one-side compaction at 10 MPa was imparted using a commercial hydraulic press (model EPH-2008, Fernco Metal Products, Capitan, NM). The CSEBs were moist cured for 14 days, reaching an average 28-day specific weight of 1640±96 kg/m^3, estimated from 16 randomly selected blocks. The production process followed standard manufacturing guidelines [4], [25], [26] and is further described in Chapter 3.

4.3.2 Experimental program

4.3.2.1 Test matrix

The test matrix, listed in Table 4.3, was extracted from a previous investigation focused on the compressive strength of the same material, as reported in Chapter 3. Here, the selected specimens were used to examine the effect of aspect ratio and cross-sectional shape on the stress-strain response determined from full-field deformation measurements. In particular, specimens with aspect ratio two (i.e., C2.0 and P2.0) were intended to characterize a stress-strain response representative of uniaxial behavior, provided that lateral platen restraining effects are reasonably minimized compared to smaller aspect ratios. The comprehensive data retrieved from the test matrix will serve to define, calibrate, and validate a constitutive numerical model of the material.

4.3.2.2 Deformation measurement setups

The experimental program included the three different setups shown in Figure 4.3 and the validation setup for 3D-DIC measurements illustrated in Figure 4.4.

The two 3D-DIC setups are intended to gain a comprehensive insight into the geometry effects on the full-field strain distribution. To this end, two different stereo-vision systems were designed to measure 3D-DIC-based deformations on either one (Figure 4.3(a)) or two (Figure 4.3(b)) surfaces of the specimens. The following section describes in detail each system.

Pointwise setup refers to a compressometer-type fixture designed to measure axial and transverse deformations within the middle third portion of cylinders with aspect ratio 2 (i.e., C2.0) for Young's modulus and Poisson's ratio estimation. In this case, 25-mm linear variable displacement transducers (LVDT) were used. The purpose of this setup

was to characterize the stress-strain response within a portion where lateral platen restraining effects could be reasonably minimized (i.e., 63.5-mm gauge length), thus being the behavior representative of the material's uniaxial behavior.

Finally, the setup denoted as Pointwise and 3D-DIC was included to validate the measuring method. Figure 4.4(a) shows the stereo-vision system, whose characteristics and components were defined to ensure adequate lighting and focus on both sample and fixture. Figure 4.4(b) shows the compressometer-type fixture and specimens C2.0 printed with a random speckle pattern. The validation was conducted by comparing compressive differential vertical displacements, indicated as “g” in Figure 4.4(b), measured with the physical LVDT and a 3D-DIC virtual extensometer located at the same position.

4.3.2.3 Stereo-vision system and speckle pattern verification for 3D-DIC

To perform 3D-DIC deformation measurements, the two stereo-vision systems shown in Figure 4.3(a-b), denoted as System 1 and System 2, were designed to (1) collect high-resolution images of flat and curved surfaces of CSEB specimens, including allowing a maximum out-of-plane displacement (for Poisson’s ratio estimates) of 10.7 mm; (2) ensure a minimum speckle sampling of 3-by-3 pixel array for accurate matching and, (3) broad gray-level distribution of the speckle pattern [27].

Table 4.4 lists the specific features of System 1 and System 2, which included a computer with a 3D-DIC image acquisition software (Vic-3D, Correlated Solutions, Inc.). System 1 was used for all cylinder specimens and specimen P0.7. System 2 included two stereo-camera sets (i.e., four total) to simultaneously monitor two side surfaces (i.e., two cameras per surface) of specimens P2.0.

The random speckle pattern was applied manually, with a stiff toothbrush, using flat black paint directly on the smoother surface of each CSEB specimen, as illustrated in Figure 4.5. The pattern surface was lighted to obtain a broad intensity distribution range and thus minimize the measurements error [27]. Figure 4.6(a) shows a close-up of a representative image taken during a test with the stereo camera identifying the pixel sampling of the speckle pattern printed on the specimen's surface, and Figure 4.6(b) shows the gray levels histogram associated with the close-up image. The resulting bell-shaped gray level distribution is suitable for accurate 3D-DIC measurements [27], as demonstrated in the case of masonry materials [28].

4.3.2.4 3D-DIC MEASUREMENT ERROR ASSESSMENT

In addition to the considerations described in the previous section concerning the stereo-vision system design and speckle pattern verification to ensure high accuracy, the measurement error was assessed as a function of two parameters: (1) the stereo angle between cameras and (2) correlation subset size. The measurement error was defined as the standard deviation (SD) of strains and displacements calculated with images taken at zero load.

The first assessment included four different stereo-angles (i.e., 14°, 18°, 26°, 39°). For each stereo-angle, sets of ten images of a specimen C2.0 with no load applied were taken for three different trials. The first trial, consisted of taking images of the specimen at an initial position, and the consecutive two trials consisted of taking zero load images after applying a body rigid movement (e.g., approximate displacement of 4 mm laterally and 3 mm forward). The results are summarized in Table 4.5. The stereo-angle was selected as 14° for providing a field of view large enough while limiting the axial strain

measurement error to 71 με, yielding a field of view with an arc length of 64 mm (32% of the nominal circumference of a given cylinder specimen). Furthermore, this assessment revealed that heatwaves were contributing to the measurement error. Thus, a fan was added to the setup, and the room temperature was monitored through every test (measured as 23±0.5°C).

Because the speckle pattern was printed manually, variations from one specimen to another were inevitable. Therefore, the influence of the correlation subset size on the measurement error was assessed for each specimen. To this end, a minimum of 50 images at zero load were taken from each specimen and analyzed to calculate the mean and standard deviation in strain and displacement for all data points to evaluate standard deviation errors. Figure 4.7 presents the standard deviation error for the axial strain as a function of the subset size for representative specimens with different aspect ratios and cross-sectional shapes. The resulting trend shows that a desirable subset size must offer a compromise between resolution (enhanced at decreasing size) and accuracy (enhanced at increasing size). The subset size selected for different specimens ranged between 41×41 and 61×61 pixel with axial strain error in the range of 12 to 94 με.

4.3.2.5 LOADING PROTOCOL AND IMAGE ACQUISITION

All specimens were tested up to failure in uniaxial compression using a servo-hydraulic frame (model 810, MTS Systems Corporation, Eden Prairie, MN) with inserts of 0.4-mm thick polytetrafluoroethylene (PTFE) sheets at the specimen-loading platen interface. For specimens C0.5, C1.0, C2.0, and P2.0, the force was applied at a rate of 0.01 mm/s and measured using a 98-kN load cell. For specimens P0.7, the loading rate was 0.03 mm/s, and the load cell capacity was 445 kN. For tests that included 3D-DIC

measurements, loading was paused at 1 to 2 kN (0.35-0.70 MPa) intervals to allow for the acquisition of a minimum of 50 images at different damage levels, as illustrated in Figure 4.8 for a representative specimen C1.0.

4.3.2.6 3D-DIC MEASUREMENT VALIDATION METHOD

The vis-à-vis comparison of displacements determined with the non-contact and pointwise measuring methods, resulted in good correspondence. To illustrate this point, Figure 4.9 presents the load-displacement curves measured, simultaneously, with the Pointwise and 3D-DIC setups on three C2.0 specimens. In Figure 4.9, the deformation data correspond to the displacement indicated as "g". Thus, the test setup was validated successfully.

4.4 RESULTS AND DISCUSSION

4.4.1 3D-DIC BASED STRAIN MAPS VARIATION ANALYSIS

The analysis and interpretation of the 3D-DIC data collected from C2.0 and P2.0 specimens served to quantify the extent of non-uniformities on the strain maps. To that end, three strain profiles were extracted over the height of each specimen. The means and coefficients of variation (CV) of strain data points within different vertically centered portions of the specimen's height (denoted as H) were calculated for each profile.

Figure 4.10 and Figure 4.11 illustrate the methodology followed in conducting the non-uniformities assessment and reporting typical results for one specimen C2.0 and P2.0, respectively. Figure 4.10(a) and Figure 4.11(a) show the axial strain maps for a given specimen at three different strain levels relative to the compressive strength, f_b, and indicate the position and denomination of each strain profile. For each profile (i.e., L0, L1, and L2), Figure 4.10(b) and Figure 4.10(b) plot the associated axial strain over the

height of the specimen, and Figure 4.10(c) and Figure 4.10(c) present the strain's mean CV as a function of the specimen's height portion considered (H) divided by its diameter (D) or by its minor cross-section dimension (b).

The strain non-uniformities assessment results in specimens C2.0 and P2.0, at a stress level of approximately $0.3f_b$, are summarized in Figure 4.12. It was observed that in C2.0 specimens, the mean CV was reduced to less than 35% when a vertically centered height's portion no longer than 1-diameter was considered. Similarly, in P2.0 specimens, a maximum mean CV maximum of 35% was obtained when a height's portion vertically centered no longer than 1.3 times the cross-section dimension was considered. The results indicated that strain nonuniformities were significant up to a distance equal to one-fourth of the specimen height from either loading platen.

The 3D-DIC based strain maps served to highlight the significant effect of lateral platen constraint, and possibly a more pronounced influence of crack propagation of specimens with aspect ratio lower than 2.0. To concisely illustrate this point, Figure 4.13 and Figure 4.14 present representative curves and envelopes of the axial stress-strain response for cylinder and prism specimens with different aspect ratios, respectively. In Figure 4.13 and Figure 4.14, the compressive stress is normalized by the specimen compressive strength, f_b, data points represent the mean, and the error bars the standard deviation of the axial strain. It is noted that strain data of specimens C2.0 and P2.0 were retrieved from the middle-third region, whereas data of specimens with aspect ratios lower than 2.0 were extracted from the entire strain map. Here, the boundary condition effects are highlighted by the inconsistencies featured in the stress-strain envelopes for specimens with aspect ratios lower than 2.0.

These results show that specimens with aspect ratios 0.5, 0.7, and 1.0, which may represent typical CSEB blocks, are unsuitable configurations for extracting stress-strain curves to define the uniaxial stress-strain response of the material.

4.4.2 UNIAXIAL STRESS-STRAIN RESPONSE

Following the identification of relatively uniform strain distribution within the middle-third of specimens with aspect ratio 2.0 and the validation of the test setup, the analysis focused on the related stress-strain response (determined with non-contact and pointwise measurements). Frist, the loss of linearity was analyzed to define elastic properties. Second, the full stress-strain response is discussed.

4.4.2.1 ELASTIC BEHAVIOR

The stress-strain data were analyzed to characterize the stress level at which the material's behavior could be reasonably approximated as linear elastic This proportional limit is an essential parameter to define an accurate constitutive model (e.g., to determine Young's modulus and Poisson's ratio). To this end, linear regression analysis, computed within different selected stress levels (i.e., from 10% to 100% of f_b), was used to assess the linearity loss of the stress-strain response, where the coefficient of determination R^2, determined by (1), (2), and (3), was selected as the linearity indicator.

$$R^2 = 1 - \frac{SSE}{SST} \tag{1}$$

$$SST = \sum(y_i - \bar{y})^2 \tag{2}$$

$$SSE = \sum(y_i - \hat{y}_i)^2 \tag{3}$$

Where SSE is the sum of squared error, SST is the sum of squared total, $y_i$is the observed data point, $\hat{y}_i$ is the predicted value of the observed data point and $\bar{y}$ is the mean of the observed data.

Figure 4.15(a-d) presents the stress-strain data, linear regression, and the resulting R^2 and E for a specimen C2.0 tested with 3D-DIC-based measurements and from other C2.0 with pointwise deformation measurements. Figure 4.15(e) displays the summary of the results for all specimens C2.0, where continuous lines represent the mean values, and the error bars indicate the standard deviation.

Similar to specimens C2.0, Figure 4.16(a-b) presents representative stress-strain data, linear regression, and resulting R^2 and E for a given P2.0 specimen tested with System 2 (as described in Table 4.4), which allows 3D-DIC measurements on two surfaces of the same specimen (i.e., Measurement_1 and Measurement_2). Figure 4.16(c) plots the E estimation error, determined by (4), as a function of the stress level, and Figure 4.16(d) presents the summary of results for all P2.0 specimens.

$$E_{estimation\ error} = \frac{|E_{Measurement_1} - E_{Measurement_2}|}{Max(E_{Measurement_1}, E_{Measurement_2})} \quad (4)$$

Results from the linearity loss assessment, from both C2.0 and P2.0 specimens, indicated that a mean R^2 equal to or higher than 0.95 is attained for stress-strain data corresponding to stress levels equal to or lower than 40% of the peak stress approximately. Thus, the proportional limit was picked at 40% stress level to define the Young's modulus, E and Poisson's ratio, ν. Figure 4.17 shows the Poisson's ratio calculated with strain data measured within the 40% stress level. Table 4.6 summarizes the experimentally characterized elastic properties for the CSEB material using cylinder and prism specimens with an aspect ratio of 2.0.

4.4.2.2 CONSTITUTIVE STRESS-STRAIN BEHAVIOR

The compressive stress-strain response measured on C2.0 and P2.0 specimens exhibited a comparable behavior, as illustrated in Figure 4.18 and with a similar fashion

to that observed in quasi-brittle materials. In fact, the linearity assessment results quantitatively describe the similarities between the compared specimens. Furthermore, the mean compressive strength of P2.0 specimens was determined as 3.32±0.67 MPa, thus agreeing with the mean strength of C2.0 specimens, which was calculated as 3.09±0.79 MPa.

These results and the minimization of platen lateral restrain effect (evidenced in the strain distribution) observed within the middle-third portion of the height of specimens with an aspect ratio of 2.0 suggest that cylinders and prisms, with such aspect ratio, are suitable configurations to experimentally characterize a stress-strain response representative of the uniaxial compressive behavior of the CSEB material. Furthermore, the observed similarities between the compressive behavior of cylinder and prism specimens provide additional evidence to support the conclusion drawn in Chapter 3 regarding the negligible effect of cross-sectional shape on the compressive strength of CSEB.

4.5 Conclusions

Based on the experimental investigation reported in this paper, for the specimens' cross-sectional shape and size considered, the following conclusions are drawn:

1. Approximately uniform axial strains are attained within a portion of the height of CSEB specimens with an aspect ratio equal to 2.0 that is one-quarter away from the loading plates. The results indicate that the lateral restraining effect is sufficiently minimized at this height portion and suggest that the corresponding stress-strain response is representative of the unconfined uniaxial compression behavior of CSEB materials and can be used to identify the modeling parameters needed to define constitutive models. To

this end, it is recommended that strain data are measured within the middle third of the specimen height.

2. The vis-à-vis comparison between the stress-strain relation from the middle-third portion of prisms and cylinders height with aspect ratio 2.0 suggested that either prisms or cylinders are suitable configurations to define the material constitutive model. Numerical simulations will allow for further verification of this conclusion.

3. The proportional limit to define the elastic properties of CSEB materials is recommended as 40% of the compressive strength. For the material investigated herein, Young's modulus and Poisson's ration were characterized as 2533±874 and 0.152±0.059, respectively.

4. Using pointwise measuring methods, such as a compressometer-type fixture, is appropriate to characterize a stress-strain response and elastic parameters that are representative of the uniaxial behavior of the material, provided that the deformations are measured within the middle-third of specimens with an aspect ratio of 2.0.

4.6 REFERENCES

[1] P. Domone, "Strength and failure of concrete," *Constr. Mater.*, pp. 155–168, 1994.

[2] AEN/CTN 41, *UNE 41410: Bloques de tierra comprimida para muros y tabiques. Definiciones, especificaciones y métodos de ensayo [Compressed earth blocks for walls and partitions. Definitions, specifications and test methods]*, AENOR. Madrid: AENOR, 2008.

[3] NZS, *NZS 4298: Materials and construction for earth buildings*. Wellington, N.Z.: Standards New Zealand, 2020.

[4] P. Walker and Standards Australia, *The Australian earth building handbook*. Australia: Standards Australia International, 2002.

[5] CEN/TC 125, *EN 772-1:2011+A1:2015: Methods of test for masonry units–Part 1: Determination of compressive strength*. Brussels: European Committee for Standardization, 2015.

[6] Standards Australia, *AS/NZS 4456: Masonry units, segmental pavers and flags - Methods of test*. Sydney, 2003.

[7] A. W. Page and R. Marshall, “The influence of brick and brickwork prism aspect ratio on the evaluation of compressive strength,” in *Proc., 7th International Brick Masonry Conference*, Melbourne, Australia, 1985, vol. 1, pp. 653–664.

[8] K. A. Heathcote and E. Jankulovski, “Aspect ratio correction factors for soilcrete blocks,” *Trans. Inst. Eng. Aust. Civ. Eng.*, vol. 34, no. 4, pp. 309–312, 1992.

[9] G. Ruiz, X. Zhang, W. F. Edris, I. Cañas, and L. Garijo, “A comprehensive study of mechanical properties of compressed earth blocks,” *Constr. Build. Mater.*, vol. 176, pp. 566–572, Jul. 2018, doi: 10.1016/j.conbuildmat.2018.05.077.

[10] A. Hakimi, O. Fassi-Fehri, H. Bouabid, S. C. D’ouazzane, and M. E. Kortbi, “Comportement mécanique non linéaire du bloc de terre comprimée par couplage élasticité endommagement [Non-linear behaviourof the compressed earthen block by elasticity-damage coupling],” *Mater. Struct.*, vol. 32, no. 7, pp. 539–545, Aug. 1999, doi: 10.1007/BF02481639.

[11] F. Champiré, A. Fabbri, J.-C. Morel, H. Wong, and F. McGregor, “Impact of relative humidity on the mechanical behavior of compacted earth as a building material,” *Constr. Build. Mater.*, vol. 110, pp. 70–78, May 2016, doi: 10.1016/j.conbuildmat.2016.01.027.

[12] C. H. Kouakou and J. C. Morel, “Strength and elasto-plastic properties of non-industrial building materials manufactured with clay as a natural binder,” *Appl. Clay Sci.*, vol. 44, no. 1–2, pp. 27–34, Apr. 2009, doi: 10.1016/j.clay.2008.12.019.

[13] P. Chauhan, A. El Hajjar, N. Prime, and O. Plé, “Unsaturated behavior of rammed earth: Experimentation towards numerical modelling,” *Constr. Build. Mater.*, vol. 227, p. 116646, Dec. 2019, doi: 10.1016/j.conbuildmat.2019.08.027.

[14] B. V. Venkatarama Reddy, R. Lal, and K. S. Nanjunda Rao, “Enhancing bond strength and characteristics of soil-cement block masonry,” *J. Mater. Civ. Eng.*, vol. 19, no. 2, pp. 164–172, Feb. 2007, doi: 10.1061/(ASCE)0899-1561(2007)19:2(164).

[15] Q.-B. Bui, S. Hans, J.-C. Morel, and A.-P. Do, “First exploratory study on dynamic characteristics of rammed earth buildings,” *Eng. Struct.*, vol. 33, no. 12, pp. 3690–3695, Dec. 2011, doi: 10.1016/j.engstruct.2011.08.004.

[16] S. A. Klink, “Actual Poisson ratio of concrete,” *ACI J.*, vol. 82, no. 74, pp. 813–817, 1985.

[17] A. Boumiz, C. Vernet, and F. C. Tenoudjif, “Mechanical properties of cement pastes and mortars at early ages,” *Adv. Cem. Based Mater.*, vol. 3, no. 3–4, pp. 94–106, 1996.

[18] R. Narayan Swamy, “Dynamic Poisson’s ratio of Portland cement paste, mortar and concrete,” *Cem. Concr. Res.*, vol. 1, no. 5, pp. 559–583, Sep. 1971, doi: 10.1016/0008-8846(71)90060-3.

[19] ASTM, *Standard test method for particle-size distribution (gradation) of soils using sieve analysis*. West Conshohocken, PA: ASTM, 2017.

[20] ASTM, *Standard test method for particle-size distribution (gradation) of fine-grained soil using the sedimentation (hydrometer) analysis*. West Conshohocken, PA: ASTM, 2017.

[21] ASTM, *Standard test methods for liquid limit, plastic limit, and plasticity index of soils*. West Conshohocken, PA: ASTM, 2017.

[22] ASTM, *Standard test methods for laboratory compaction characteristics of soil using standard effort (12 400 ft-lbf/ft3 (600 kN-m/m3))*. West Conshohocken, PA: ASTM, 2012.

[23] ASTM, *Standard practice for classification of soils for engineering purposes (Unified Soil Classification System)*. West Conshohocken, PA: ASTM, 2011.

[24] M. C. Jiménez Delgado and I. C. Guerrero, “The selection of soils for unstabilised earth building: A normative review,” *Constr. Build. Mater.*, vol. 21, no. 2, pp. 237–251, Feb. 2007, doi: 10.1016/j.conbuildmat.2005.08.006.

[25] T. Morton, *Earth masonry design and construction guidelines*. Bracknell: IHS BRE Press, 2008.

[26] H. Houben, V. Rigassi, and P. Garnier, *Compressed earth blocks: production equipment*, 2nd ed. Brussels: CDI and CRATerre-EAG, 1996. [Online]. Available: https://books.google.com/books?id=g1ogAAAACAAJ

[27] M. A. Sutton, J. J. Orteu, and H. Schreier, *Image correlation for shape, motion and deformation measurements: basic concepts, theory and applications*. Springer, 2009.

[28] R. Ghorbani, “Context-sensitive seismic strengthening and repair of substandard confined masonry,” Doctoral dissertation, University of South Carolina, Columbia, 2014. [Online]. Available: https://scholarcommons.sc.edu/etd/3038

[29] D. Silveira, H. Varum, and A. Costa, “Influence of the testing procedures in the mechanical characterization of adobe bricks,” *Constr. Build. Mater.*, vol. 40, pp. 719–728, Mar. 2013, doi: 10.1016/j.conbuildmat.2012.11.058.

4.7 TABLES

Table 4.1 Modulus of elasticity reported in the literature for earthen materials

Reference	Material	Mean [MPa]	Definition	Specimen type	Aspect ratio	Measuring method
[9]	CSEB	5640±1800	Not specified	Prism	2	Extensometer
[29]	Adobe	13214	Secant at 1/3 of peak stress	Cylinder	1.8	Extensometer
[29]	Adobe	1777	Secant at peak stress	Cylinder	1.8	Extensometer
[14]	Mortar	6574	Initial tangent	Prism	2	Extensometer
[14]	CSEB[1]	8000	Initial tangent	Prism	2	Extensometer
[11]	CEB cores	2000-5000	Secant modulus[2]	Cylinder	2	3D-DIC
[12]	Pressed adobe blocks	950	Equivalent modulus[3]	Prism	2	Sensors between machine pistons
[12]	Pressed adobe blocks	450	Initial tangent modulus[3]	Prism	2	Sensors between machine pistons

[1]Saturated condition
[2]Specimen tested at 25% relative humidity and with unload-reload cycles up to 60% of peak stress
[3]Unload-reload cycles up to 30% of peak stress

Table 4.2 Soil properties

Test method	Range
Particle size distribution (ASTM D6913 [19], D7928 [20])	
Sand passing No.4 sieve and retained on No. 200 sieve	14-59%
Silt size, 0.074 to 0.005 mm	11-63%
Clay size, smaller than 0.005 mm	22-37%
Liquid Limit, Plastic Limit, and Plasticity Index (ASTM D4318 [21])	
Liquid limit	30-49%
Plastic index	10-23%
Optimum moisture content (ASTM D698 [22])	12-22%

Table 4.3 Testing matrix

ID	Aspect ratio	Nominal dimensions [mm]			Number of specimens			Loading rate	
		Diameter or base	Length	Height	Test setup		Total	mm/ sec	με/ sec
Cylinders									
C0.5	0.5	64	—	32	3D-DIC	4	4	0.01	313
C1.0	1.0	64	—	64	3D-DIC	5	5	0.01	156
C2.0	2.0	64	—	127	3D-DIC	5	23	0.01	79
					Pointwise and 3D-DIC	3			
					Pointwise	15			
Prisms									
P0.7	0.7	127	178	90	3D-DIC	6	6	0.03	333
P2.0	2.0	84	89	178	3D-DIC	9	9	0.01	79

Table 4.4 Stereo-vision systems features

Feature		System 1	System 2	
Lenses	Reference	AF Nikkor 50mm f/1.8D	XENOPLAN 1.9/35-0511	TAMRON 23FM16SP
	Focal length	50 mm	35 mm	16 mm
	Aperture	f/8	f/8	f/8
Camera	Reference	GRAS-50S5M-C	GS3-U3-91S6M-C	
	Sensor name	Sony ICX625	Sony ICX814	
	Megapixels	5	9.1	
LED lights		3	2	
Working distance		~2200 mm	~1200 mm	~600 mm
Stereo angle		14°	13°	15°

Table 4.5 3D-DIC measurements error as function of stereo-angle

	Strain		Displacement	
Angle	Transverse [με]	Axial [με]	Transverse [mm]	Axial [mm]
14°	359	71	0.0014	0.0009
18°	227	65	0.0010	0.0006
26°	94	51	0.0006	0.0006
39°	165	100	0.0004	0.0008

Table 4.6 Summary of experimentally characterized CSEB elastic properties

Property	Specimen type	Mean	SD	CV
Young's modulus [MPa]	C2.0	2457	697	28%
	P2.0	2533	874	35%
Poisson's ratio ν [-]	C2.0	0.152	0.059	36%

4.8 FIGURES

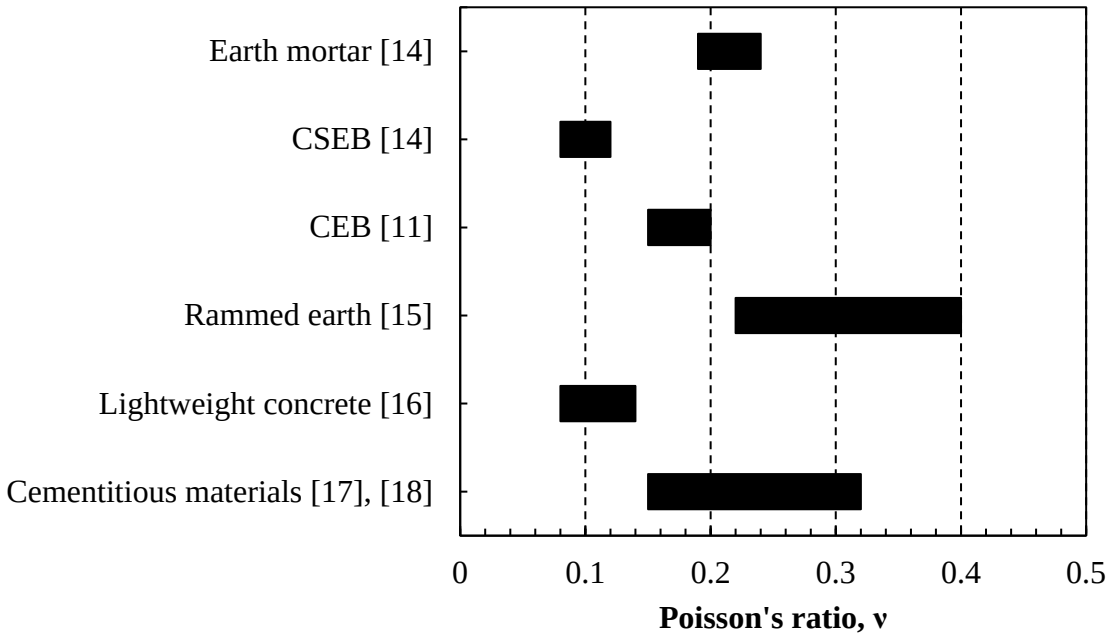

Figure 4.1 Poisson's ratio reported in literature for earthen materials and cementitious materials

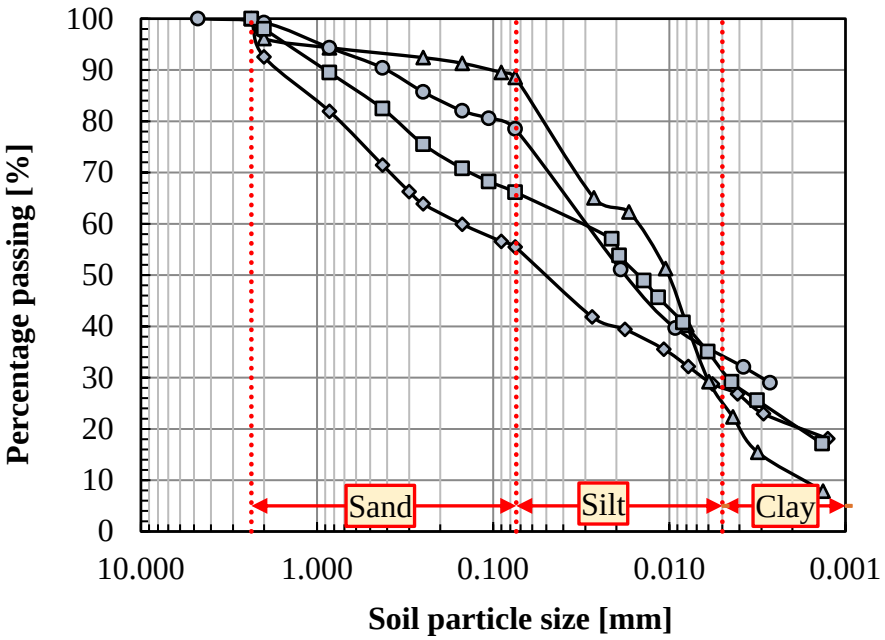

Figure 4.2 Representative particle particle-size distribution curves

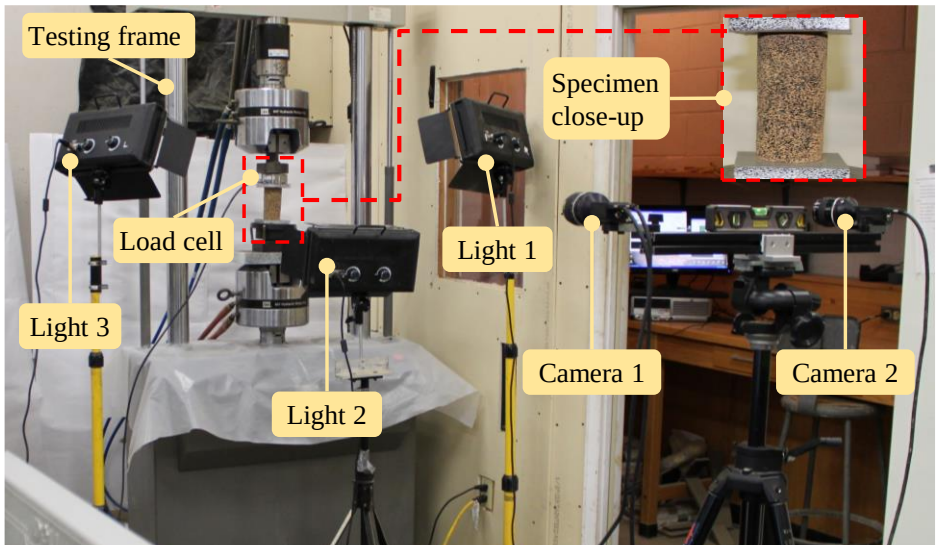

(a)

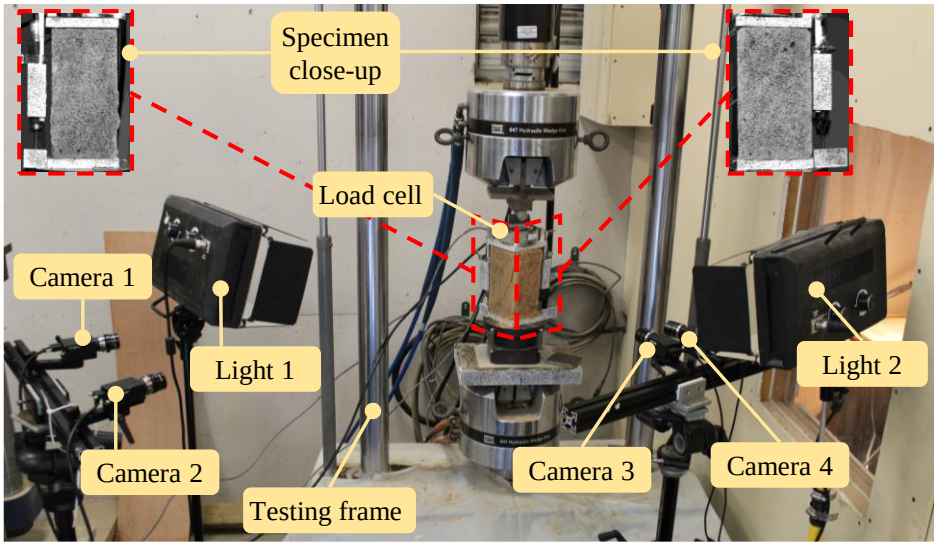

(b)

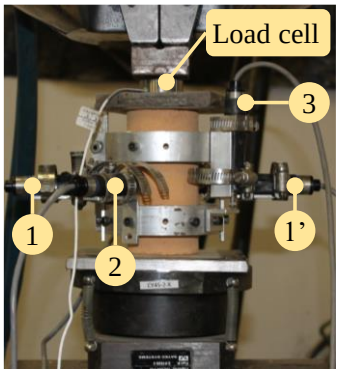

(c)

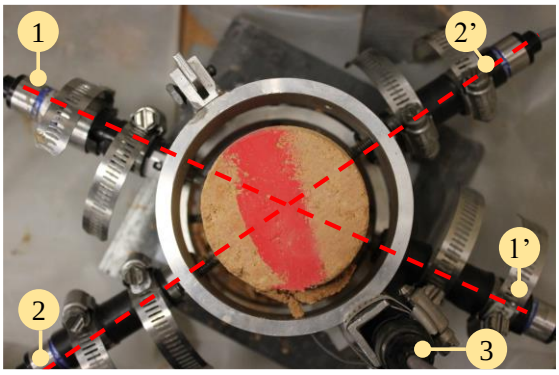

(d)

Figure 4.3 Compression tests setups:3D-DIC setup with stereo-vision (a) System 1 and (b) System 2; (c-d) Pointwise setup for C2.0 with two aligned pairs of horizontal displacement transducers, 1-1', 2-2', and one vertical displacement transducer, 3

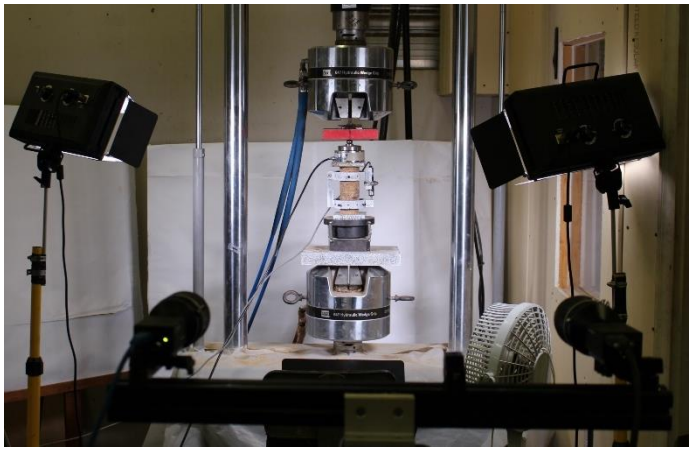

(a)

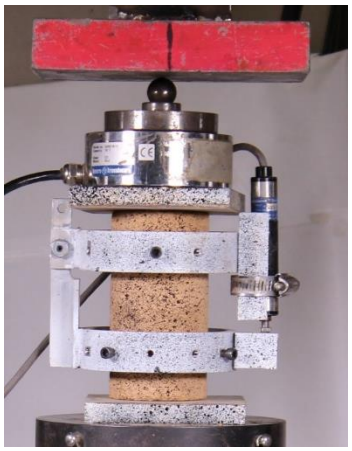

(b)

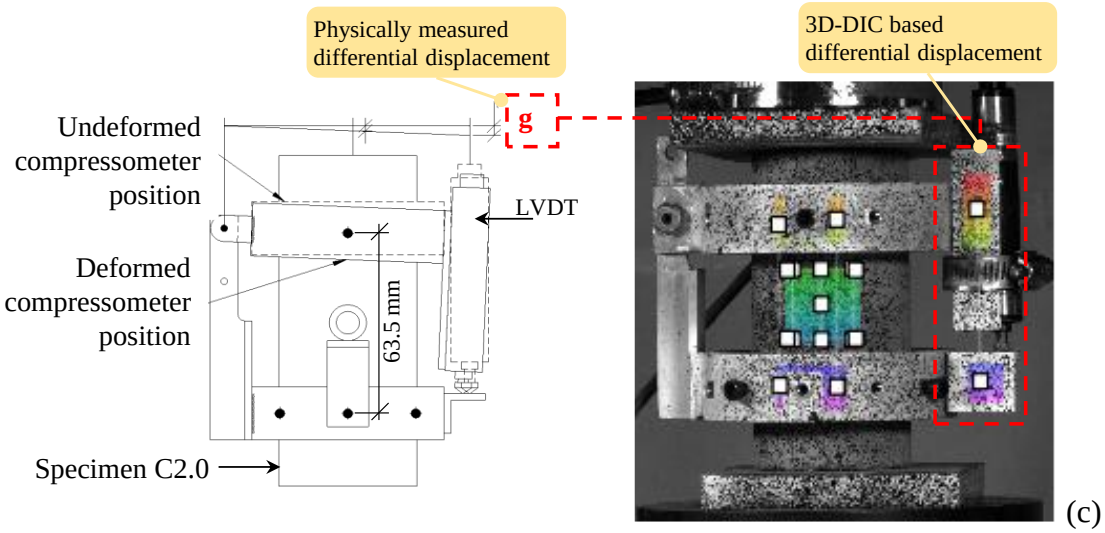

(c)

Figure 4.4 Pointwise and 3D-DIC setup for measuring method validation


(a)

(b)


(c)

Figure 4.5 Specimen's surface preparation for 3D-DIC measurements: (a) manual printing of speckle pattern with a stiff toothbrush; final result for representative (b) C2.0 and (c) P0.7 specimens

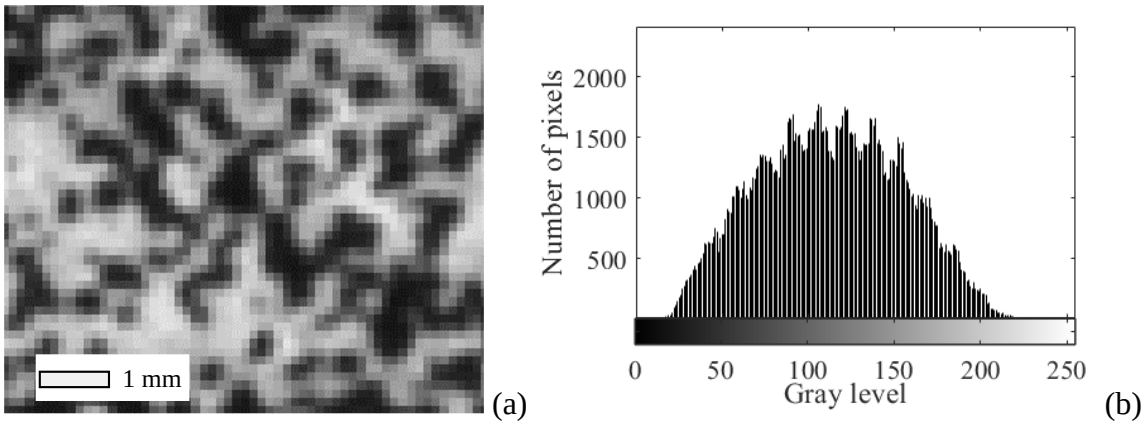

Figure 4.6 Speckle-pattern: (a) close-up view of speckle-pattern sampled by at least 3 x 3 pixels (2) representative histogram of gray levels

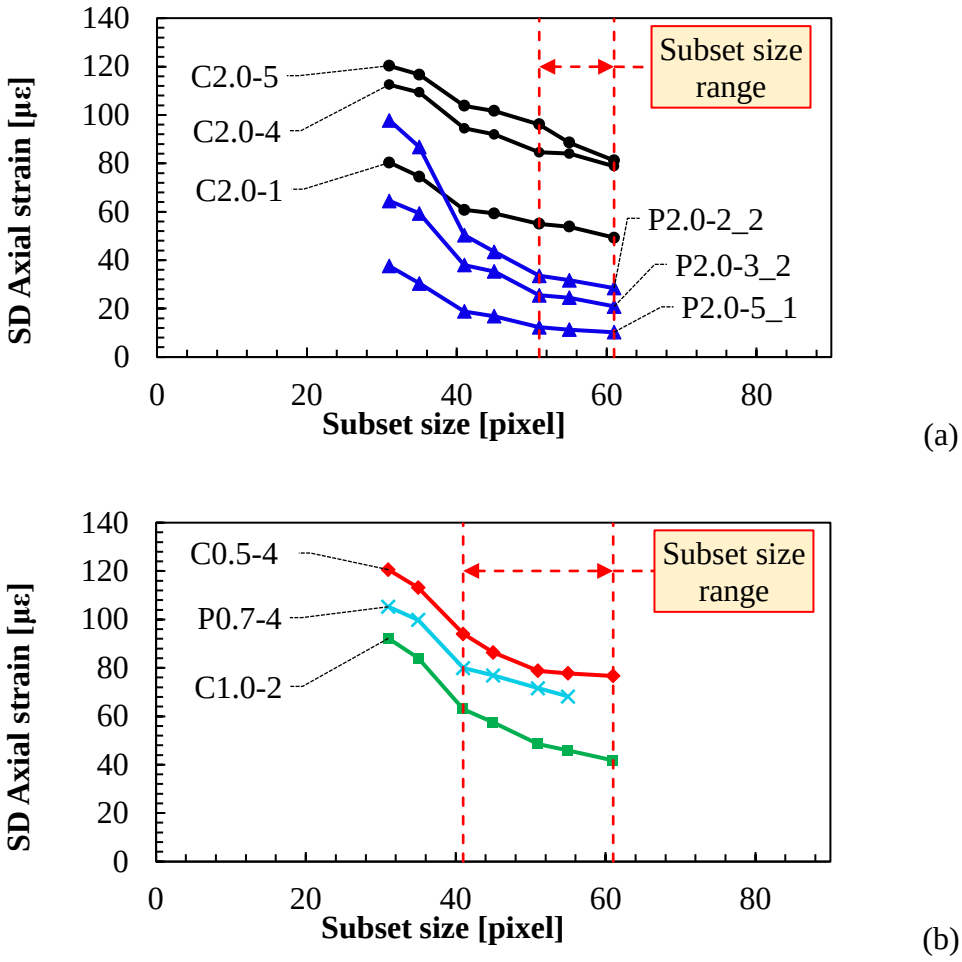

Figure 4.7 Representative results of 3D-DIC analysis subset size based on standard deviation error assessment for axial strain as function of subset size

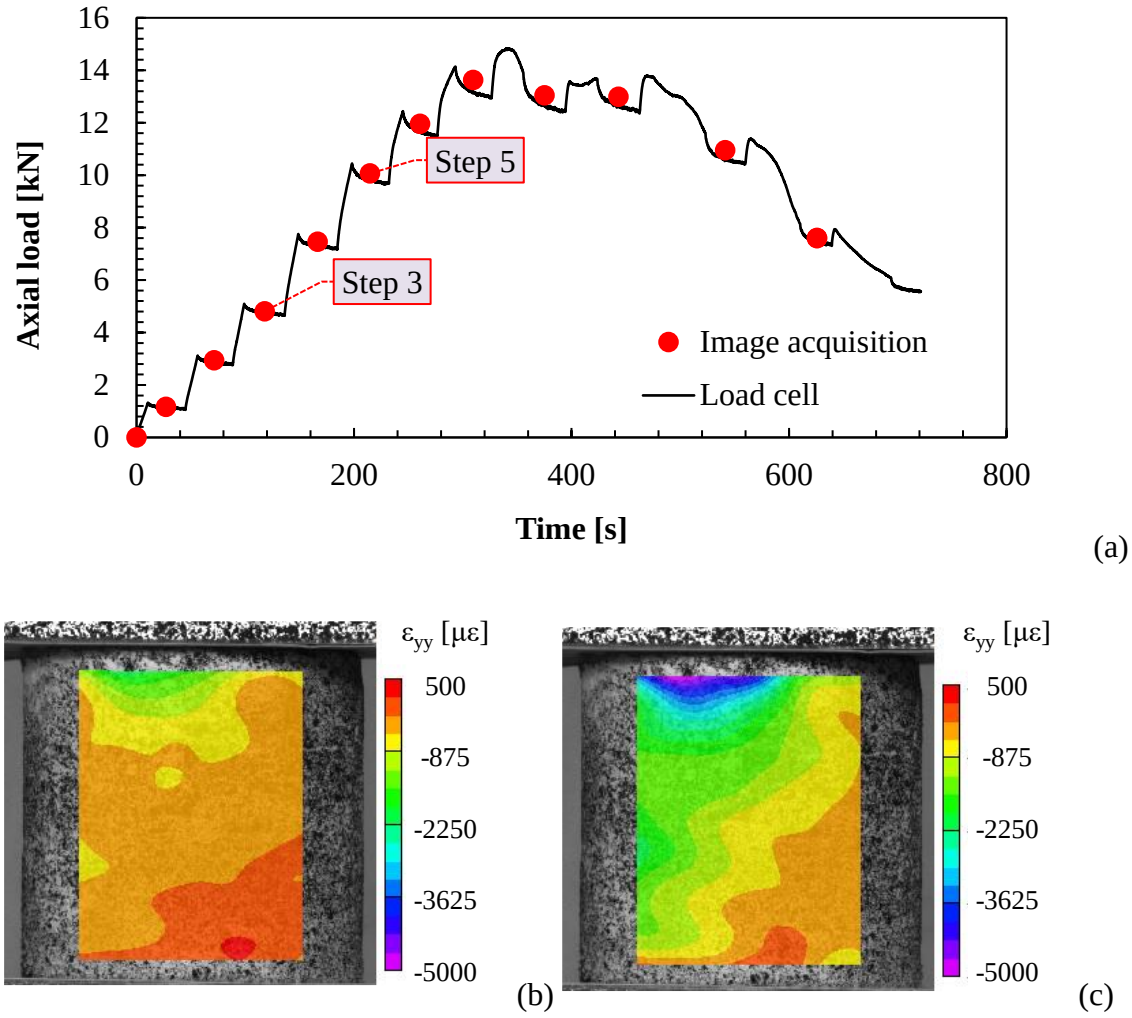

Figure 4.8 3D-DIC acquisition during uniaxial compression tests: (a) loading protocol indicating load steps for image acquisition of a specimen C1.0, (b) 3D-DIC based axial strain map at Step 3, and (c) at Step 5

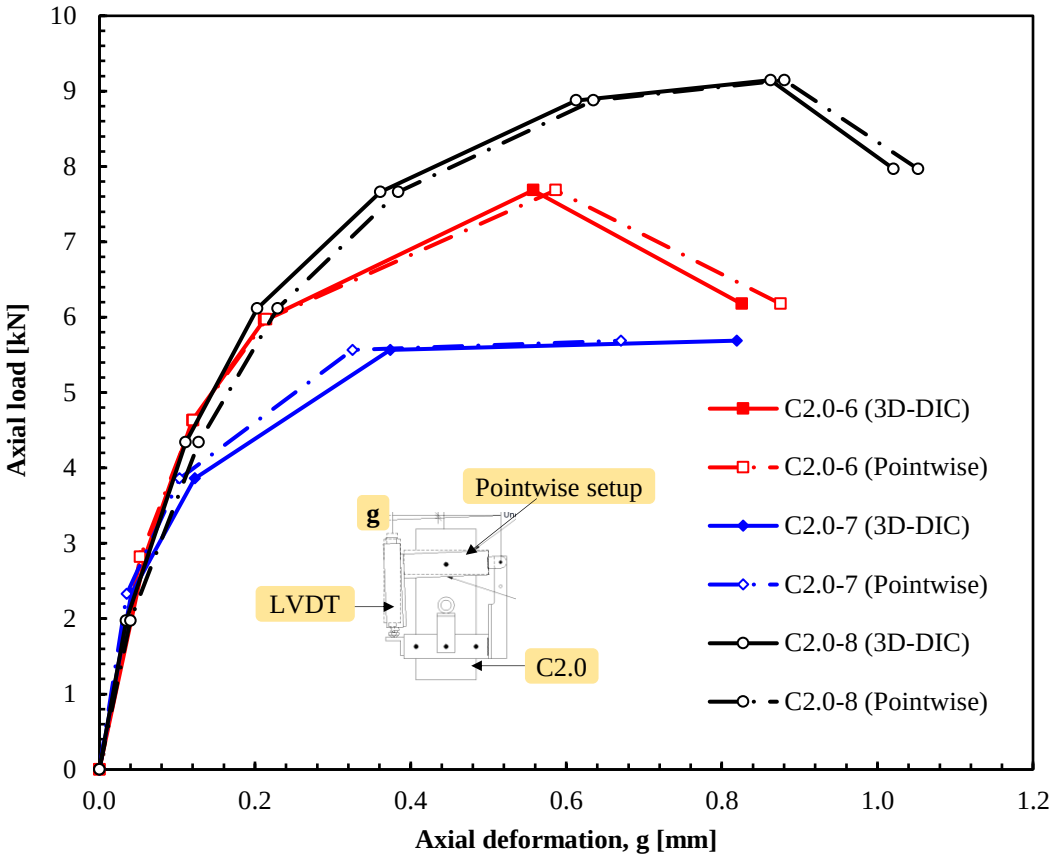

Figure 4.9 Representative validation test results comparing load-displacement relations simultaneously measured at point “g” using Pointwise and 3D-DIC setups

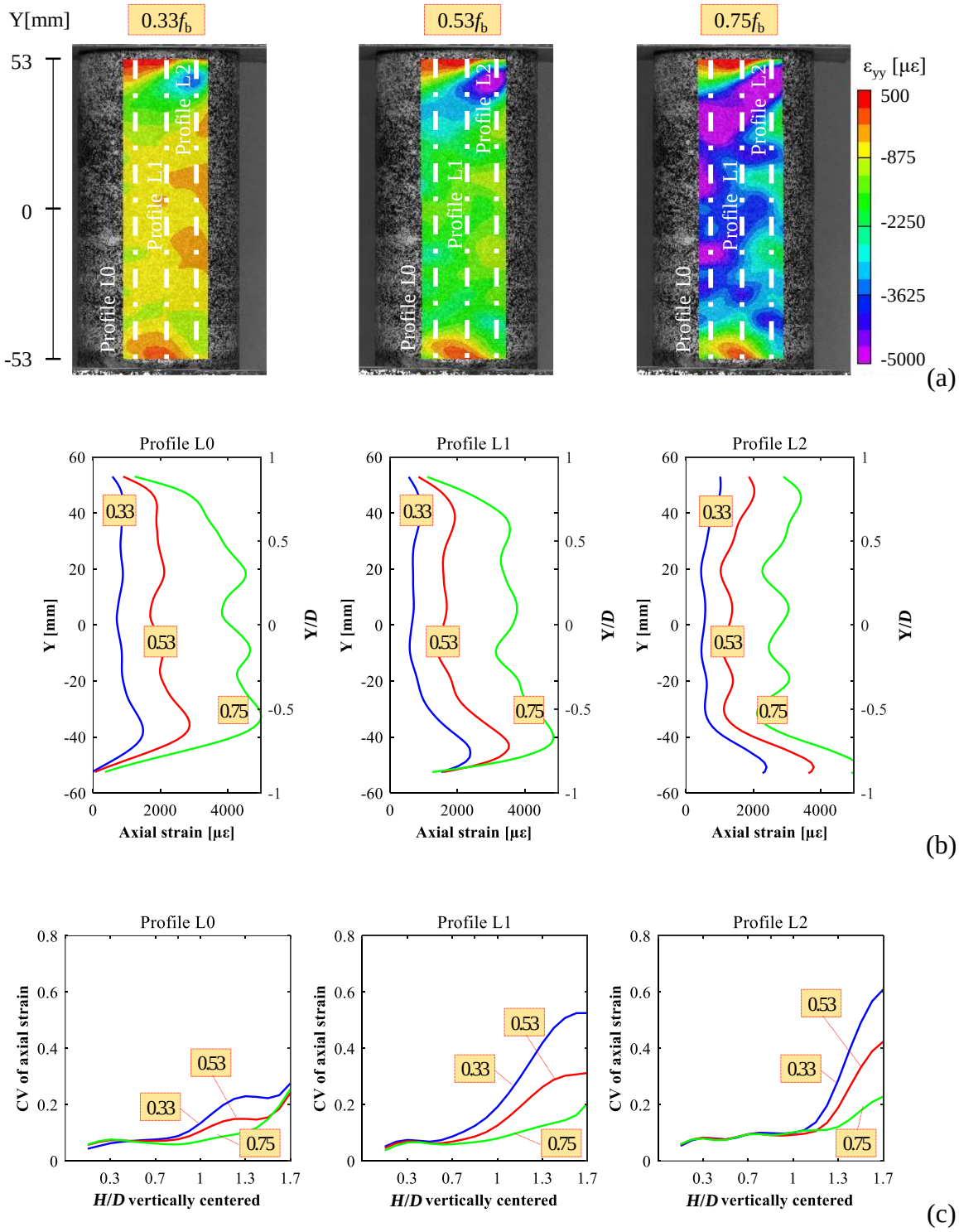

Figure 4.10 Representative results of nonuniformities assessment on strain distribution in a specimen C2.0: (a) axial strain map indicating planes from which strain profiles were extracted; (b) axial strain distribution at different stress levels relative to f_b; (c) CV of axial strain along different height portions

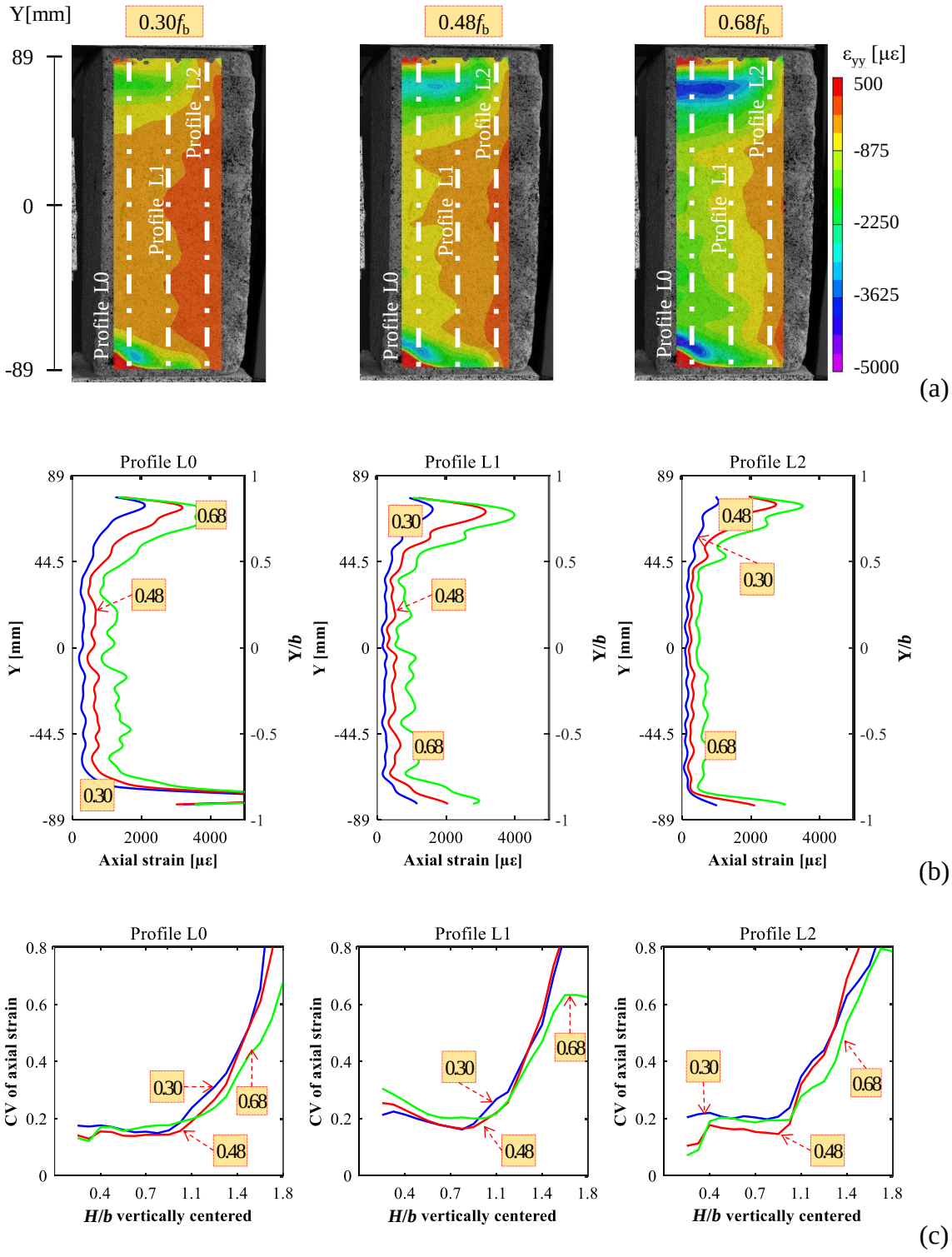

Figure 4.11 Representative results of nonuniformities assessment on strain distribution in a specimen P2.0: (a) axial strain map indicating planes from which strain profiles were extracted; (b) axial strain distribution at different stress levels relative to f_b; (c) CV of axial strain along different height portions

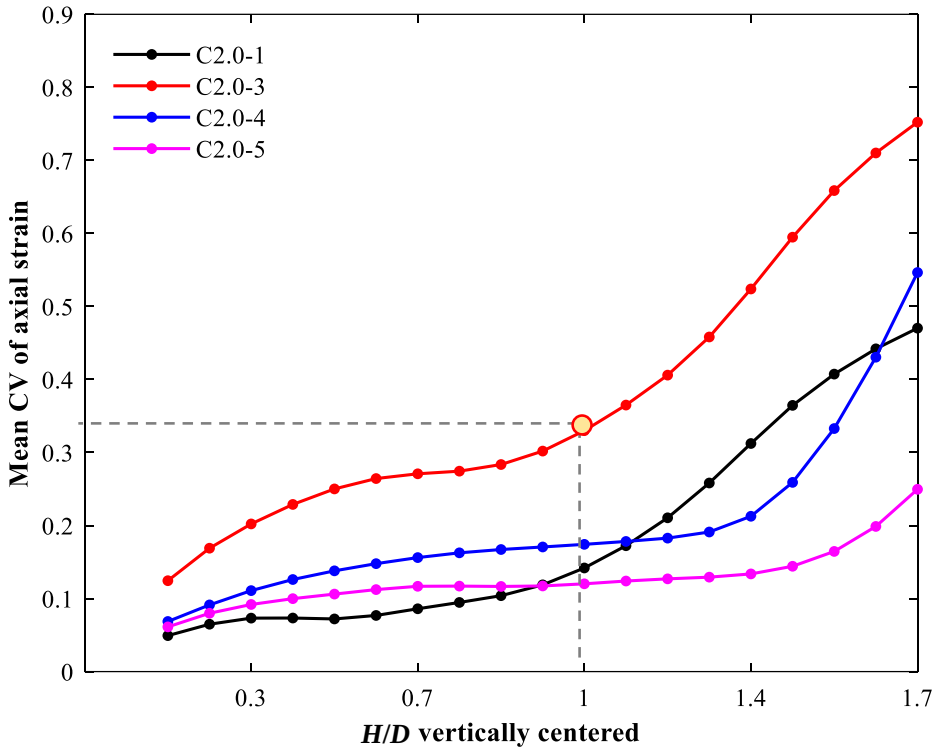

(a)

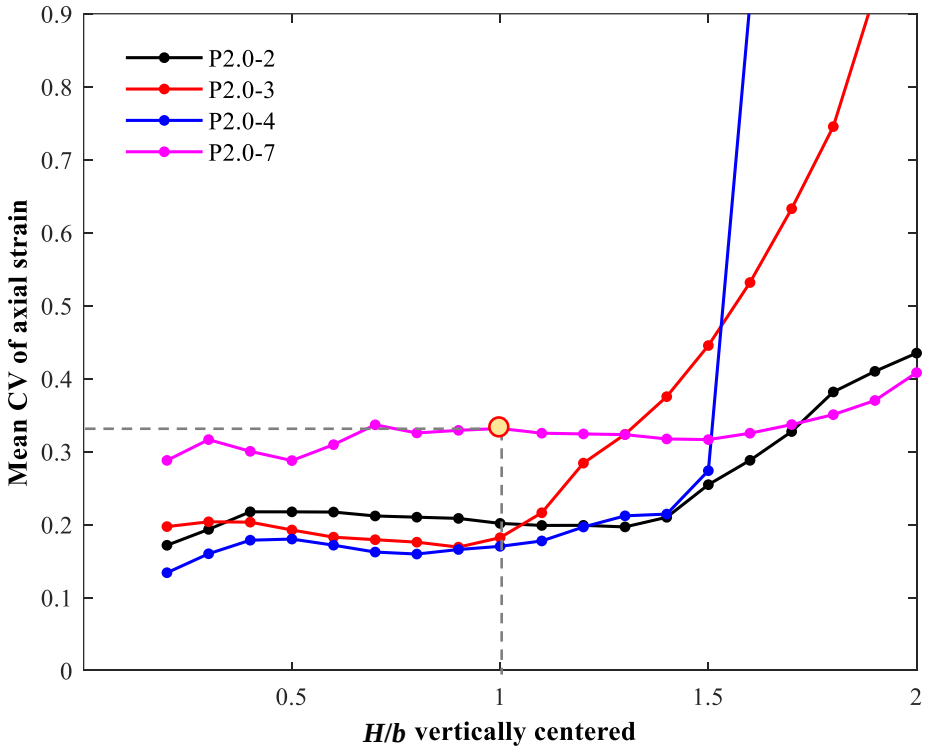

(b)

Figure 4.12 Summary of strain variation assessment throughout specimen height at approximately 0.3f_b: (a) specimens C2.0; (b) specimens P2.0

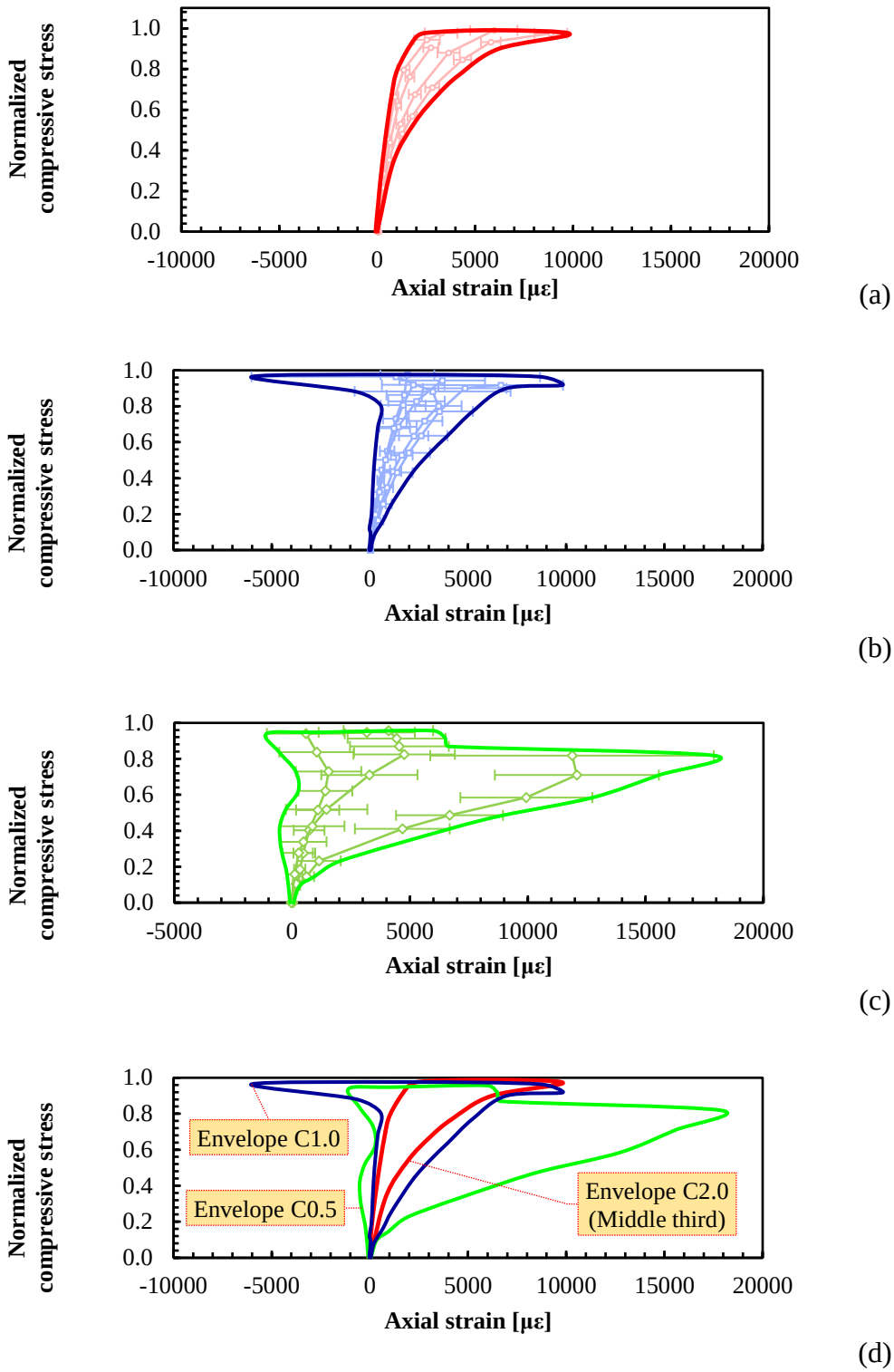

Figure 4.13 Normalized stress-strain response of cylinder specimens: (a) C2.0; (b) C1.0; (c) C0.5; (d) envelopes

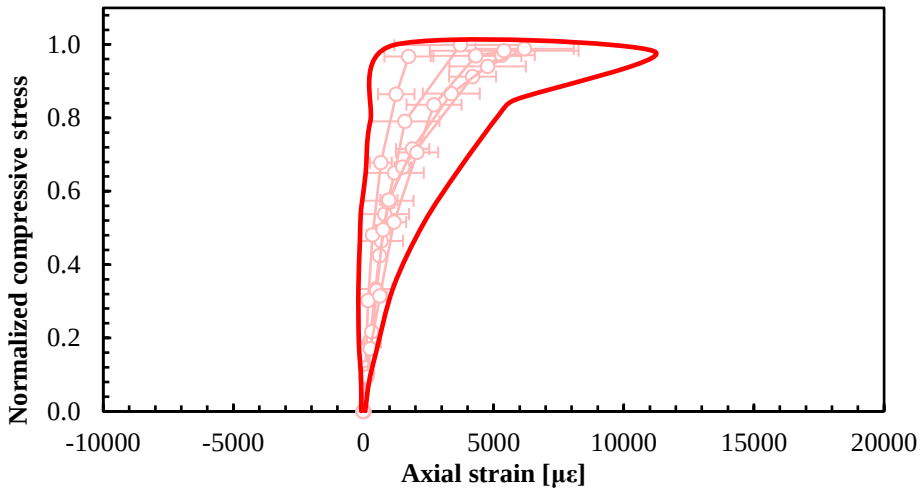

(a)

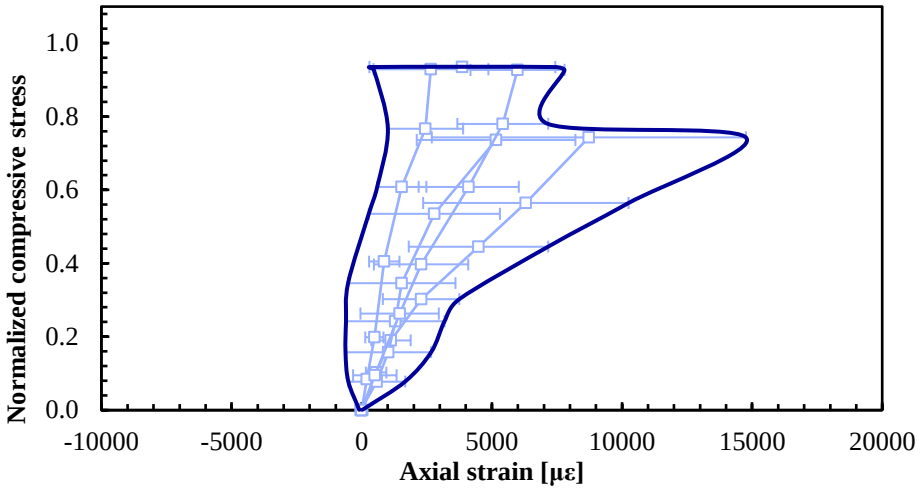

(b)

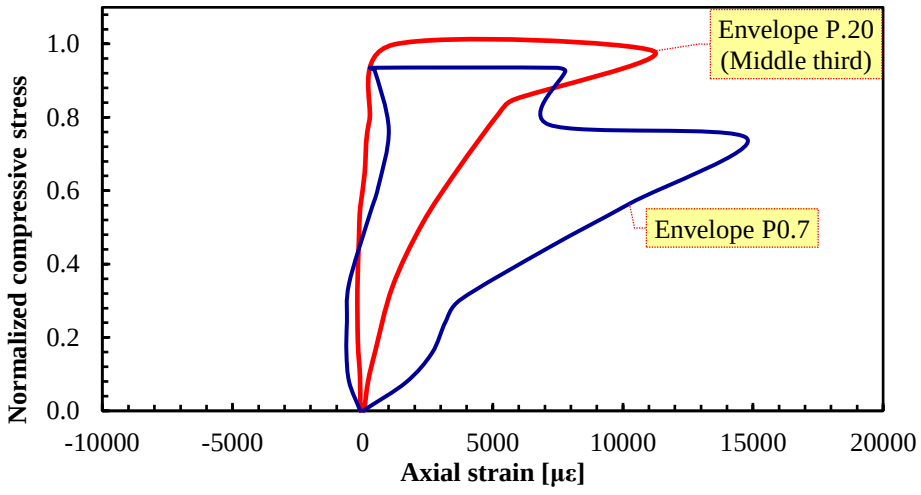

(c)

Figure 4.14 Normalized stress-strain prism specimens: (a) P2.0; (b) P0.7; (c) envelopes

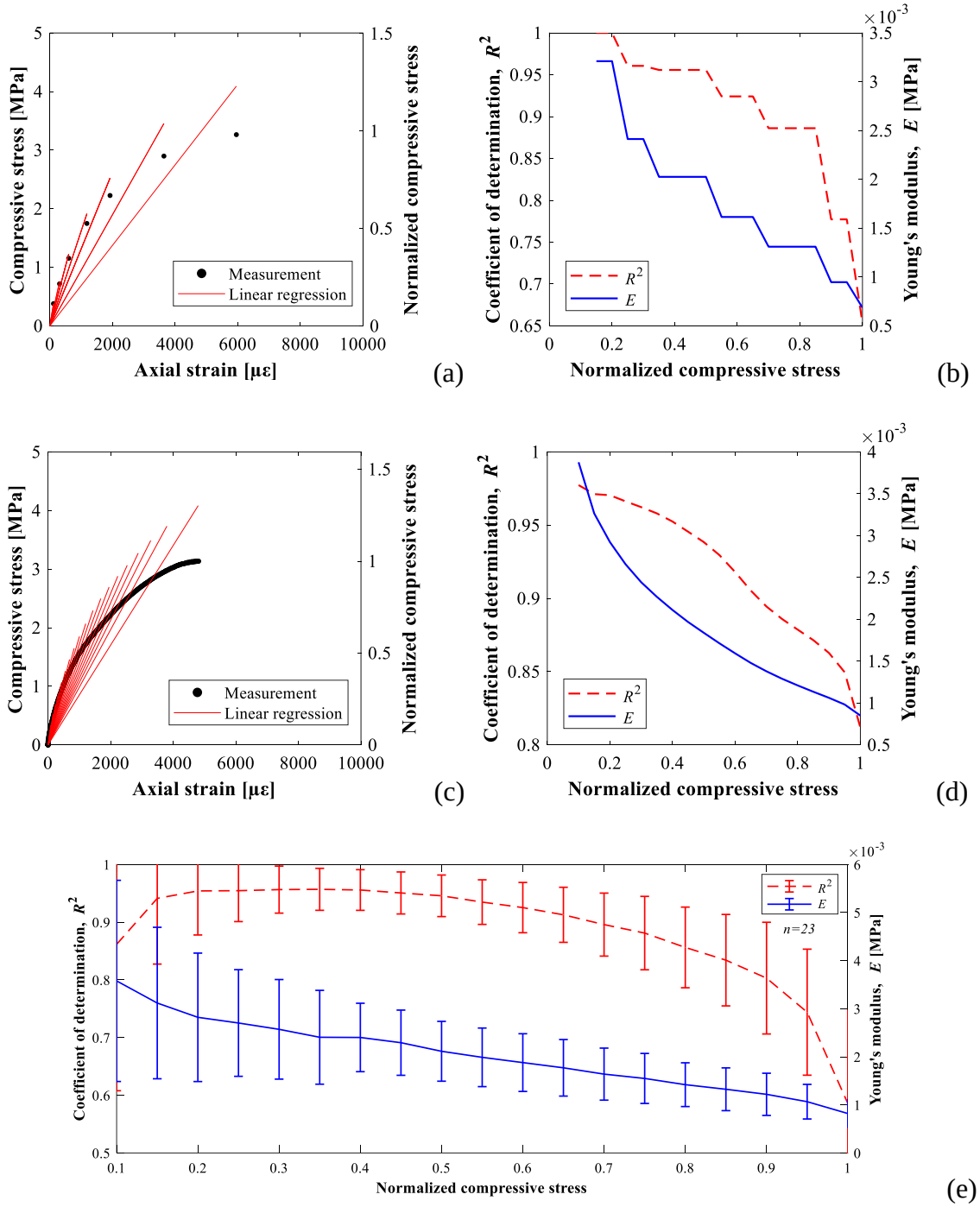

Figure 4.15 Representative results of assessment of loss of linearity for C2.0 specimens: stress-strain response with linear regressions at different stress levels (a) based on 3D-DIC for C2.0-5, (c) and based on pointwise deformation measurements for C2.0-17; R^2 and E as a function of normalized compressive stress for (b) C2.0-5 and (d) C2.0-17; (e) mean and SD (error bars) of R^2 and E from all specimens as a function of normalized compressive stress

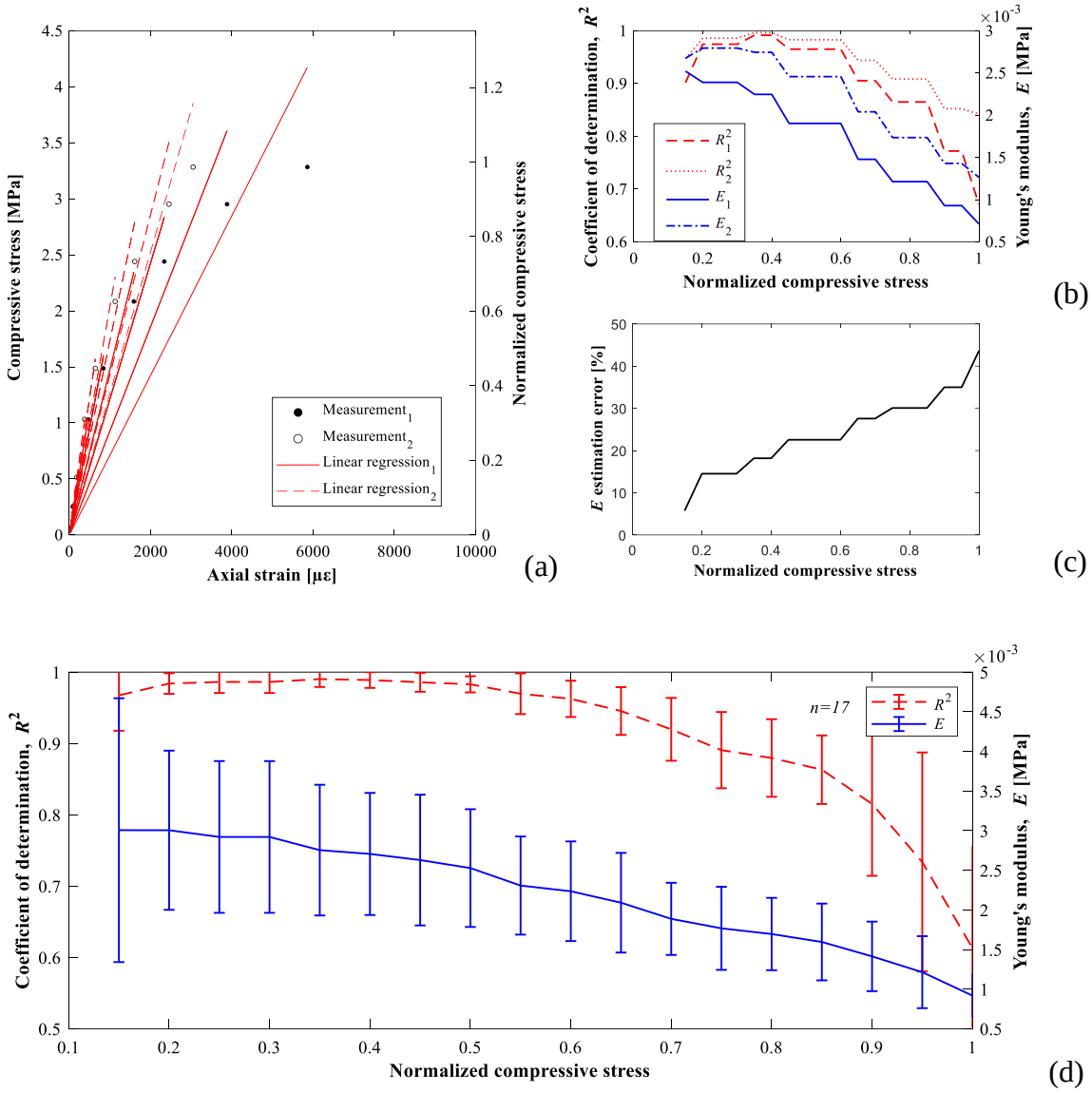

Figure 4.16 Representative results of assessment of loss of linearity for P2.0 specimens: (a) stress-strain response with linear regressions at different stress levels based on 3D-DIC measurements on two surfaces of the same specimen; (b) R^2 and E as a function of normalized compressive stress; (c) error in estimation of E with measurements on two surfaces; (d) mean and SD (error bars) of R^2 and E from all specimens as a function of normalized compressive stress

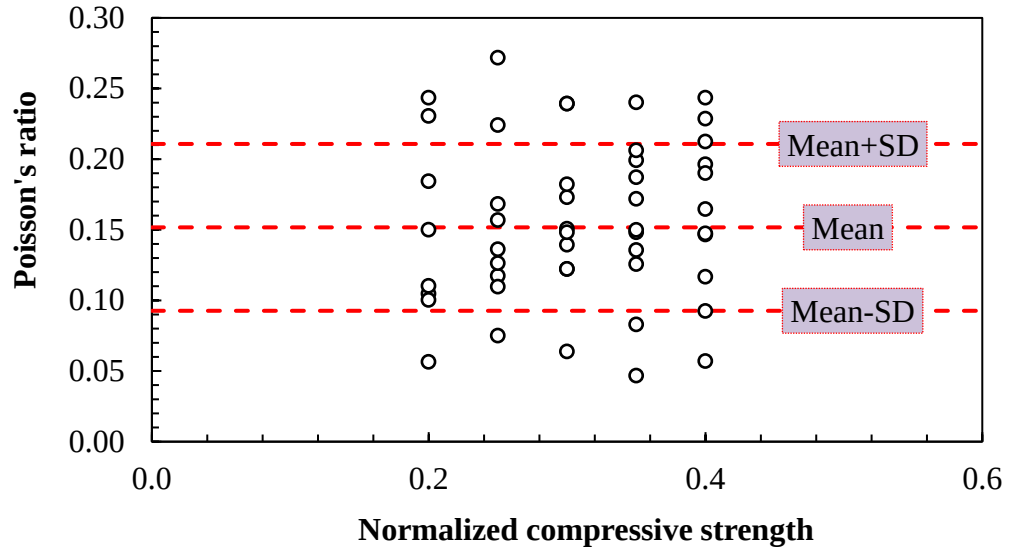

Figure 4.17 Poisson's ratio determined up to 0.4f_b from deformation measurements within middle-third of C2.0 specimens

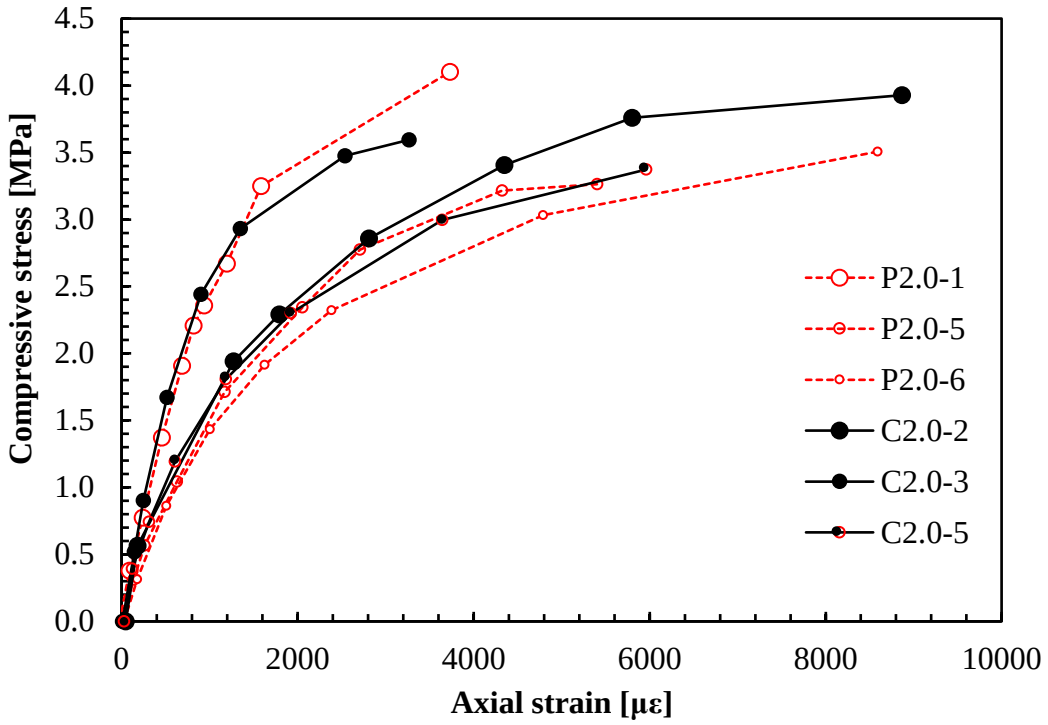

Figure 4.18 Representative stress-strain curves from middle third of C2.0 and P2.0 specimens

CHAPTER 5: COLLABORATIVE HANDS-ON LEARNING FOR STEM OUTREACH: MULTI-YEAR ASSESSMENT OF K-12 WORKSHOP ON HAZARD-RESISTANT EARTH MASONRY CONSTRUCTION[4]

[4] Erika L. Rengifo-López., Charles E. Pierce, and Fabio Matta. To be submitted to *Journal of STEM Education Innovations and Research*.

ABSTRACT. Conducting K-12 outreach programs on university or college campuses focused on science, technology, engineering, and mathematics (STEM) disciplines is an essential part of the multifaceted effort for preparing future generations of engineers and scientists. However, the lack of knowledge to design programs that maximize the potential impact poses a challenge. This paper contributes to reducing this gap through a five-step adaptable framework whose intent is to provide meaningful structure for on-campus STEM outreach activities that emphasize collaborative, hands-on learning experiences for pre-college students. Successful implementation of the framework is demonstrated through the design of a civil engineering workshop on hazard-resistant earth masonry, and its evaluation through the analysis of students' feedback from three summer workshops between 2017 and 2019.

5.1 INTRODUCTION

Preparing students to be the engineers and scientists of tomorrow remains a critical challenge for our national education system. The science, technology, engineering, and mathematics (STEM) workforce in the United States is essential to improve our standards of living, sustain economic growth, and ensure global competitiveness [1]. Demand for STEM workers continues to rise as more occupations require their expertise. The Bureau of Labor Statistics [2] estimates a 9.5% growth in science and engineering employment during the 10-year period from 2019-2029. This rate is about 2.5 times higher than the projected increase of 3.7% for all occupations. Meeting the future demand for STEM professionals requires a sustained and multifaceted effort to inform and motivate pre-college students to pursue STEM in higher education.

Informal learning during out-of-school time is one important mechanism for educating K-12 students about STEM fields. Beyond-the-classroom experiences are crucial to student growth and development [3] and can influence their decisions on career choices [4]. Outreach programs, in particular, provide an informal learning environment for pre-college students to explore personal interests and test their abilities without the pressure to perform for a grade [5]. Thus, most outreach programs become important recruitment tools for increasing enrollments and broadening representation in STEM majors at colleges and universities. Whether or not students choose to pursue STEM careers, the broader impacts of outreach on changing negative perceptions of engineers and scientists [6] and improving scientific literacy [7] are significant.

Jeffers et al. [7] categorized STEM outreach programs into six general approaches: develop and/or deliver K-12 classroom materials; conduct outreach activities at K-12 schools or on a college or university campus; conduct or sponsor student contests or competitions; sponsor college student teaching fellows or offer service-learning opportunities; and professional development for K-12 teachers. Regardless of approach, two main characteristics of outreach are the inclusion of real-life context and active involvement of people (e.g., faculty, professionals, students) not affiliated with K-12 schools [5]. Those individuals are an important part of the program, as a common theme of successful outreach is having engaged role models to share knowledge and excite participants about STEM fields [7]. Engaged role models can also facilitate active learning through hands-on activities, which is a significant feature of most programs [4]–[7]. Bugallo and Kelly [6] found that outreach to K-12 students is most effective when

using inductive learning approaches, such as discovery-based learning, inquiry-based learning, and problem-based learning.

There are three models for K-12 student programs held on a college campus. The first model is for after-school events that take place during the school year. Most can be characterized as one-time, short-duration activities that span an hour or two, although some events are designed for a full day. After-school events can be structured to accommodate a larger number of students, although it varies as a function of format, location, and contact time. Examples include on-campus events for Science Days and Engineers Week, or E-Week, which is a national outreach effort that occurs annually in February. The second model is a summer camp, residential and non-residential, where students spend a moderate to extended period on campus. A one-week camp is the most common, although some camps run for two weeks or more. Camps can expose students to multiple disciplines, like the chemical, civil, electrical, environmental, and mechanical engineering fields [8] or immerse students in a discipline-specific experience, such as the transportation camp described in [9]. Most camps limit student participation and therefore tend to impact fewer students than after-school events. The third model is a research internship. In most cases, internships engage one or a few high-achieving high school students in authentic research experiences on campus. The experience can be concentrated in the summer, often in an 8 to 10-week period, or spread across the academic year.

One of the challenges with K-12 outreach on campus is the lack of knowledge on how to construct and deliver an experience that maximizes potential impact. The purpose of this paper is to (1) propose an adaptable framework for developing STEM outreach

activities; (2) demonstrate the framework with a civil engineering example from a summer camp; and (3) evaluate student feedback as a measure of successful implementation of the framework.

5.2 METHODS

A pedagogical framework is proposed to provide meaningful structure for on-campus STEM outreach activities that emphasize collaborative hands-on learning experiences for pre-college students. The framework, shown in Figure 5.1, is an adaptation of the six-step developmental framework for Environments for Fostering Effective Critical Thinking, or EFFECTs, described in [10]. EFFECTs are problem-based learning (PBL) modules that feature active learning and collaborative learning. Modules constructed within this framework have proven successful across a range of instructional environments, including undergraduate engineering courses in a conventional classroom setting [11], [12], laboratory courses [13], [12], and high school science classes [14]. While civil engineering has been the focus for most modules, EFFECTs have been structured around other STEM content such as solar power [15] and software engineering [16]. Such broad application of this PBL framework in formal STEM instruction suggests it can be adapted for informal learning environments, including outreach programs.

5.2.1 SITUATED LEARNING

Establishing a situated learning environment is at the core of the modified EFFECTs framework for outreach. Situated learning is an instructional approach that places students at the center of the learning environment and engages them in cooperative participation throughout the experience. To situate learning, one must think and act with other learners in a specific place and time to acquire knowledge and create meaning from

their activities [17]. In other words, situated learning integrates content, context, community, and participation [17]. Learning is a social process and working together to solve real life problems is essential to that process. Situated learning centralizes student learning in co-participation [18], [17], [19], [20].

Selecting an appropriate and authentic context where activities take place is important. The context provides the setting for examining experience [17] and should be situated in the same space that experts use to perform relevant knowledge- and skill-oriented tasks [20]. This means that students are often immersed in unfamiliar environments and challenged to use their intellect, critical thinking skills, and kinesthetic abilities to address a real problem. For example, situated learning environments have been created in undergraduate science and engineering undergraduate lab courses delivered via traditional face-to-face [21] or virtual instruction [22]. Similarly, K-12 outreach activities on campus can leverage STEM research labs to create situated learning environments. Having students perform activities in a research lab provides opportunities to explore how concepts and skills can be applied in the context of conducting research.

The proposed five-step framework is shown in Figure 5.1. The first two steps are intertwined. Step 1 is to identify the core knowledge that is most significant or desirable for students to learn. That knowledge can be represented through a set of concepts or ideas of what something is or how something works. In other words, there should be a plan for what content knowledge could or should be acquired during the outreach activity. However, the goal is not to enforce or limit learning to a prescribed set of concepts. In fact, the nature of situated learning can give rise to unintended or unexpected

conceptual learning. Step 2 is to design student-centered activities that can reveal the pre-identified concepts. Activities can be conducted using one or more active learning strategies or achieved through purposeful exercises. Exercises can be mental or physical and should represent something performed or practiced to develop a specific cognitive or psychomotor skill. Whether activities are designed for hands-on or minds-on learning, having students exchange ideas and navigate tasks in a cooperative manner is essential. As illustrated in Figure 5.1, the selection of concepts and activities is often an iterative back-and-forth process.

Step 3 considers the practical applications of core knowledge identified in Step 1. The purpose of this step is to choose one representative application for the students to learn about, rather than presenting them with all the possibilities. In this way, their experience is focused on how specific STEM concepts can be used in a singular scientific or engineering practice, which could involve analysis, design, development, or prediction associated with that particular application. A civil engineering example of an application is the design of a dam. Step 4 intends to provide a meaningful context for the selected application. The purpose is to shift learning from a generic example to one that involves something significant or recognizable, such that it fosters a higher level of self-interest and motivation. The unique circumstances of how the Hoover Dam was designed and built in the 1930s represent one example of an historical context. Referencing a dam that is local to the area, specifically one that students would know about, is another approach for selecting a context. This context is for *situating the concepts* that have been identified within the framework and is not the same as the situated learning context that students experience in a real workplace environment, such as a research lab.

5.2.2 EXPLICIT VS. IMPLICIT PROBLEMS

In steps 1-4, there is an implicit problem that creates a backdrop for student activities. These should be real problems that are studied through scientific and engineering research. In an ideal situated learning environment, outreach activities are derived from or associated with a current research project being conducted in that particular laboratory. The spatial and temporal dimensions of that setting can create a sense of community amongst the students, making them feel a part of a real research lab in that moment. Students should be aware that their experience, regardless of how simple or complex it might seem, is affiliated with authentic research practices that contribute to making something better or discovering something new.

If the problem is implicit, then the students do not need to solve it. In practice, this means that the students are not expected to demonstrate, describe, or document a solution. Such an approach is appropriate and more convenient when instructional contact time is limited, or the problem is too complicated. In some cases, however, the outreach program can accommodate a problem-based learning approach. As shown in Figure 5.1, the framework can be extended to develop a driving question about an explicit problem using optional Step 5. The driving question frames and directs the entire learning experience, and students are tasked with concluding their experience with an answer. It is similar to a research question in that it prompts students to acquire new knowledge during the process of discovering an answer. More discussion on how to formulate driving questions can be found in [10].

5.3 Application example

The proposed pedagogical framework was applied to design a workshop on sustainable and hazard-resistant earth masonry for K-12 students. The workshop took place at the University of South Carolina (UofSC) within the Partners for Minorities in Engineering & Computer Science (PMECS) resident summer workshop program for three consecutive years (2017-2019) in which a total of 85 sophomore high-school students participated.

5.3.1 PMECS overview

PMECS is a business and education partnership formed in 1977 whose mission is to prompt underrepresented communities' participation in engineering and computer science professional careers. PMECS designs one-week technical workshops to motivate minority students in local high schools to pursue engineering and computer science degree programs in higher education. The specific objectives of PMECS's workshops are to (1) stimulate increased interest in applied math and science problems, (2) familiarize academically qualified minority students with career opportunities in engineering, and engineering-related fields, (3) inform students of the high school prerequisites necessary to enter a college of engineering or computer science, and (4) inspire students pursuing academic excellence in their high school course work. Nominated participants, appointed by a school representative (e.g., counselor, teacher) through an online form, must be a minority (i.e., African American, Native American, or Hispanic), be a rising 9^{th} through 12^{th} grader, and have a minimum overall B grade-point average [23]. PMECS provides grants to eligible students to attend the summer camp at minimum to no cost, and 9^{th}-grade students may apply to participate in the program for the three following years [24].

The workshops are held at UofSC every summer, hosting approximately 120 students. Through activities intended to be challenging and enjoyable, the program introduces different engineering fields to the participants, exposes them to role models in a college environment, and offers socializing opportunities [23]. The agenda typically starts with a welcoming day followed by four days of technical workshops, and a closure day. The sophomores' program includes three to five workshops every day, separated by lunch, dinner breaks, and social events. During 2017, 2018, and 2019, sophomores participated in a total of 12, 16, and 14 technical workshops, respectively. It is noted that the engineered earth masonry workshop (i.e., framework application example), was delivered in different schedules among consecutive years. In 2017, the workshop took place at the beginning of the week, and there were no preceding civil engineering-related activities. In 2018 and 2019, the workshop was scheduled on the last day of the workshop's series and after at least one other civil engineering-related activity.

5.3.2 ENGINEERED EARTH MASONRY WORKSHOP

The first four steps of the proposed modified EFFECTs framework (i.e., implicit problem approach) were implemented to design a half-day workshop on engineered earth masonry for K-12 students. This workshop was conceived as part of the broader impacts' integrated plan for a research project supported by the National Science Foundation (NSF) through grant 1537776 at UofSC, and companion grants 1537078 and 1850777 at Louisiana State University and University of California, Davis, and entitled "Collaborative Research: Engineered Earth Masonry for Affordable Seismic Resistant Low-Rise Buildings"[25]–[27]. This project addresses the growing demand for affordable, sustainable, and hazard-resistant low-rise buildings for households and

businesses. In fact, it fosters the use of locally available materials, such as soil, and job creation by applying low-cost technologies to offer reliable alternative solutions for real-life problems such as safe and energy-efficient housing shortage. Broader impacts, defined as the "project's potential to benefit society and contribute to the achievement of specific, desired societal outcomes," are fundamental components of an NSF-supported research project [28].

The objectives of the engineered earth masonry workshop were to (1) raise interest in pre-college students towards civil engineering, (2) enhance the understanding of civil engineering research efforts, and (3) create awareness about the relevance of low-tech research to address real-life problems. These objectives were addressed by introducing fundamental technical terminology and highlighting the potential of earth masonry as a sustainable, affordable, and structurally appropriate material through disseminating research results.

The program included two activities entailing hands-on and minds-on experiences. In the first one, the students participated in a 45-minute introductory presentation on engineered earth masonry for high-wind and seismic resistant houses. In the second activity, the students were taken to the materials laboratory to manufacture compressed and stabilized earth blocks (from hereon, referred to as CSEB making). Figure 5.2 illustrates the relation between the four steps of the framework and the engineered earth masonry workshop components.

According Step 1, three learning concepts were selected: (1) construction materials, (2) structures, and (3) natural-hazard resiliency. These concepts are fundamental for civil engineering materials and structures' core knowledge.

In compliance with Step 2, the introductory presentation and brick-making activities propitiated opportunities for collaboration, reflection, observation, judgment, assessment, decision making, and enjoyment, which constitute active learning components, as illustrated in Figure 5.3. The introductory presentation included four Think-Pair-Share exercises to inquire about the students' level of understanding and perception regarding the concepts defined in Step 1 before they would be introduced or defined. To this end, slides with supportive images were used to formulate questions that the students had to address individually and then in discussion groups. Using poster wallpaper and sticky notes, each discussion group shared their answers with the rest of the class. On the other hand, for the CSEB making activity, the students worked in the materials laboratory in groups to (1) determine the amount of water and cement given by soil weight percentage, (2) measure the weight proportions of soil, cement, and water, (3) manually mix the materials, (4) assess the appropriateness of the moisture content of the mix conducting an empirical test, (5) mold and compact the mix into a CSEB and (5) wrap it in plastic for curing.

Placing the workshop in a practical application (Step 3) and providing a meaningful context (Step 4) that facilitates the students linking the concepts (e.g., materials) with their reality are essential points of the proposed framework. In this case, engineered CSEB masonry represents a singular but generic practical use of civil engineering materials and structures (i.e., core knowledge), whereas building a new house in Columbia, SC, serves as a tangible example of the application. Furthermore, this context provides the students with an illustration of the relevance of conducting research

to provide affordable, sustainable, and high-quality natural-hazard-resistant housing solutions.

5.4 Results and discussion

5.4.1 Post-workshop survey

A two-section survey was conducted at the end of the workshop. The first section evaluated the students' inclination towards pursuing college, STEM, and civil engineering education using a five-point Likert scale. The second section examined the participants' insights about the workshop's activities by asking two open-ended questions. The survey was completed by 80% of the participants, of which 38% were female, 41% were male, and 21% did not specify. Table 5.1 describes the survey completion data.

The divergent stacked bar chart shown in Figure 5.4 summarizes the responses per year to the following questions: "*After today's activities, how likely is it that you will pursue: (Q1) a college education?, (Q2) STEM in college?, and (Q3) civil engineering?*". In the vertical axis, the responses with favorable inclination (i.e., somewhat more likely and much more likely) are stacked in the positive domain, and the responses with unfavorable inclination (i.e., somewhat less likely and much less likely) in the negative domain. The value noted within the black circles represents the Net Promoter Score (NPS). This value results from subtracting the unfavorable inclination percentage from the favorable inclination percentage. NPS is a metric introduced by Reichheld [29] to measure customer satisfaction, and its value can range from -100% to 100%. The general benchmark classifies values between 0 and 50% as "good," above 50% as "excellent," and above 70% as "world-class" [30], [31], [29]. This metric has expanded to higher education applications to help describe students' reactions towards different instructional

processes and environments. For instance, NPS has been used in academic engineering programs study cases to identify preferences about online learning platforms for remote instruction [32] and evaluate the impact of accreditation processes on students' satisfaction concerning education services [33]. In the investigation presented herein, the NPS was used to help describe the participant's attitude towards pursuing higher education and, to a limited extent, gauge the workshop's effectiveness to foster interest in it.

In general, the results from the three consecutive years (i.e., 2017 to 2019) indicate that the respondents have a favorable inclination to pursue a college education. The total NPSs fell within the "good" range with values of 38%, 44%, and 4% for pursuing a college education, STEM in college, and civil engineering, respectively. These results seem reasonable considering the students' profile targeted for PMECS. In particular, the comparatively low interest in civil engineering is not surprising given that this is a specific discipline. It is noted that in 2017, the engineered earth masonry workshop took place at the beginning of the week and was the only technical workshop related to civil engineering. In contrast, the workshop was scheduled at the end of the week, after three civil engineering-related activities in the next two years.

The annual breakdown of the results (Figure 5.4) displays a significant improvement in the NPS obtained in 2019 compared to 2017. The overall respondents' inclination was consistently positive for college and STEM education through the first two years, with NPS falling within the "good" range. In the third year, the NPS was enhanced, falling within ranges of "world-class" and "excellent." In the case of civil engineering, there was a radical shift in the respondents' attitude through the years. In

2017, the unfavorable and favorable inclination percentages were the same, thus resulting in an NPS of 0%, whereas, in 2018, the net inclination was negative. Interestingly, in 2019 there was a radical change with a relatively high NPS of 41%, corresponding to the "good" range.

The positive shift in the respondents' interest in pursuing civil engineering, observed in the third year, might be influenced by the combined effect of the participants' exposure to multiple civil engineering workshops and the instructor's increased expertise and experience with leading the workshop, as indicated by the annotations in Figure 5.4. The same instructor delivered the workshop over the three years of the framework implementation, which, over time, prompted the growth of her understanding of the related instructional and learning objectives, thus positively impacting the workshop's quality and effectiveness.

Thematic analysis was applied responses to two open-ended questions: *(Q4)* "*Which was your favorite session from today's activities? Please tell us why*." and *(Q5)* "*How do engineers make a difference through research?*" Based on the six-step framework described by Braun and Clarke [34], the responses were examined to identify patterns and then define outstanding aspects. For Question 4, the identified aspects were reaction and sentiment, in addition to the favorite session. For Question 5, the identified aspects were participants' insight about the purpose of research in engineering and response elaboration. Table 5.2 indicates the codebook defined for the thematic analysis.

For presenting the results, the workshop's activities (i.e., introductory presentation and CSEB-making) are referred to from now on as sessions. CSEB-making was selected by 87% of the total respondents as their favorite session. Although this is not a surprising

result, given that there were only two sessions, some responses to the question's part "please tell us why?" were particularly insightful. The students' remarks highlighted the brick-making session because it was enjoyable, challenging, and collaborative (e.g., *"Finding the right amount of sand and water to go with cement. It was challenging"*). Specifically, interest, enjoyment, and apathy were identified in 22%, 16%, and 9% of the responses, respectively, and 53% of them as neutral.

The students' reaction indicates that the workshop's agenda fulfilled the original intent of PMECS activities. Furthermore, some relatively well-elaborated responses displayed that the students recognized the relevance of the context (i.e., engineered CSEB masonry) and application (i.e., building a new house in Columbia, SC) of the concepts introduced in the workshop. For instance, a respondent pointed out: *"When we made our own brick, because it was cool to do [,] and people can use [it] for their house."* In other cases, answers indicated an understanding of some basic terminology associated with the learning concepts, such as construction materials (e.g., *"I enjoyed making the bricks, as I got a closer look at cement vs. concrete"*).

Six themes represented the respondents' insights about research in engineering. Figure 5.5 presents the results relative to the grand total (i.e., 61) and total respondents per year. It is noted that from a single response, one or more themes could have been identified. Interestingly, all the identified themes relate to the introductory presentation content, and some were illustrated through the brick-making session. Overall, innovation was the theme with the highest frequency, with an associated relative rate of 30%.

Figure 5.6 presents the relative percentage of response elaboration associated with each theme for all years. The responses related to the natural hazard risks mitigation and

experimentation themes showed the highest elaboration rate. The former is the most distinctive theme of the workshop because it is one of the three intentionally introduced concepts.

The results from the thematic analysis to responses to Question 5 showed a connection between the identified themes and the learning concepts introduced by the workshop. Furthermore, it was determined that responses associated with the most distinctive workshop themes were the most elaborate, indicating that the participants paid attention to the presentation content even though the brick-making activity was what they overwhelmingly liked the most.

5.4.2 CAMP SURVEY

Students completed a simple evaluation form on the last day of the program. It contained three open-ended questions: *(1) What did you like best about the program? (2) What do you wish could be changed about the program? (3) Give suggestions for improvement.* A total of 71 evaluation forms were collected from 2017 and 2018 sophomore residential camps. Data from 2019 were not available.

Most responses provided feedback on what students liked best about the program as a whole. There are three main themes present in the responses. First, students recognized and appreciated the daily workshops. Students did not use the word "workshop" and instead referred to them with words such as activities, challenges, exercises, laboratories and projects. One student commented that the workshops were *"very informative and interesting",* and another described them as *"very challenging and competitive [with] constraints that made [them] difficult.*" Second, the hands-on nature of the workshops was valued. A number of students commented that building, creating, and

making things was the best part of the program. Third, students highlighted the teamwork required to complete workshops. One student liked *"working together to get projects done."* Other responses stated the workshops *"made us get along and bond"* because students had to *"put everyone's minds together."*

Fifteen of the 71 evaluation forms singled out a specific workshop as the best part. Seven of them identified the engineered earth masonry workshop. Those responses included comments such as *"loved making the bricks"* and *"creating bricks from raw materials"* as highlights of the program. One student specifically liked the presentation from the first half of the workshop. These observations were consistent in 2017 (3 of the 8 mentions of an individual workshop) and 2018 (4 of 7). The findings are notable because students participated in 5 different hands-on workshops in 2017 and 12 workshops in 2018. The 2018 summer program was expanded to include abbreviated (90-120 minutes) workshops in addition to the half-day workshops that were offered in 2017.

5.5 LIMITATIONS

The proposed framework was implemented and evaluated with a single workshop example (i.e., on engineered earth masonry). Furthermore, because PMECS' nomination criteria target a specific student profile, participants were likely already interested in STEM disciplines. However, this limitation enhances the robustness of the assessment, given that it ensures that samples from different years pertain to a similar participant population. On the other hand, although the results indicate that the workshop contributed to the favorable attitude of the students towards STEM disciplines, the extent of such impact cannot be differentiated from the influence of other components of the PMECS

program. Including a pre-workshop survey in future applications of the framework would facilitate a more comprehensive evaluation of the impact of the outreach activity.

5.6 Conclusions

This paper proposes a pedagogical framework to provide meaningful structure to design on-campus STEM outreach activities for pre-college students. The core of the proposed framework lies in establishing a situated learning environment, in which activities develop around tangible applications and allocate within meaningful contexts. The successful implementation of the framework is demonstrated through the design and evaluation of a workshop on engineered earth masonry delivered to underrepresented gifted K-12 students within the context of a summer camp program for STEM disciplines.

Structuring on-campus STEM outreach activities following the proposed framework prompts their impact and facilitates the achievement of objectives associated with outreach programs. The participants' open-ended responses indicated that the engineered earth masonry workshop accomplished its objectives and contributed to fulfilling the PMECS program's specific objectives. For instance, natural hazard mitigation, which is one of the concepts introduced by the workshop, was identified as one of the outstanding themes describing the respondent's insights about research in engineering, and the related responses exhibited the highest rate of elaboration. Moreover, the camp survey results showed that the brick-making activity and the related introductory presentation were singled out consistently throughout the three years, suggesting that the participants liked how the engineered earth masonry workshop was delivered. Overall, the participant's feedback described appreciation and understanding of

the context and concepts' application introduced in the workshop and the participants' enjoyment and excitement towards the topic.

Providing continuity in the framework's instructional and structural components was identified as a key contributing factor for a successful implementation. In the described application example, the same instructor delivered the workshop throughout the three years of implementation, which potentially facilitated the increment in understanding the related instructional and learning objectives, consequently positively impacting the workshop's quality. This impact is evidenced in the survey results from the third year, which exhibited a radical positive shift in the respondents' interest in pursuing civil engineering compared with the first year.

5.7 References

[1] National Science Board, “The STEM labor force of today: scientists, engineers, and skilled technical workers,” National Science Foundation, Alexandria, VA, Special reports NSB 2021-2, 2021. Accessed: Mar. 10, 2022. [Online]. Available: https://ncses.nsf.gov/pubs/nsb20212

[2] Bureau of Labor Statistics, “Special tabulations of 2019–29,” 2020.

[3] X. Kong, K. P. Dabney, and R. H. Tai, “The association between science summer camps and career interest in science and engineering,” *Int. J. Sci. Educ. Part B*, vol. 4, no. 1, pp. 54–65, Jan. 2014, doi: 10.1080/21548455.2012.760856.

[4] R. Hammack, T. Ivey, J. Utley, and K. High, “Effect of an engineering camp on students’ perceptions of engineering and technology,” *J. Pre-Coll. Eng. Educ. Res. J-PEER*, vol. 5, no. 2, Nov. 2015, doi: 10.7771/2157-9288.1102.

[5] J. Vennix, P. den Brok, and R. Taconis, “Do outreach activities in secondary STEM education motivate students and improve their attitudes towards STEM?,” *Int. J. Sci. Educ.*, vol. 40, no. 11, pp. 1263–1283, Jul. 2018, doi: 10.1080/09500693.2018.1473659.

[6] M. F. Bugallo and A. M. Kelly, “Engineering outreach: yesterday, today, and tomorrow [SP education],” *IEEE Signal Process. Mag.*, vol. 34, no. 3, pp. 69–100, May 2017, doi: 10.1109/MSP.2017.2673018.

[7] A. T. Jeffers, A. G. Safferman, and S. I. Safferman, “Understanding K–12 engineering outreach programs,” *J. Prof. Issues Eng. Educ. Pract.*, vol. 130, no. 2, pp. 95–108, Apr. 2004, doi: 10.1061/(ASCE)1052-3928(2004)130:2(95).

[8] M. Yilmaz, J. Ren, S. Custer, and J. Coleman, “Hands-on summer camp to attract K–12 students to engineering fields,” *IEEE Trans. Educ.*, vol. 53, no. 1, pp. 144–151, Feb. 2010, doi: 10.1109/TE.2009.2026366.

[9] J. Yan, K. Wen, and L. Li, “Effects of summer transportation institute on minority high school student’s perception on STEM learning,” *J. STEM Educ.*, vol. 20, no. 2, 2019, Accessed: May 27, 2021. [Online]. Available: https://www.jstem.org/jstem/index.php/JSTEM/article/view/2306

[10] C. E. Pierce, “Problem-Based Learning with EFFECTs: Part I – Preparing Future Faculty to Integrate Teaching and Research – SFGE 2016,” presented at the SFGE 2016 – Shaping the Future of Geotechnical Education International Conference on Geo-Engineering Education, Belo Horizonte, Brazil, Oct. 2016.

[11] C. E. Pierce, J. M. Caicedo, J. R. Flora, N. D. Berge, R. Madarshahian, and B. Timmerman, “Integrating professional and technical engineering skills with the EFFECTs pedagogical framework,” *Int. J. Eng. Educ.*, vol. 30, no. 6, pp. 1579–1589, 2014.

[12] C. E. Pierce, S. L. Gassman, and J. T. Huffman, “Environments for fostering effective critical thinking in geotechnical engineering education (Geo-EFFECTs),” *Eur. J. Eng. Educ.*, vol. 38, no. 3, pp. 281–299, Jun. 2013, doi: 10.1080/03043797.2013.800021.

[13] R. D. Starcher and C. E. Pierce, “Problem-based learning with EFFECTs: part II–ground improvement module for lab courses,” presented at the International Conference on Geo-Engineering Education, ISSMGE, Belo Horizonte, Brazil, 2016.

[14] N. Berge, D. D. Thompson, C. Ingram, and C. Pierce, “Engineering design and EFFECTs,” *Sci. Scope*, vol. 38, no. 3, pp. 16–27, Nov. 2014.

[15] I. W. Wait, “Solar power system design to promote critical thinking in freshman engineering students,” in *Proc. 2012 ASEE Annual Conference & Exposition*, 2012, pp. 25–1167.

[16] C. E. Pierce *et al.*, “Infusing STEM courses with problem-based learning about transportation disruptive technologies,” presented at the ASEE Annual Conference & Exposition, 2019.

[17] D. Stein, *Situated learning in adult education*. ERIC Clearinghouse on Adult, Career, and Vocational Education, Center on …, 1998.

[18] P. H. Henning, “Everyday cognition and situated learning,” in *Handbook of research on educational communications and technology: A project of the association for educational communications and technology*, 2004, pp. 829–861.

[19] W. J. Clancey, “A tutorial on situated learning,” in *Proc. International Conference on Computers and Education (Taiwan)*, Charlottesville, VA, 1995, pp. 49–70. Accessed: Mar. 09, 2022. [Online]. Available: http://cogprints.org/323/

[20] J. Lave and E. Wenger, *Situated learning: legitimate peripheral participation*. Cambridge university press, 1991.

[21] M. Pérez-Sanagustín, P. J. Muñoz-Merino, C. Alario-Hoyos, X. Soldani, and C. Delgado Kloos, “Lessons learned from the design of situated learning environments to support collaborative knowledge construction,” *Comput. Educ.*, vol. 87, pp. 70–82, Sep. 2015, doi: 10.1016/j.compedu.2015.03.019.

[22] A. L. Steele and C. Schramm, “Situated learning perspective for online approaches to laboratory and project work,” *Proc. Can. Eng. Educ. Assoc. CEEA*, 2021.

[23] College of Engineering and Computing at the University of South Carolina, “Partners for Minorities in Engineering and Computer Science,” *College of Engineering and Computing*. https://sc.edu/study/colleges_schools/engineering_and_computing/connect/k-12_outreach/summer_camps/pmecs/index.php (accessed Jul. 06, 2021).

[24] Central Carolina Community Foundation, “Partners for Minorities in Engineering and Computer Science,” *Midlands Gives*. https://www.midlandsgives.org/PMECS (accessed Jul. 06, 2021).

[25] “NSF Award Search: Award # 1537776 - Collaborative Research: Engineered Earth Masonry for Affordable Seismic Resistant Low-Rise Buildings.” https://nsf.gov/awardsearch/showAward?AWD_ID=1537776 (accessed Apr. 03, 2022).

[26] “NSF Award Search: Award # 1537078 - Collaborative Research: Engineered Earth Masonry for Affordable Seismic Resistant Low-Rise Buildings.” https://nsf.gov/awardsearch/showAward?AWD_ID=1537078 (accessed Apr. 03, 2022).

[27] “NSF Award Search: Award # 1850777 - Collaborative Research: Engineered Earth Masonry for Affordable Seismic Resistant Low-Rise Buildings.” https://www.nsf.gov/awardsearch/showAward?AWD_ID=1850777 (accessed Apr. 03, 2022).

[28] National Science Foundation, “Proposal & award policies & procedures guide secion II.C.2.d,” *NSF-National Science Foundation*, 2020. https://www.nsf.gov/pubs/policydocs/pappg20_1/pappg_2.jsp#IIC2d (accessed Aug. 25, 2021).

[29] F. F. Reichheld, “The one number you need to grow,” *Harv. Bus. Rev.*, p. 12, 2003.

[30] D. Ø. Madsen, “One marketing metric to rule them all? an examination of the emergence and rise of Net Promoter Score as a marketing fashion,” Social Science Research Network, Rochester, NY, SSRN Scholarly Paper ID 3738866, Nov. 2020. doi: 10.2139/ssrn.3738866.

[31] J. Yan, “Good Net Promoter Score (NPS): what is it?,” *QuestionPro*, Apr. 25, 2017. https://www.questionpro.com/blog/nps-considered-good-net-promoter-score/ (accessed Dec. 10, 2021).

[32] S. V. Thakker, J. Parab, and S. Kaisare, “Systematic research of e-learning platforms for solving challenges faced by Indian engineering students,” *Asian Assoc. Open Univ. J.*, vol. 16, no. 1, pp. 1–19, May 2021, doi: 10.1108/AAOUJ-09-2020-0078.

[33] J. O. Cruz, E. E. Moreno, and W. C. Silupu, “Effect of the implementation of university accreditation on the satisfaction of engineering students using the Net Promoter Score,” in *Proc. 2019 IEEE Sciences and Humanities International Research Conference (SHIRCON)*, Lima, Peru, Nov. 2019, pp. 1–4. doi: 10.1109/SHIRCON48091.2019.9024870.

[34] V. Braun and V. Clarke, “Using thematic analysis in psychology,” *Qual. Res. Psychol.*, vol. 3, no. 2, pp. 77–101, Jan. 2006, doi: 10.1191/1478088706qp063oa.

[35] FEMA, “FEMA fact sheet: seismic building code provisions for new buildings to create safer communities.” FEMA, 2020.

[36] Adobe in Action, “Earth USA News Issue #5,” *Earth USA 2022*. https://www.earthusa.org/earthusa-news/2020/10/22/earthusa-news-issue-5 (accessed Apr. 04, 2022).

[37] College of Engineering and Computing at the University of South Carolina, “Building affordable and hazard-resistant houses with earth bricks and recycled plastic reinforcement,” *College of Engineering and Computing*. https://www.sc.edu/study/colleges_schools/engineering_and_computing/news_events/news/2021/building_affordable_and_hazard_resistant_houses.php (accessed Apr. 04, 2022).

5.8 TABLES

Table 5.1 Survey completion data

	Workshop Participants	Survey Respondents	Completion rate	Respondents' demographics		
				Female	Male	Not specified
2017	28	28	100%	57%	29%	14%
2018	31	23	74%	22%	48%	30%
2019	26	17	65%	41%	41%	18%
Total	85	68	80%	38%	41%	21%

Table 5.2 Thematic analysis codebook

Aspect	Code	Definition	Example
Question 4: Which was your favorite session from today's activities? Please tell us why.			
Favorite session	Brick making	The response refers to the hands-on activity	*"My favorite part was mixing the water, soil, and cement."*
	Presentation	The response refers to concepts introduced in the presentation	*"When we learn about the materials and the pros and cons of making buildings, as well as how natural disasters"*
Reaction and sentiment	Neutral	There is not a discernible reaction in the response	"*Making the brick because I'm a hands-on person*"
	Apathy	There is no response at all	"*IDK" [I do not know]*
	Enjoyment	The response reflects enjoyment or excitement towards the concepts or activities	*"Making the brick because it was awesome. I made the brick with clay [,] and everything was really cool"*
	Interest	The response indicates curiosity for learning, intellectual engaging or detailed attention towards the concepts or activities	*"Finding the right amount of sand and water to go with cement. It was challenging"*
Question 5: How do engineers make a difference through research?			
Insight about purpose of research in engineering	Innovation	The response refers to processes associated with creativity, improvement, or technological advancement	*"They find ways to make things better or more suitable for a certain environment"*
	Life improvement	The response refers to human wellbeing	*"They create things that people need"*
	Problem solving	The response refers to the search of solutions to different problems or situations	"*They solve problems that affect the environment"*
	Discovery and learning	The response refers to learning, knowledge gain, or discovering	*"They research to find out needed information"*
	Natural hazard risk mitigation	The response refers to safety, risk, and the need to protect life and goods	"*Making constructions safer and reliable*"
	Experimentation	The response refers to gaining knowledge or evidence by experimenting or simulating.	"*They use their research to find out what material is best and how it can be used*"
Elaboration	Little elaborate	The response does not state a clear idea	*"A lot"*
	Fair elaborate	The response states a general idea without further elaboration	*"They protect people"*
	Elaborate	The response states a clear idea and there is an attempt to elaborate by providing at least one supportive example or application	*"By researching they redefine constraints and eliminate risks that could have been present before"*

5.9 FIGURES

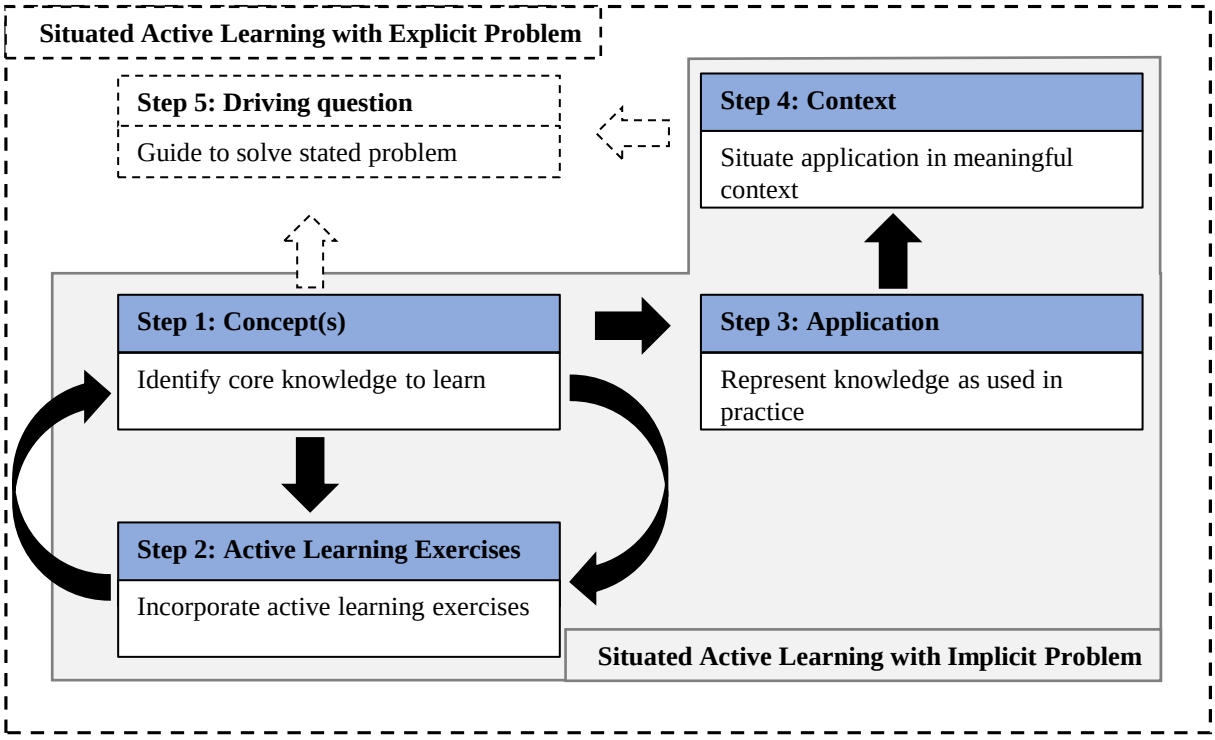

Figure 5.1 Adaptable framework for on-campus STEM outreach activities

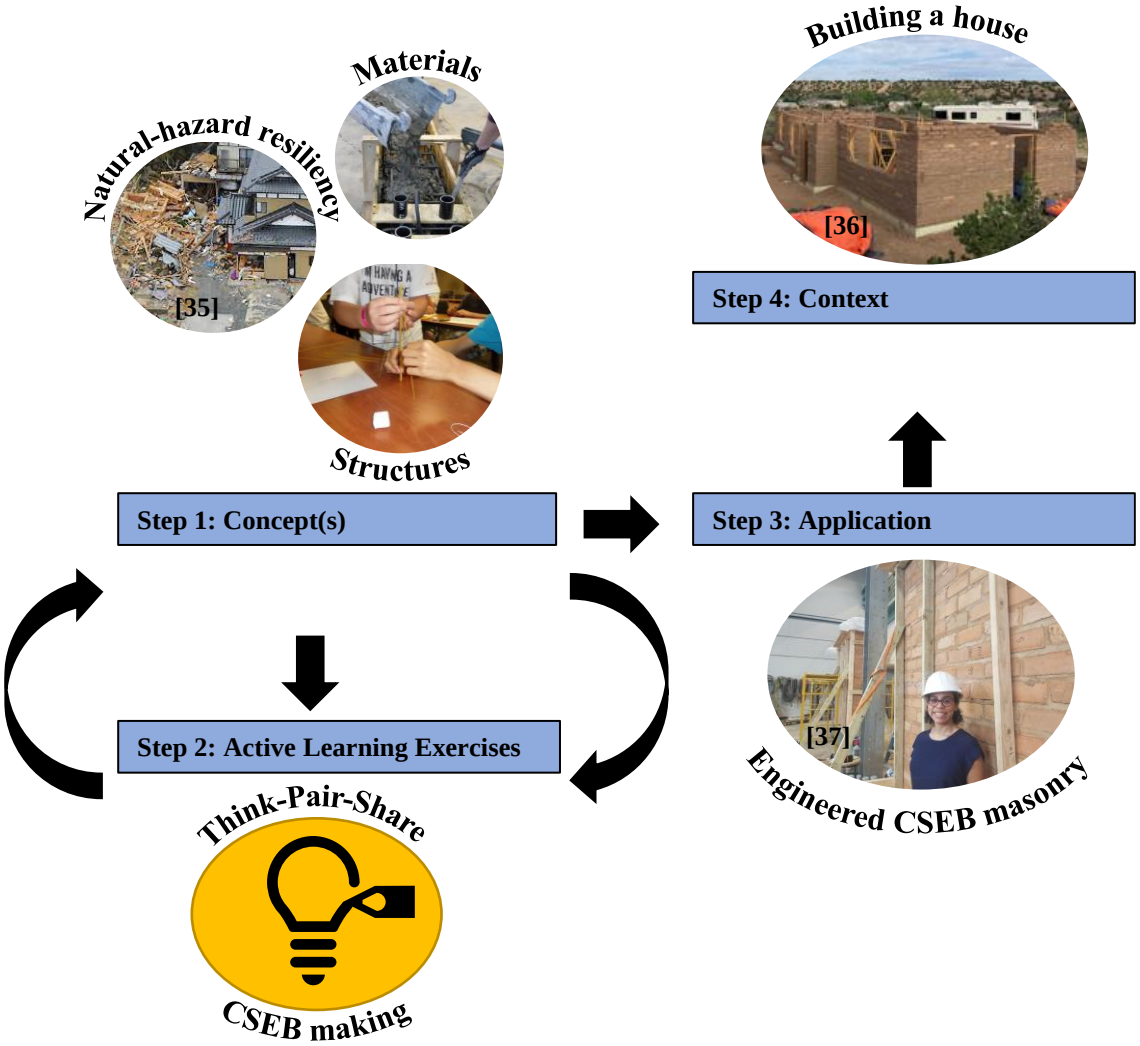

Figure 5.2 Framework steps application for workshop on hazard-resistant earth masonry construction. Images taken from [35]–[37]

INTRODUCTORY PRESENTATION

Instructor posts **questions** using supportive images

Students **think** about posted questions and write down answer(s)

Students discuss in teams and come to a consensus to **pair** their ideas.

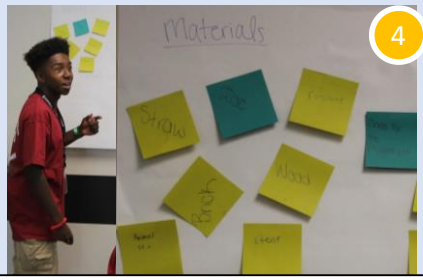

Student **shares** group's conclusion with class

CSEB MAKING

Students **calculate** and **measure** **materials**' amount based on prescribed soil weight percentages

Students manually mix material until they **observe** a uniform consistency

Students **assess** moisture content with an empirical test and **make decisions** to adjust water content with **instructor's feedback**

Students have **fun**

Figure 5.3 Active learning components of engineered masonry workshop

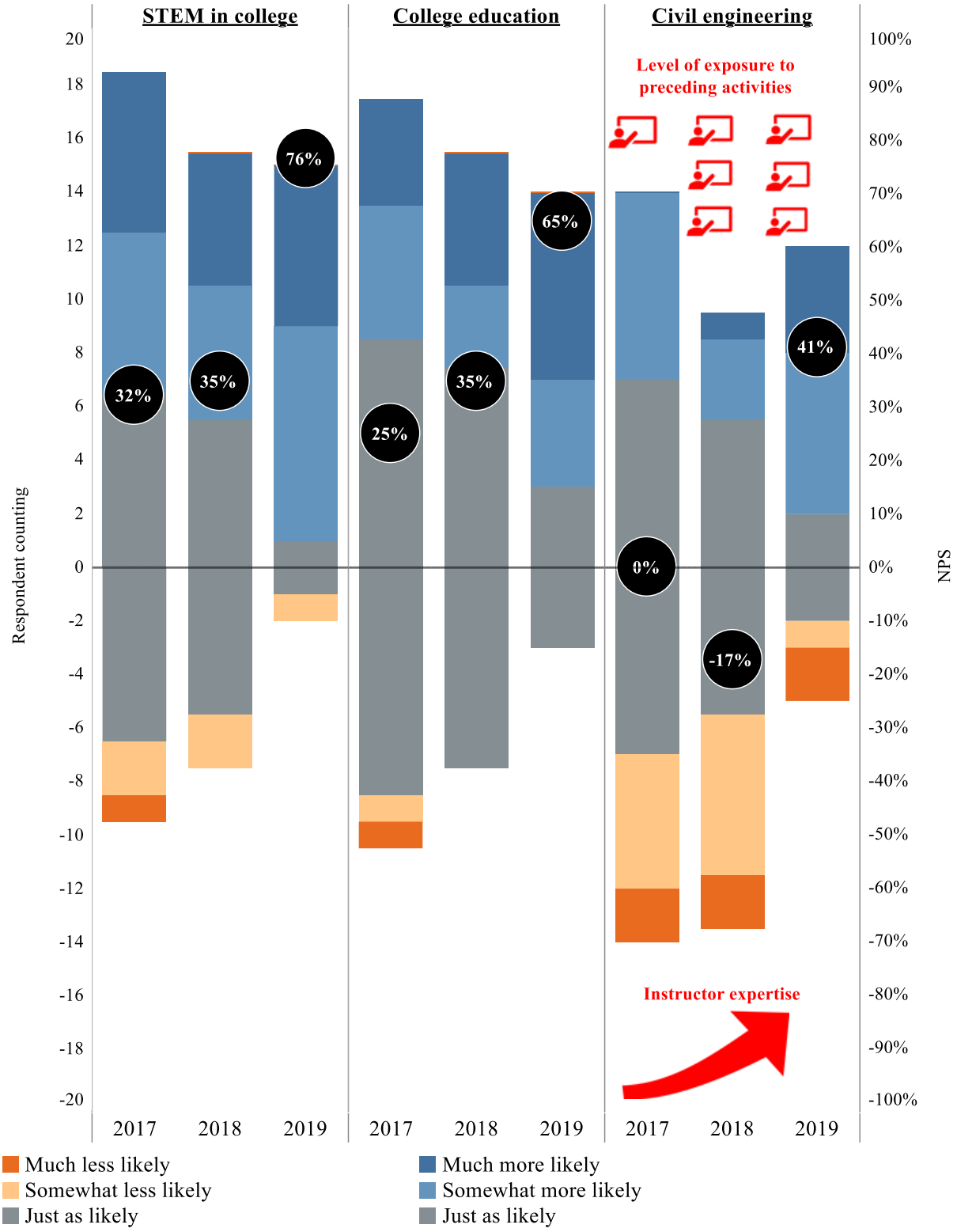

Figure 5.4 Results of inclination assessment to pursue different levels of college education

Figure 5.5 Thematic analysis: how do engineers make a difference through research?

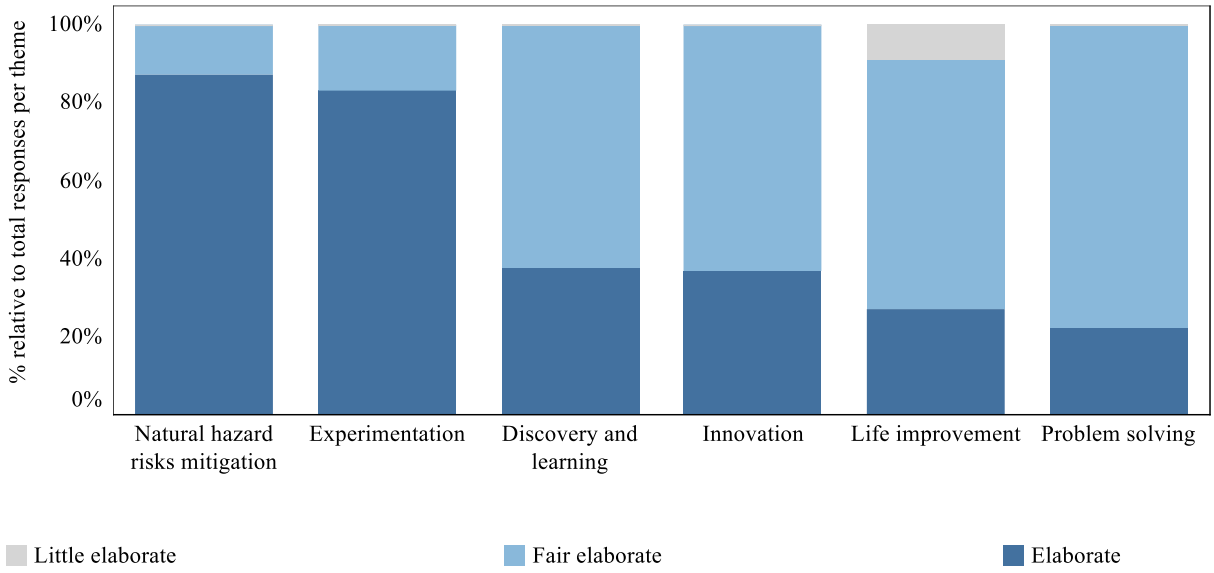

Figure 5.6 Elaboration in responses to Question 5 as a percentage relative to each theme

CHAPTER 6: CONCLUSIONS AND RECOMMENDATIONS FOR FUTURE WORK

This chapter presents a recompilation of the primary conclusions drawn from the experimental projects presented in Chapter 2 through Chapter 4 and the investigation conducted on outreach programs for K-12 presented in Chapter 5. Moreover, this chapter includes recommendations for future work.

Chapter 2 focused on the experimental characterization of the physico-mechanical homogeneity and isotropy of a prototype earth block material manufactured with one-sided compaction and the statistical analysis of the collected experimental data. The main conclusions of this research are summarized as follows.

1.The compressive strength and initial tangent stiffness are homogeneous and isotropic properties for earth blocks fabricated with the technique used in this paper. The combined results of ANOVA and Levine's test suggest that all data, regardless of loading direction and source location within a given block, belong to the same population. A single probability distribution describes the variability of all results. Therefore, for practical purposes, the inherent heterogeneity of the soil used for manufacturing CSEBs, the variability of its properties (e.g., particle size distribution, plastic limits), and the factors associated with the block manufacturing process (e.g., internal friction, particle alignment), do not significantly affect the uniform distribution of the mechanical properties within a given block.

2.A normal distribution is recommended for applications focused on the body of the distribution (e.g., probabilistic response, stochastic dynamics), whereas the

truncated normal distribution is recommended for use in applications focused on the distribution tails (e.g., structural reliability).

Chapter 3 presents the results of an experimental investigation on the compressive strength of the same material studied in Chapter 2, focusing on the effect of friction at the loading interface and specimen geometry. The key conclusions of this research are summarized as follows.

1. There is a negligible difference between the effect of using either low- or high-friction inserts at the loading interface, in a uniaxial compression test, on the compressive strength of CSEB specimens. The experimental results indicate that the order of magnitude of the CoF developed between the CSEB material surface and inserts of either PTFE or sandpaper (i.e., CoF higher than 0.37) pertains to a range in which the relation between friction and compressive strength approaches an asymptote.

2. In uniaxial compression tests, the CSEB specimens' aspect ratio (i.e., minor dimension-to-height ratio) has a significant effect on the resulting compressive strength. The compressive strength decreases as the aspect ratio increases due to the minimization of platen restraining effects, and such effect becomes clear for aspect ratios higher than one. In contrast, the effect of cross-sectional shape was characterized as negligible. CSEB prisms and cylinders with comparable size and aspect ratio yield comparable compressive strength results.

3. The extent of cutting to manufacture CSEB laboratory specimens affects uniaxial compression tests results. The surface abrasion, caused by cutting and or drilling used to manufacture prism and cylinder specimens, increases the test results' variability

and impair, to some extent, the specimen's strength. This effect is mitigated as the specimen aspect ratio increases and cutting involved in its manufacturing is minimized.

4. Prisms and cylinders with an aspect ratio of 2.0 are suitable configurations to characterize the compressive strength of CSEB materials. Using specimens with an aspect ratio of 2.0 provides minimization of platen restraining and manufacturing effects on the compressive strength.

Further is needed to understand the effect of the specimen manufacturing process. For cut CSEB specimens with an aspect ratio equal to or lower than 1.0, the interplay between the extent of strength increments due to platen restraining effect and the extent of strength impairment due to manufacturing effect is unclear. While the importance of this effect remains uncertain, it is recommended to opt for prisms with an aspect ratio of 2.0 and minimize the number of cut surfaces to manufacture the specimens. When practical constraints oblige extracting drilled cores (e.g., in existing structures), the specimens' aspect ratio should be near two.

Chapter 4 continued the study reported in Chapter 3 by extending the experimental program and data analysis focusing on the stress-strain response to identify a suitable configuration to characterize the constitutive behavior of the material. The main conclusions are listed as follows.

1. Approximately uniform axial strains are attained within a portion of the height of CSEB specimens with an aspect ratio equal to 2.0 that is one-quarter away from the loading plates. The results indicate that the lateral restraining effect is sufficiently minimized at this height portion and suggest that the corresponding stress-strain response is representative of the unconfined uniaxial compression behavior of CSEB materials and

can be used to identify the modeling parameters needed to define constitutive models. To this end, it is recommended that strain data are measured within the middle third of the specimen height.

2. The vis-à-vis comparison between the stress-strain relation from the middle-third portion of prisms and cylinders height with aspect ratio 2.0 suggested that either prisms or cylinders are suitable configurations to define the material constitutive model. Numerical simulations will allow for further verification of this conclusion.

3. The proportional limit to define the elastic properties of CSEB materials is recommended as 40% of the compressive strength. For the material investigated herein, Young's modulus and Poisson's ration were characterized as 2533±874 and 0.152±0.059, respectively.

4. Using pointwise measuring methods, such as a compressometer-type fixture, is appropriate to characterize a stress-strain response and elastic parameters that are representative of the uniaxial behavior of the material, provided that the deformations are measured within the middle-third of specimens with an aspect ratio of 2.0.

Finally, in Chapter 5, an adaptable pedagogical framework is proposed to provide meaningful structure for on-campus STEM outreach activities that emphasize collaborative, hands-on learning experiences for pre-college students. The successful implementation of the framework was demonstrated through the design and evaluation of a workshop on engineered earth masonry delivered to underrepresented gifted K-12 students within the context of a summer camp program for STEM disciplines. The highlighted takeaways of this investigation are described as follows.

1. Structuring on-campus STEM outreach activities following the proposed framework prompts their impact and facilitates the achievement of objectives associated with outreach programs. The participants' open-ended responses indicated that the engineered earth masonry workshop accomplished its objectives and contributed to fulfilling the PMECS program's specific objectives. For instance, natural hazard mitigation, which is one of the concepts introduced by the workshop, was identified as one of the outstanding themes describing the respondent's insights about research in engineering, and the related responses exhibited the highest rate of elaboration. Moreover, the camp survey results showed that the brick-making activity and the related introductory presentation were singled out consistently throughout the three years, suggesting that the participants liked how the engineered earth masonry workshop was delivered. Overall, the participant's feedback described appreciation and understanding of the context and concepts' application introduced in the workshop and the participants' enjoyment and excitement towards the topic.

2. Providing continuity in the framework's instructional and structural components was identified as a key contributing factor for a successful implementation. In the described application example, the same instructor delivered the workshop throughout the three years of implementation, which potentially facilitated the increment in understanding the related instructional and learning objectives, consequently positively impacting the workshop's quality. This impact is evidenced in the survey results from the third year, which exhibited a radical positive shift in the respondents' interest in pursuing civil engineering compared with the first year.

APPENDIX A: SOIL CHARACTERIZATION

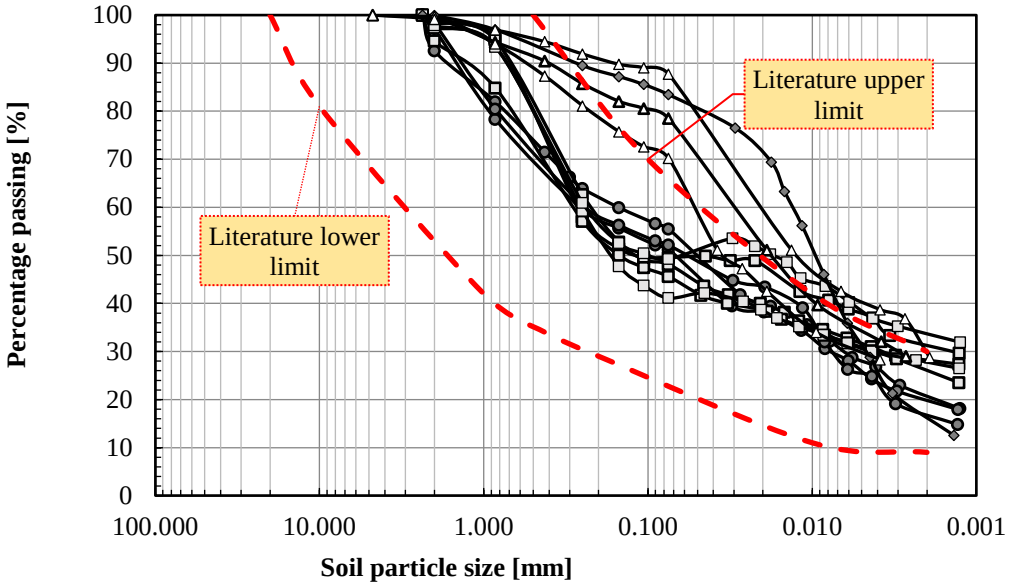

Figure A.1 Particle size distribution of multiple trials on 13 batches of soil used to manufacture prototype CSEB material

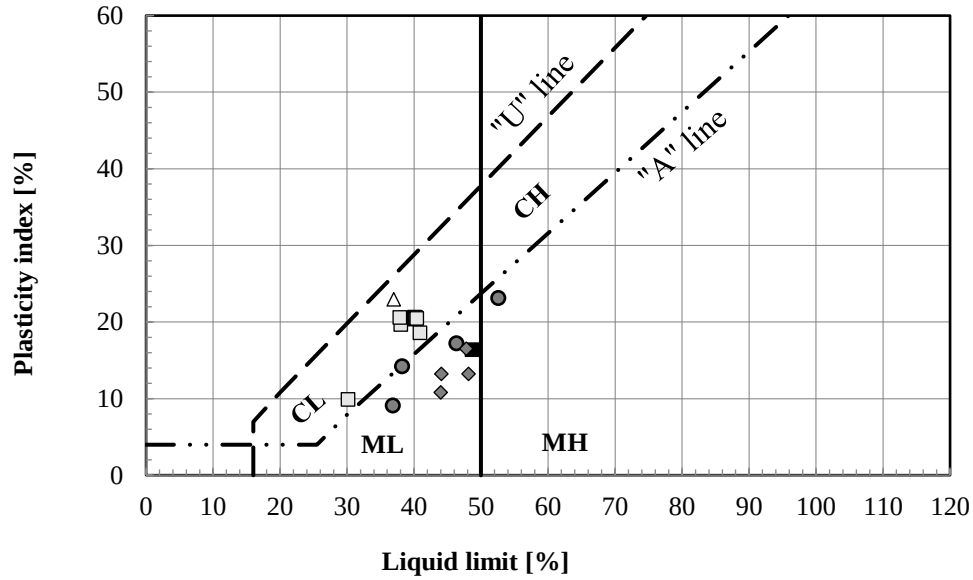

Figure A.2 Plasticity chart of multiple trials on 13 batches of soil used to manufacture prototype CSEB material

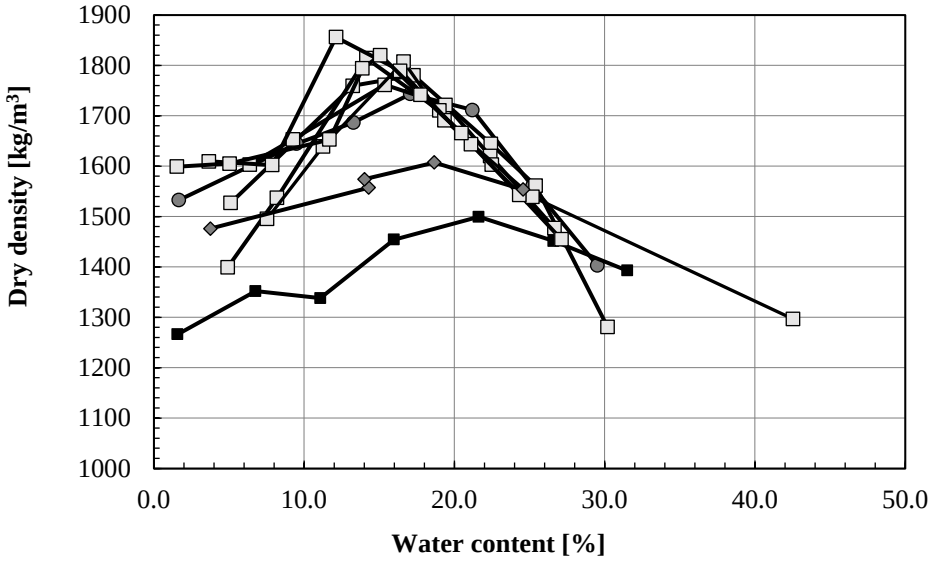

Figure A.3 Compaction curve of Particle size distribution of multiple trials on 13 batches of soil used to manufacture prototype CSEB material

Table A.1 Soil properties for representative results of different batches used to manufacture prototype CSEB material

Model ID (Soil batch ID)	USCS		OMC (%)	Average sand %	Average silt %	Average clay %	Fines %	LL	PL	PI
	Group name	Group name								
1-2015	Silt	ML	17-18	41	37	22	59	46	29	17
1-2016	Silt	ML	21-22	15	63	22	85	49	32	16
2-2019	Clayey sand	CS	17	51	13	36	49	40	20	21
3-2019	Clayey sand	CS	15-16	53	15	32	47	41	22	19
4-2019	Clayey sand	CS	14	55	16	30	45	38	18	20
5-2019	Clayey sand	CS	17	56	14	31	44	40	20	21
6-2019	Clayey sand	CS	12-16	59	11	30	41	30	20	10
7-2019	Clayey sand	CS	15	51	12	37	49	38	17	21
1-2021	Silt	ML	14	19	55	26	81	48	31	17
2-2021	Silt	ML		19	52	28	81	44	31	13
3-2021	Silt	ML		34	37	29	66	44	33	11
4-2021	Silt	ML		14	59	27	86	48	35	13
NSF award 1131161	Lean clay	CL	17	21	46	33	79	37	14	23

APPENDIX B: CSEB MANUFACTURING QUALITY CONTROL

Table B.1 Quality control data for manufacturing of CSEBs with recycled plastic fibers

			Average						
Soil batch ID	Block ID	Fibers	Length	Width	Height	Weight	Moisture content	Dry density	Compressive strength
		Y / N	[mm]	[mm]	[mm]	[kg]	[%]	[kg/m3]	[MPa]
6-2019	401-A	Y	181	122	97	3.8	2.1%	1762	7.2
6-2019	401-B	Y	183	127	99	4.0	1.3%	1722	6.4
7-2019	429-A	Y	177	125	91	3.6	0.9%	1776	8.8
7-2019	429-B	Y	179	126	93	3.7	2.2%	1747	8.9
7-2019	469-A	Y	177	122	90	3.2	2.5%	1594	4.2
7-2019	469-B	Y	176	127	90	3.4	1.7%	1643	5.4
							Average	1707	6.81
							SD	73	1.88
							CV	4%	28%

Table B.2 Quality control data for manufacturing of CSEBs

			Average						
Soil batch ID	Block ID	Fibers	Length	Width	Height	Weight	Moisture content	Dry density	Compressive strength
		Y / N	[mm]	[mm]	[mm]	[kg]	[%]	[kg/m3]	[MPa]
3-2019	73-1	N	127	125	89	2.5	3.1%	1679	4.52
3-2019	73-2	N	127	127	92	2.5	1.9%	1681	4.22
3-2019	96-1	N	127	127	92	2.6	2.3%	1734	6.34
3-2019	96-2	N	126	125	92	2.5	2.4%	1716	5.98
3-2019	109-1	N	127	124	92	2.4	2.8%	1587	4.65
3-2019	109-2	N	127	127	92	2.5	3.9%	1588	4.61
4-2019	149-1	N	127	127	92	2.9	7.0%	1821	5.65
5-2019	271-A	N	176	123	98	3.6	1.3%	1655	5.53
5-2019	271-B	N	175	127	97	3.6	1.1%	1676	5.65
5-2019	227-A	N	178	127	97	3.7	0.0%	1684	0.00
5-2019	227-B	N	178	125	96	3.6	0.0%	1704	6.88
5-2019	254-A	N	180	128	98	3.8	2.0%	1677	6.87
5-2019	254-B	N	177	123	97	3.7	1.6%	1705	6.68
6-2019	328-A	N	180	126	100	3.8	1.8%	1664	6.11
6-2019	328-B	N	180	124	99	3.8	1.9%	1673	6.19
6-2019	352-A	N	180	125	97	3.6	1.4%	1618	5.20
6-2019	352-B	N	181	125	95	3.6	3.3%	1617	5.79
6-2019	384-A	N	184	127	97	4.2	0.0%	1859	8.98
6-2019	384-B	N	183	126	96	4.0	1.8%	1806	8.57
5-2019	235-A	N	177	125	95	3.7	2.0%	1704	7.67
5-2019	235-B	N	178	126	96	3.8	1.3%	1736	7.88
6-2019	297-A	N	177	124	100	3.6	1.4%	1628	5.37
6-2019	297-B	N	176	126	98	3.7	1.1%	1676	5.79
7-2019	436-A	N	176	126	95	3.6	2.9%	1639	7.62
7-2019	436-B	N	176	125	94	3.6	2.5%	1680	8.07
1-2016	550-1	N	94	100	104	1.5	0.0%	1524	2.74
1-2016	550-2	N	132	101	75	1.6	0.0%	1582	1.95
1-2016	547-1	N	180	125	103	3.4	0.0%	1486	4.69
1-2016	547-2	N	180	125	100	3.5	0.0%	1541	5.08
1-2021	569-1	N	180	127	97	3.3	1.2%	1476	5.58
1-2021	569-2	N	177	102	95	2.7	0.9%	1555	5.40
1-2021	570-1	N	177	129	95	3.3	1.2%	1496	5.35
1-2021	570-2	N	178	123	99	3.1	0.9%	1421	4.62
							Average	1645	5.64
							SD	99	1.82
							CV	6%	32%

APPENDIX C: MICROANALYSIS

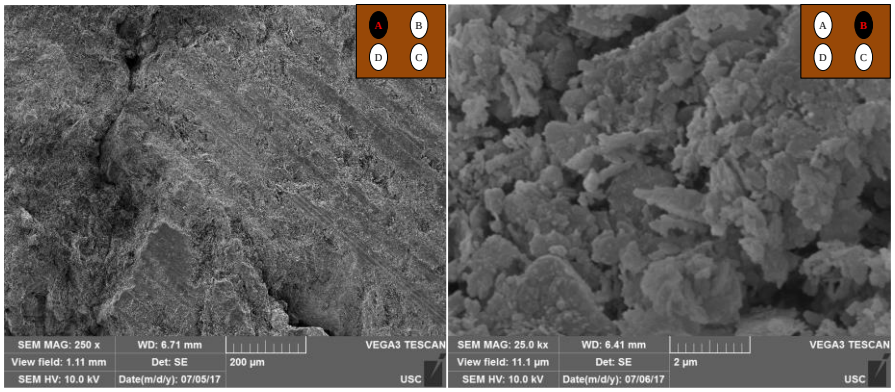

Figure C.1 SEM micrographs of Sample 1

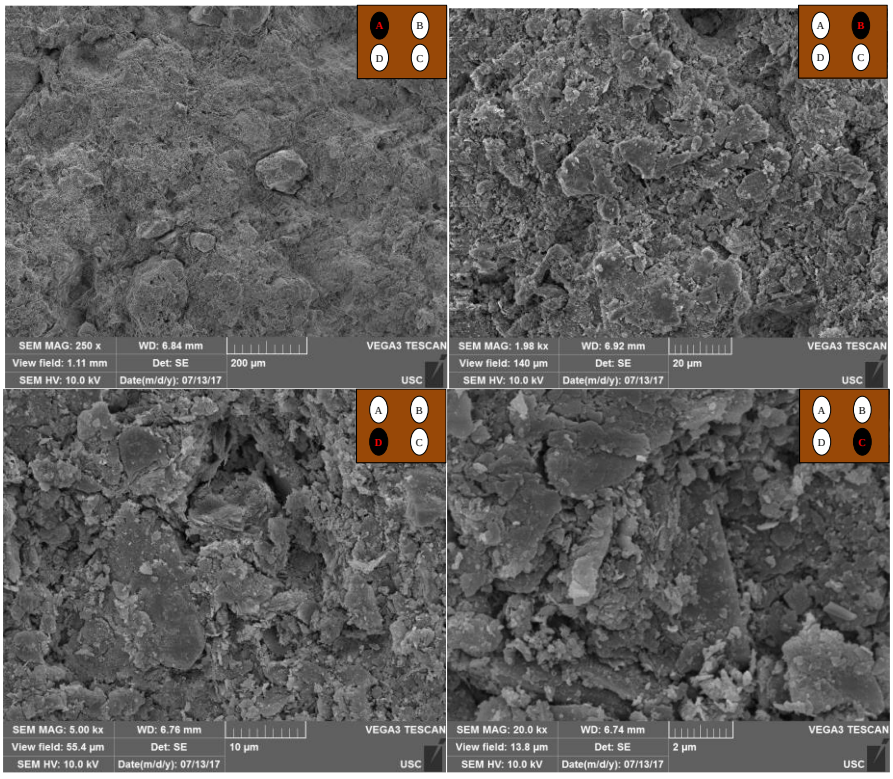

Figure C.2 SEM micrographs of Sample 2

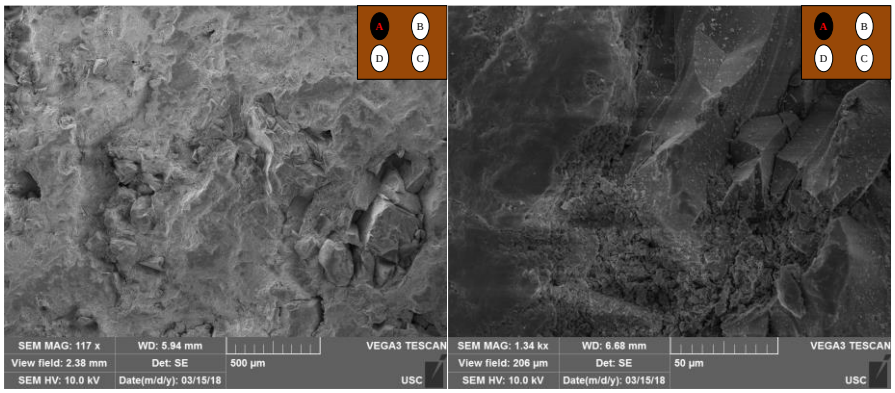

Figure C.3 SEM micrographs of Sample 3

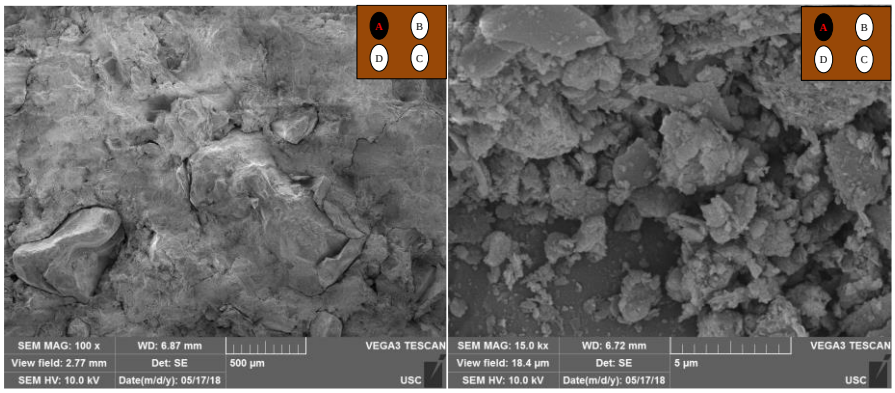

Figure C.4 SEM micrographs of Sample 4

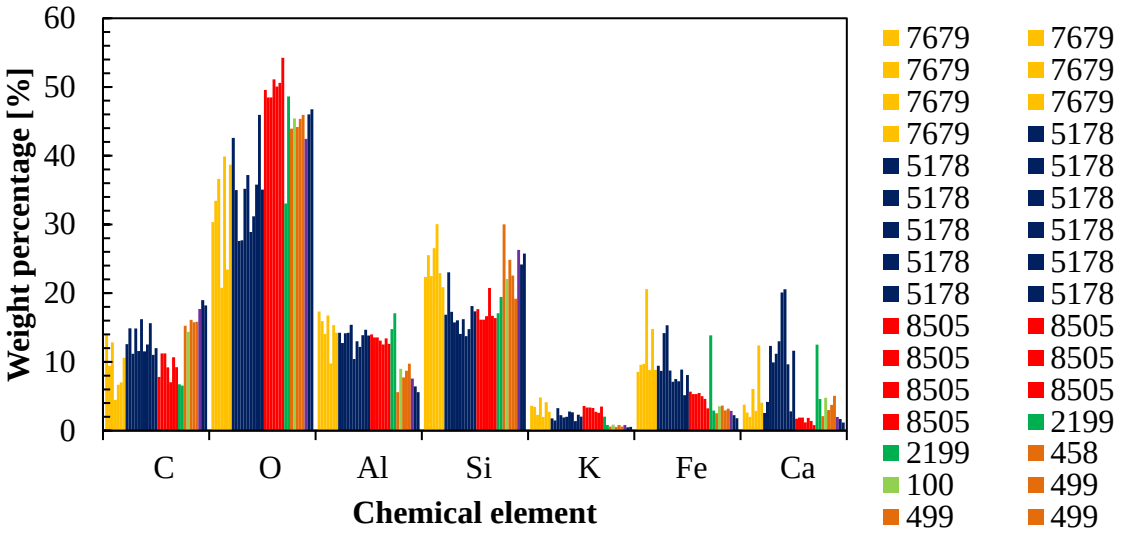

Figure C.5 Overall summary of EDS analysis color-coded per magnification

APPENDIX D: COF CHARACTERIZATION

Table D.1 CoF characterization test matrix

Interface	Number of CSEB specimens	Number of surfaces	Additional weight [N]			Total trials
			0.0	4.5	8.9	
CSEB-PTFE	3	2	X	X	X	18
CSEB-Sandpaper 220	3	2	X	X	X	18
CSEB-Polished steel	3	2	X	X	X	18
CSEB-Steel	3	2	X	X	X	18
CSEB-Sandpaper 60	3	2	X	X	X	18

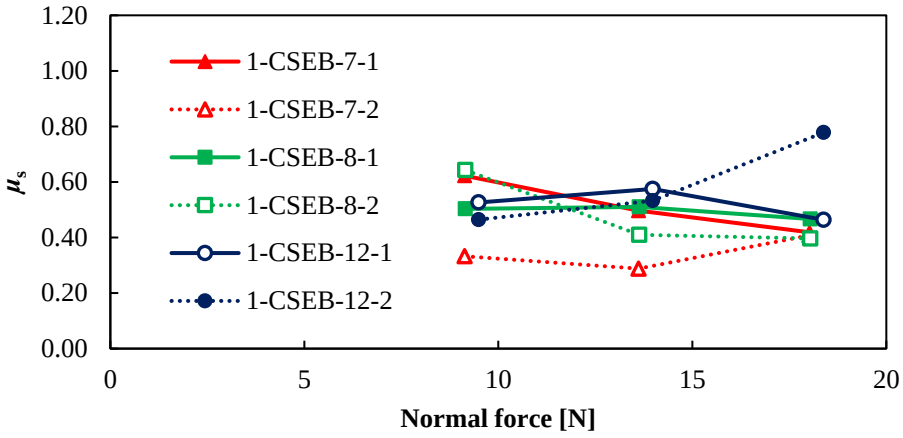

Figure D.1 CoF characterization results for CSEB-PTFE interface

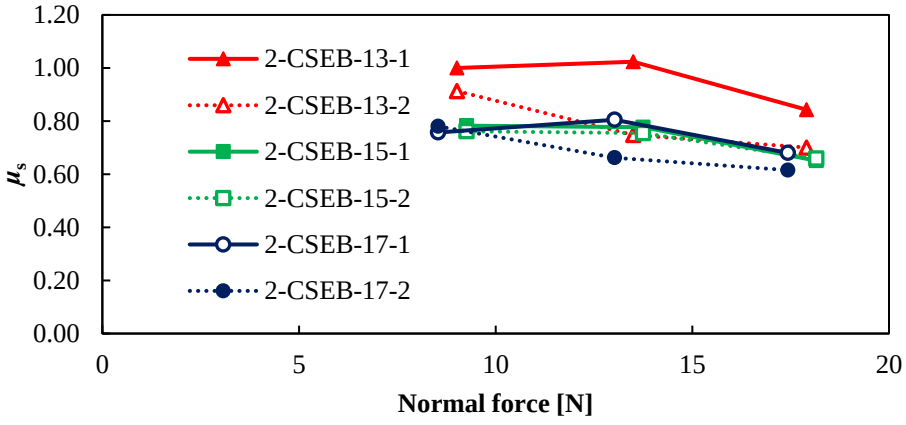

Figure D.2 CoF characterization results for CSEB-Sandpaper 220 interface

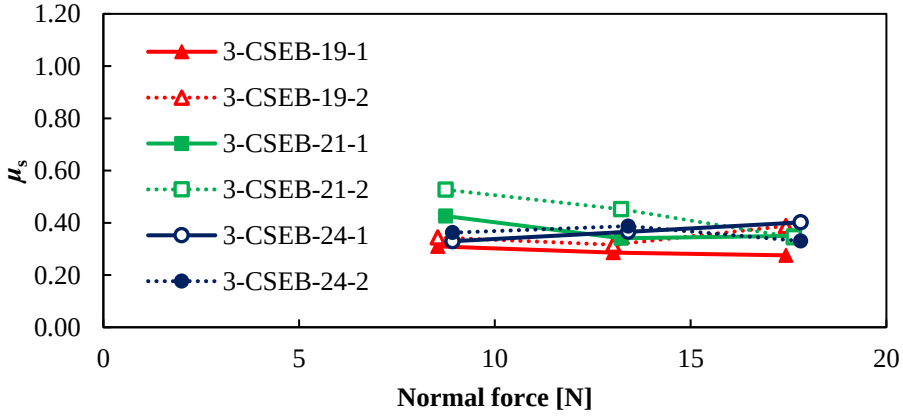

Figure D.3 CoF characterization results for CSEB-Polished steel interface

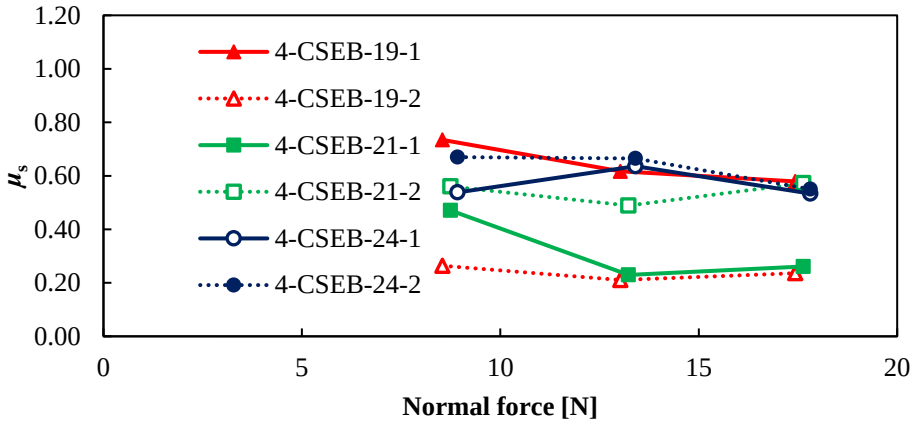

Figure D.4 CoF characterization results for CSEB-Steel interface

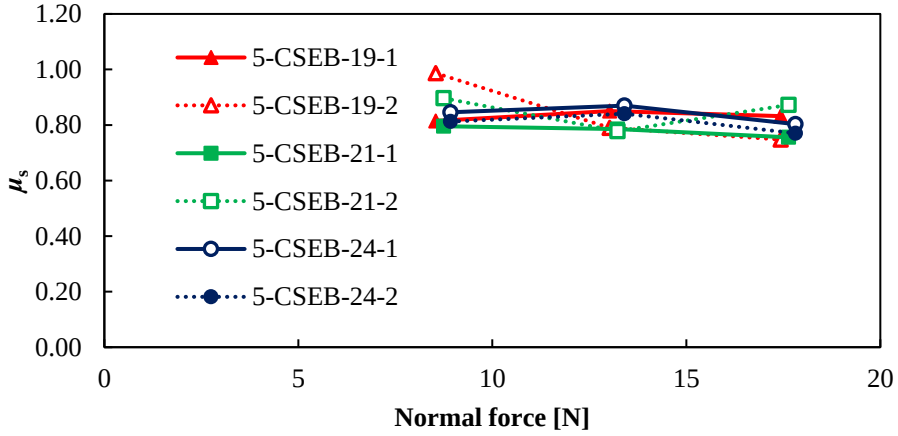

Figure D.5 CoF characterization results for CSEB-Sandpaper 60 interface

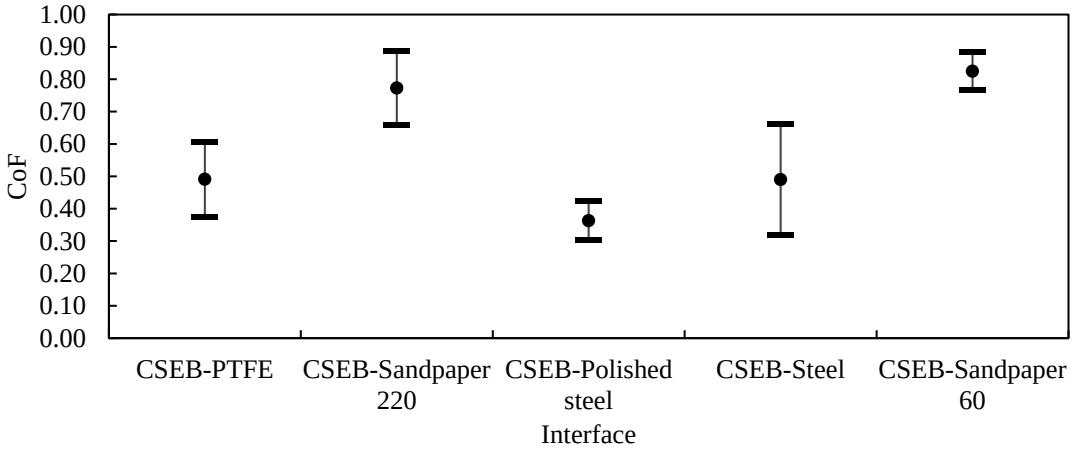

Figure D.6 Summary of CoF characterization

APPENDIX E: 3D-DIC

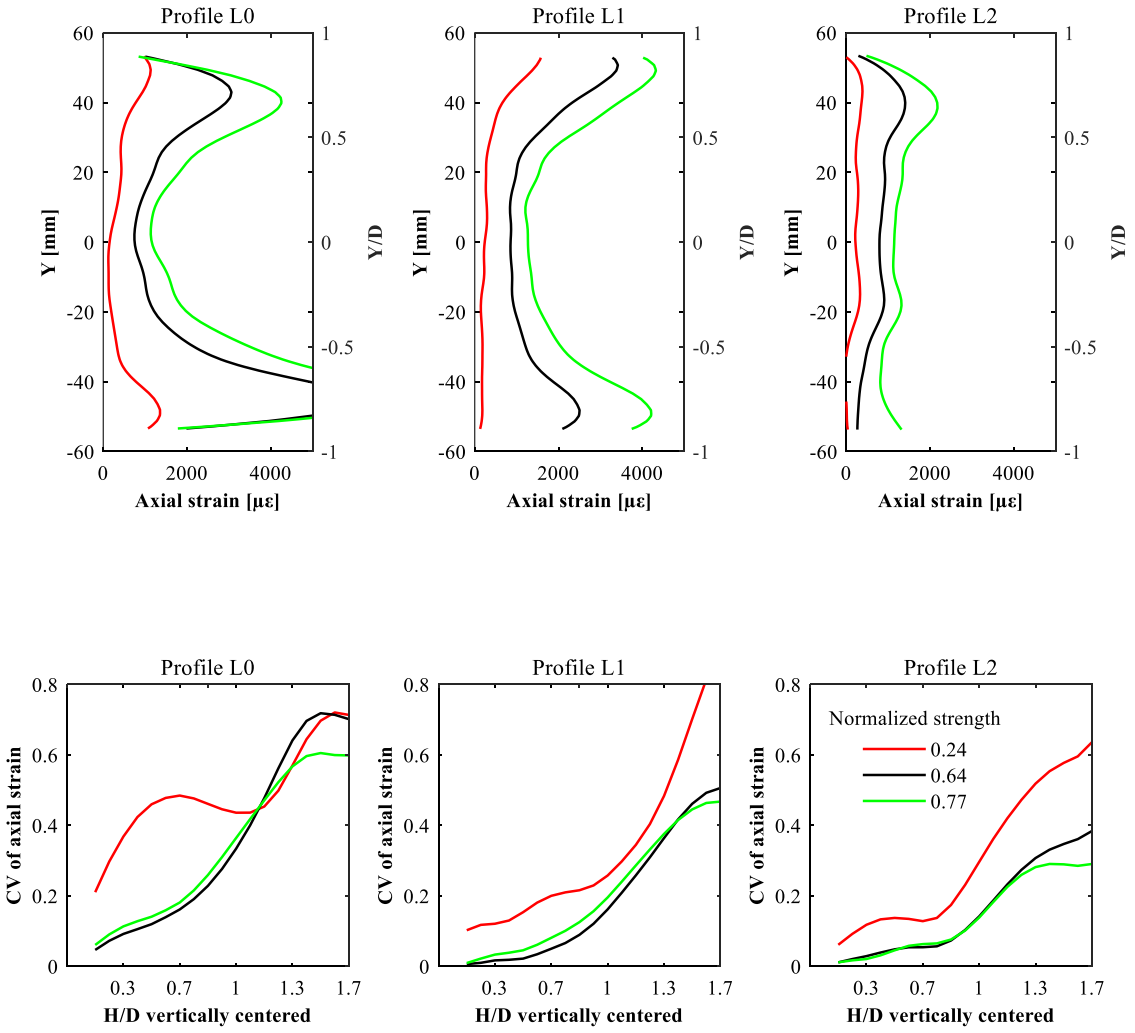

Figure E.1 Nonuniformities assessment on strain distribution in a specimen C2.0-3

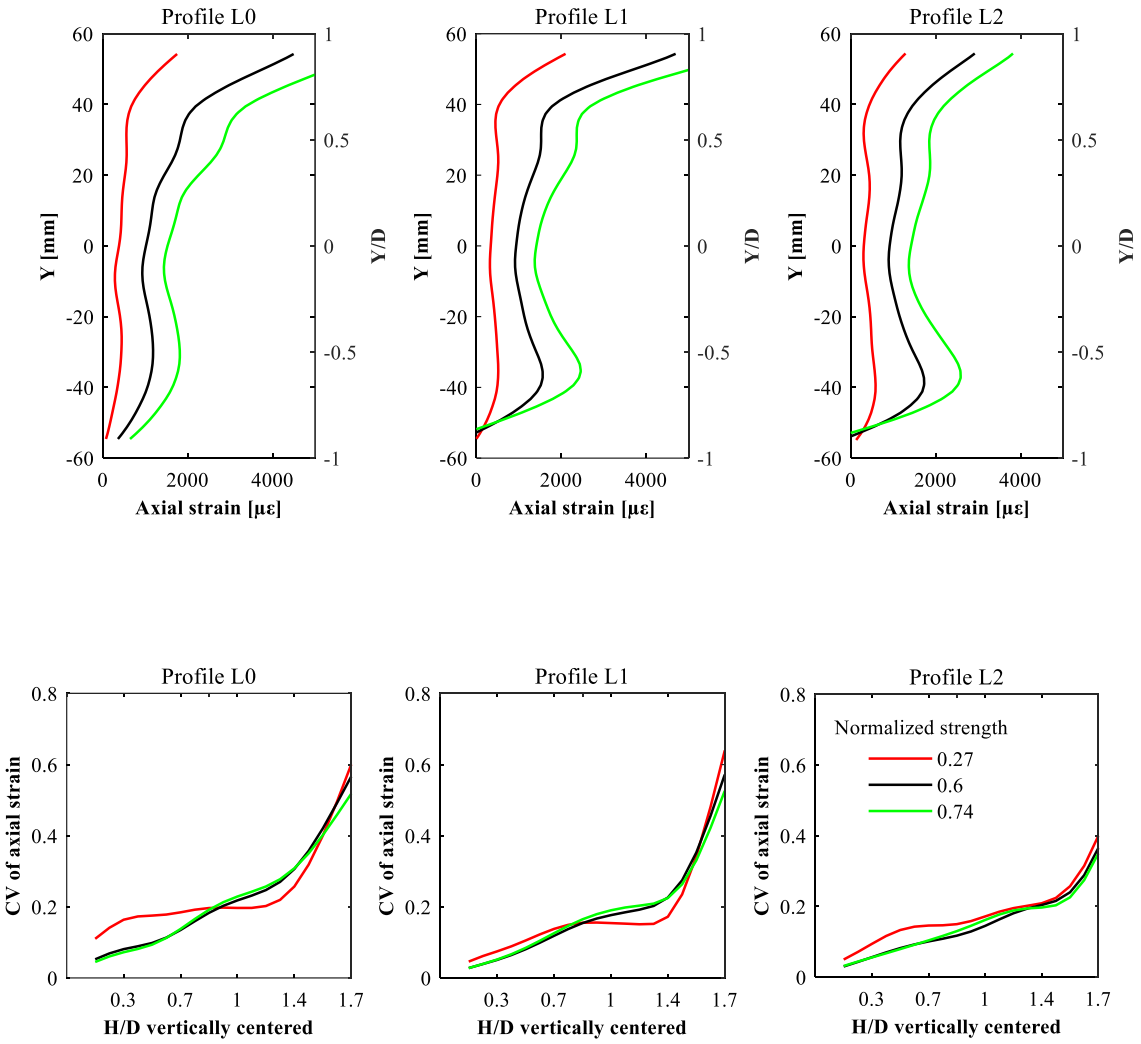

Figure E.2 Nonuniformities assessment on strain distribution in a specimen C2.0-4

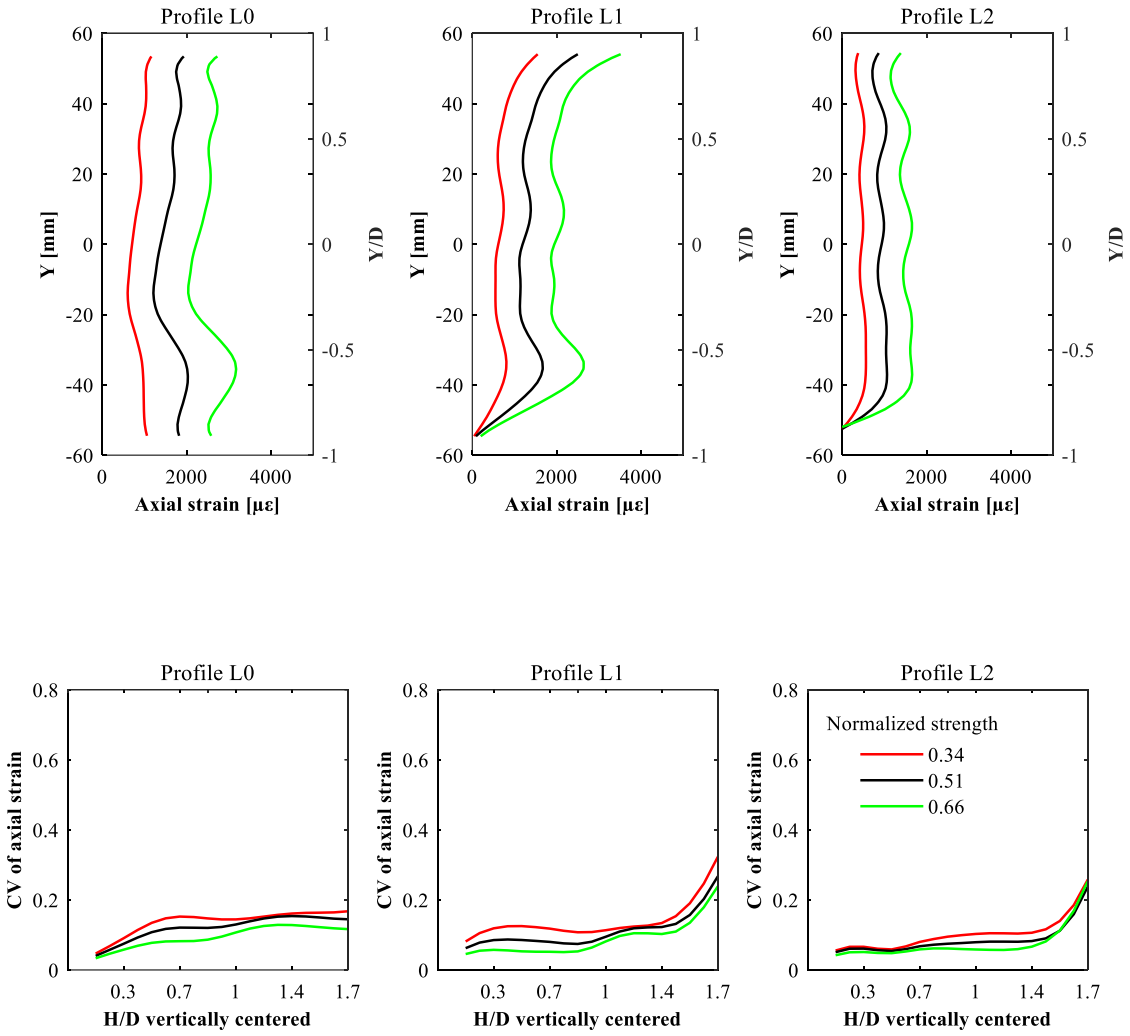

Figure E.3Nonuniformities assessment on strain distribution in a specimen C2.0-5

Table E.1 Experimental setup information

Experiment		3D-DIC	3D-DIC	3D-DIC		Pointwise and 3D-DIC
Model (Specimen type)		C0.5, C1.0, C2.0	P0.7	P2.0		C2.0
				System 1	System 2	
Room temperature [°C]		23	23	23		23
Sensors	Displacement			50-mm LVDT		25-mm LVDT
	Load cell capacity [kN]	98	445	98		98
Max. Peak load (range) [kN]		(15-25)	146	33		15
Bounday conditions		PTFE	PTFE	PTFE		PTFE
Loading frame		245 kN MTS	245 kN MTS	245 kN MTS		245 kN MTS
Loading rate [mm/s]		0.01	0.03	0.01		0.01
Lenses	Reference	AF Nikkor 50mm f/1.8D	AF Nikkor 50mm f/1.8D	XENOPLAN 1.9/35-0511	TAMRON 23FM16SP	AF Nikkor 50mm f/1.8D
	Focal length [mm]	50	50	35	16	50
	F number (lense aperture)	11 or 8	8	8	8	11 or 8
Cameras	Part number	GRAS-50S5M-C	GRAS-50S5M-C	GS3-U3-91S6M-C		GRAS-50S5M-C
	Sensor name	Sony ICX625	Sony ICX625	Sony ICX814		Sony ICX625
	Megapixels	5	5	9.1		5
LED lights		3	3	2		3
Working distance [mm]		2200	2200	1200	600	2200
Stereo angle		14°	14°	13°	15°	14°
Calibration grid		18-mm	18-mm	18-mm or 4-mm	18-mm or 4-mm	18-mm
Images per load step		100	100	50	100	
Subset size (range) [pixel]		(41-61)	51	51		(51-61)

APPENDIX F: ASSESSMENT INSTRUMENT FOR WORKSHOP ON HAZARD-RESISTANT EARTH MASONRY CONSTRUCTION FOR K-12 STUDENTS

Gender (Optional): _____

PART I

1. After today's activities, how likely is it that you will pursue a college education? (Select one)

    a. ___ Much more likely than before
    b. ___ Somewhat more likely than before
    c. ___ Just as likely as before
    d. ___ Somewhat less likely than before
    e. ___ Much less likely than before

2. After today's activities how likely is it that you will pursue Science, Technology, Engineering, or Math (STEM) in college? (Select one)

    a. ___ Much more likely than before
    b. ___ Somewhat more likely than before
    c. ___ Just as likely as before
    d. ___ Somewhat less likely than before
    e. ___ Much less likely than before

3. After today's activities, how likely is it that you will pursue Civil Engineering in college? (Select one)

    a. ___ Much more likely than before
    b. ___ Somewhat more likely than before
    c. ___ Just as likely as before
    d. ___ Somewhat less likely than before
    e. ___ Much less likely than before

PART II

4. Select the Civil Engineering sub-disciplines you heard of for the first time today. (Select all that apply)

___ Materials science and Engineering	___ Coastal Engineering
___ Construction Engineering	___ Earthquake Engineering
___ Environmental Engineering	___ Geotechnical Engineering
___ Water Resources Engineering	___ Structural Engineering
___ Municipal or Urban Engineering	___ Transportation Engineering
___ Forensic Engineering	___ Research

5. Which was your favorite session from today's activities? Please tell us why.

6. How do engineers make a difference through research?

PART III

7. Which of the following buildings is most likely to suffer severe damage during an earthquake event? (Select one)

   a. Wood framing building
   b. Masonry walled building
   c. Earth masonry walled building
   d. Concrete walled building
   e. Don't know

8. Which of the following buildings is most likely to be classified as sustainable construction? (Select one)

   a. Wood framing building
   b. Masonry walled building
   c. Earth masonry building
   d. Concrete walled building
   e. Don't know